UNIVERSITÉ DU QUÉBEC À RIMOUSKI

ÉTUDE DE LA STRUCTURE ET DE LA DYNAMIQUE DES HOUPPIERS A PARTIR DE DONNEES DE LIDAR TERRESTRE

THÈSE

PRÉSENTÉE

COMME EXIGENCE PARTIELLE

DU DOCTORAT EN BIOLOGIE

EXTENSIONNÉ DE

L'UNIVERSITÉ DU QUÉBEC À MONTRÉAL

PAR

OLIVIER MARTIN

AOUT 2017

Composition du jury :

Daniel Kneeshaw, président du jury, UQAM

Robert Schneider, directeur de recherche, UQAR

Richard Fournier, codirecteur de recherche, USherbrooke

Hans Pretzsch, examinateur externe, TUM (Technische Universität München)

Alain Paquette, examinateur interne, UQAM

Dépôt initial le 7 avril 2017   Dépôt final le 02/09/2017

iv

UNIVERSITÉ DU QUÉBEC À RIMOUSKI
Service de la bibliothèque

Avertissement

À mes parents, à mes frères,

REMERCIEMENTS

Les personnes qui ont participé à l'aboutissement de cette thèse, autant d'un point de vue professionnel qu'humain sont très nombreuses. Bien que ces personnes ne soient probablement pas toutes citées dans ce manuscrit, je les remercie chaleureusement.

Je ne peux que commencer ces remerciements par mon directeur de recherche Robert Schneider. Robert, merci tout d'abord de m'avoir accueilli dans ton équipe et de m'avoir confié ce sujet de doctorat. Durant ces années passées à travailler avec toi j'ai pu développer mon esprit et mon autonomie scientifique et je te le dois en grande partie. Merci pour toutes tes relectures de documents, tes conseils avisés et les nombreuses discussions que nous avons pu avoir pour faire aboutir nos idées. Je garde des souvenirs mémorables de ces discussions autour d'une feuille en essayant désespérément de dessiner ou de mimer nos idées respectives en 3D (ça n'a pas toujours été un succès…). Merci finalement pour le côté humain de ton encadrement, tu as su être à l'écoute des problèmes et des frustrations que j'ai pu ressentir dans l'avancement de ma thèse et toujours proposer des solutions pour me sortir des mauvaises passes.

Je tiens ensuite à remercier mon codirecteur Richard Fournier. Richard, merci pour tous tes précieux conseils et tout ce que tu as pu m'apprendre dans le domaine de la télédétection. Merci également d'avoir parfois réorienté mes objectifs trop ambitieux avec ta vision réaliste. Je garde encore en tête le principe KISS (« keep it super simple ») que tu m'avais une fois partagé lors de la rédaction difficile de mon premier manuscrit.

Merci à Batistin Bour pour ces heures passées ensemble sur le terrain et les parties d'échecs enflammées pendant que le LiDAR travaillait. Merci aussi pour ton temps passé devant un ordinateur à isoler avec rigueurs mes arbres-études. Ton aide a été déterminante pour le bon déroulement de ma thèse.

Merci à toutes les personnes du labo de sylviculture et aménagement, Tony, Vincent, Sharad, Alexa, Laurie, Emmanuel, Bérengère pour leur aide, les discussions qu'on a pu avoir et pour leurs accueils lors de mes visites à Rimouski.

x

Merci à tous mes ami(e)s. Martha d'avoir été là de m'avoir soutenue et accompagné pendant plusieurs années dans ce projet. Mes amis de cordée, Antoine, Jean-Nic, JS et les autres qui ont fait de mon passage au Québec une aventure humaine et verticale incomparable.

Merci à toi Madoka d'être là, de me rendre heureux, de me donner confiance dans mes réalisations et de partager nos aventures.

Finalement, merci à mes parents Dominique et Marie Hélène et mes frères Fabien et Nicolas. Vous êtes toujours là pour m'écouter et soutenir mes décisions malgré la distance qui nous sépare. Je pense à vous dans toutes les étapes importantes de ma vie et celle-ci en est une. Vous êtes les personnes les plus importantes pour moi et je vous dédie cette thèse.

RÉSUMÉ

La structure de la canopée joue plusieurs rôles importants dans le fonctionnement des écosystèmes forestiers. Elle est définie par l'emplacement, la taille et la forme des arbres qui la compose. Elle peut donc être étudiée à l'échelle du peuplement entier, ou à celle des arbres individuels. Toutefois, les dimensions, la complexité et la longévité des arbres rendent l'étude de leur structure difficile. Depuis une dizaine d'années, des technologies comme le LiDAR (Light Detection And Ranging) ont fait leur apparition dans le monde de l'écologie et de l'aménagement des forêts. Ce type d'outil fournit une représentation tridimensionnelle (3D) très précise de la structure de la canopée. L'objectif global de ma thèse était d'étudier la structure et la dynamique des houppiers d'arbres individuels à l'aide du LiDAR terrestre (LiDAR-t) dans un contexte de réponse à la diversité du peuplement.

Dans le premier chapitre, l'objectif était d'étudier l'effet de la mixité sur la structure du houppier de l'érable à sucre et sur la pression de compétition qu'il subit. De nouvelles métriques de structure du houppier et des indices de compétition ont été développées à partir de données de LiDAR-t. Les résultats montrent que la pression de compétition est moins forte en peuplement mixte et que les érables occupent l'espace de façon plus efficace. Ces résultats illustrent la grande plasticité du houppier de l'érable à sucre. Par ailleurs, ils soutiennent l'importance d'un aménagement des forêts plus complexe où la diversité spécifique peut entrainer une complémentarité des traits de houppier et une meilleure exploitation de l'espace. Finalement, la capacité du LiDAR-t à décrire la structure des houppiers et la compétition pour la lumière est mise en évidence au travers de l'approche utilisée.

Dans le deuxième chapitre, l'objectif était de quantifier des profils verticaux des feuilles et du bois à partir de données de LiDAR-t et de comparer la forme des distributions entre espèces (érable à sucre et sapin baumier) et types de peuplement (pur et mixte). Une méthode a été mise au point pour discriminer la matière foliaire de la matière ligneuse à partir d'une approche géométrique sur le nuage de point. Les résultats montrent que la distribution du feuillage de l'érable à sucre est plus basse en peuplement mixte qu'en peuplement pur. L'inverse est observé pour le sapin baumier. Ceci suggère une fois de plus que l'érable à sucre est avantagé en peuplement mixte par rapport au peuplement pur. Ce n'est en revanche pas le cas pour le sapin baumier. Finalement les avantages et les limites de la méthode de séparation du feuillage et du bois sont soulevés.

L'objectif du troisième chapitre était de mettre au point une méthode permettant de quantifier les changements du houppier des arbres à partir de données multitemporelles de LiDAR-t. Le principe de la méthode est de récupérer tous les points du nuage de points au temps t_x qui se trouvent au-delà de la limite du houppier au temps t_0 (défini par une enveloppe). L'approche a été appliquée à titre d'exemple pour quantifier la réponse d'érable à sucre et de

sapin baumier aux trouées. Les résultats montrent que les érables à sucre ont une réponse beaucoup plus forte que les sapins baumiers. Par ailleurs, les deux espèces ont tendance à ouvrir leur houppier en réponse au dégagement des compétiteurs et à réoccuper l'espace vers le bas. Ces résultats révèlent une fois de plus l'importante plasticité de l'érable à sucre et l'importance de quantifier les changements de la végétation dans toutes les directions. Finalement, les applications potentielles de la méthode à d'autres espèces et à la dynamique des trouées sont discutées.

Au travers de ces trois chapitres, ma thèse de doctorat a permis de relever plusieurs défis méthodologiques liés à l'utilisation du LiDAR-t en forêt. À partir de ces méthodes, ma thèse a répondu à des questions d'écologie et du développement des arbres. Ainsi, des approches statiques comparant, des indices de compétition, des métriques 3D et des profils de houppier à un instant donné dans différents types de peuplement ont été utilisées dans le premier et deuxième chapitre. Une approche dynamique permettant un suivi précis de la réoccupation de l'espace par les houppiers a été utilisée dans le troisième chapitre. Ces approches ont permis de caractériser l'occupation de l'espace des deux espèces en fonction de l'environnement local. La plasticité importante du houppier des érables à sucre et les effets bénéfiques de la diversité du peuplement sur son développement ont été mis en évidence. Le sapin baumier montre une réponse à la diversité du peuplement plus mitigé. Ces résultats soulèvent alors plusieurs questions et ouvrent des perspectives de recherche quant à l'effet de la diversité sur l'occupation de l'espace à l'échelle du peuplement.

Mots clés: LiDAR-t, peuplement mixte, plasticité, compétition pour la lumière, structure du houppier, développement du houppier, distribution vertical.

ABSTRACT

The canopy structure plays many roles in the processes occurring in forest ecosystems. Canopy structure can be defined as the position, size and shape of the tree crowns that compose it. It can be studied at the stand or at the tree scale. The dimensions, complexity and longevity of trees make it hard to study the canopy. In the last decade, LiDAR (Light Detection and Ranging) technologies have increased in popularity in forest ecology and management studies. These tools offer a very accurate three-dimensional representation of the canopy. In the context of tree response to stand diversity, the objective of my thesis was to study the structure and the dynamics of tree crowns using terrestrial LiDAR data (t-LiDAR).

The objective of the first chapter was to study the effect of mixing on the competition for light and on sugar maple tree crown structure. New crown metrics and competition indices were developed using t-LiDAR data. Results show that competitive pressure is lower in mixed stands than in pure ones. Moreover, sugar maple occupies the space more efficiently in mixed stands. These results revealed the high plasticity of sugar maple tree crowns and highlighted the potential advantages of managing forests in a more complex way, in order to optimize the use of the canopy space. Finally, our approach underlines the t-LiDAR efficiency to quantify tree crown structure and competition for light.

The objective of the second chapter was to quantify vertical distribution profiles of the leaves and wood using t-LiDAR data. The distributions between two species (sugar maple and balsam fir) and between two types of stands (pure and mixed) were compared. We developed a method to separate woody from leafy material from the point cloud using a geometrical approach. Results on sugar maple show that the foliage distribution is lower in the crown in mixed stands than in pure ones and the opposite behaviour was observed for balsam fir. This suggests, once again, that sugar maple can take advantage of the diversity in mixed stands. This is, however, not the case for balsam fir. Finally, advantages and limitations of the wood/leaf separation method were discussed.

The objective of the third chapter was to develop a method to quantify crown changes using multi-temporal t-LiDAR data. The idea of the approach was to extract all the points at time t_x outside the crown hull of t_0. The method was used to quantify sugar maple and balsam fir response to gap formation. Results show that sugar maple has a stronger response than balsam fir to canopy opening and that both species reoccupy the space downward after a gap formation. These results highlight once again the high tree crown plasticity of sugar maple

and the importance to quantify changes in all directions. Finally, the potential applications of the method to other species and to study gap dynamics were discussed.

My PhD thesis has faced important methodological challenges in t-LiDAR data treatment in forest science. The proposed developments enabled me to answer questions about tree development and ecology. In the first and second chapters, static approaches were used to compare at a given time vertical distributions, three-dimensional metrics and competition indices in different stand types. In the third chapter, a dynamic approach was proposed to accurately follow the space colonization of tree crowns. These approaches quantified canopy space occupation of the two studied species in various local environments. The high plasticity of sugar maple and its positive response to mixing in terms of space occupation was highlighted. Balsam fir responses were, on the other hand, not as strong. These results brings up questions and opens research perspectives about the positive effect of diversity at the stand scale.

Keywords: t-LiDAR, Mixed stands, plasticity, competition for light, crown structure, crown development, vertical distribution.

TABLE DES MATIÈRES

CHAPITRE I

INTRODUCTION GÉNÉRALE

CHAPITRE II

REPONSE DE LA STRCTURE DU HOUPPIER DE L'ERABLE A SUCRE (*ACER SACCHARUM*, MARSH) EN PEUPLEMENT PUR ET MIXTE

CHAPITRE III

ETUDE DE LA DISTRIBUTION VERTICALE DE LA MATIERE DANS LE
HOUPPIER A PARTIR DE DONNEES DE LiDAR-t

CHAPITRE IV

UNE METHODE POURQUANTIFIER LES CHANGEMENTS DE LA
CANOPEE A PARTIR DE DONNEES MULTI-TEMPORELLES DE LIDAR
TERRESTRE : LA REPONSE DES ARBRES AUX TROUEES
ENVIRONNANTES

CHAPITRE V

CONCLUSION GÉNÉRALE

xx

LISTE DES TABLEAUX

xxii

LISTE DES FIGURES

LISTE DES ABRÉVIATIONS, DES SIGLES ET DES ACRONYMES

ALS   *Airborn LiDAR System*

CC-PC   *competition cone point cloud*

CDI   *competition density index*

CHI   *competition heterogenity index*

CM   *crown metrics*

CP   *changed point*

CPA   *crown projected area*

CPI   *competition pressure index*

CrD   *crown density*

CrL   *crown length*

Cr-PC   *crown point cloud*

CrW:CrL   *crown width to length ratio*

Cr%   *crown proportion*

DB   *displaced biomass*

DBH   *diameter at breast height*

DS   *developmental stage*

GE   *global expansion*

HE   *horizontal expansion*

HE:GE   *horizontal to global expansion ratio*

HL   *height level*

LAD   *leaf area density*

LAI   *leaf area index*

LiDAR   *light detection and ranging*

LR   *leaf return*

LRDI   *leaf relative density index*

PACr   *projected area of the crown*

RDI   *relative density index*

SC   *stands characteristic*

SP   *species*

STT-PC   *surrounding target tree point cloud*

ST   *stand type*

TLS   *terrestrial laser scanner*

TT   *target tree*

TT-PC   *target tree point cloud*

VE   *vertical expansion*

WR   *wood return*

WRDI   *wood relative density index*

CHAPITRE I
INTRODUCTION GÉNÉRALE

1.1 LA STRUCTURE DE LA CANOPEE

La canopée a longtemps été une partie de la forêt délaissée des scientifiques. Non pas parce qu'elle ne suscitait aucun intérêt, mais du fait de sa complexité et son inaccessibilité. Les études en forêt étaient ainsi initialement limitées à ce qui est facilement observable depuis le sol : le tronc des arbres, les espèces de sous canopée ou les jeunes arbres. La canopée était alors simplement définie comme la couche supérieure de la végétation (Richards et Champion, 1954). Aujourd'hui l'importance de la canopée dans le fonctionnement des écosystèmes forestiers et ses rôles à différentes échelles sont largement acceptés et étudiés par la communauté scientifique. À titre d'exemple, on connait l'impact de la structure de la canopée à l'échelle de la planète sur la régulation du climat en intervenant dans des processus physico-chimiques liée aux échanges gazeux avec l'atmosphère et à l'interception du rayonnement solaire. À une échelle plus fine, elle régule des processus micrométéorologiques impliqués dans la diversité spécifique locale et la dynamique naturelle de l'écosystème. Bien que le nombre de méthodes qui s'appliquent à l'étude de la canopée aient augmenté significativement, l'accès au houppier demeure une limite importante pour des mesures *in situ*. Plusieurs stratégies d'accès à la canopée se sont alors développées. Par exemple, il est possible d'abattre un ou plusieurs arbres pour mesurer leurs différents compartiments. Toutefois, la structure de l'arbre est souvent modifiée lorsque l'arbre s'affaisse au sol, ce qui limite les mesures fines de la

structure du houppier. Par ailleurs, l'aspect destructif de cette approche exclut la possibilité de suivi des individus. Une autre alternative implique de grimper dans les arbres à partir de techniques de corde utilisées en escalade ou en installant une tour ou une structure permettant de se déplacer dans les houppiers. Ces approches peuvent demander un effort technique considérable ou la mise en place de structure coûteuse et requièrent du temps à installer. Le radeau des cimes mis en place par l'équipe de Francis Hallé dans les années 80 est une démonstration typique du désir d'accéder à la canopée. En complément de ces stratégies d'accès aux arbres, les techniques de télédétection procurent des moyens d'estimer la structure des arbres sans contact direct. L'imagerie par avion ou par satellite permet d'appuyer l'inventaire forestier par de nouvelles mesures. Toutefois, les mesures à l'aide des technologies LiDAR (Light Detection And Ranging) procurent de l'information 3D sur les houppiers.

Malgré un consensus sur l'importance de mieux connaître les caractéristiques structurelles et fonctionnelles des houppiers, il ne semble pas y avoir de définition unique quant à la structure de la canopée découlant des différentes approches pour la mesurer. Ses définitions sont donc très diverses et dépendantes du domaine d'étude. Ainsi un écologiste du paysage, un forestier et un botaniste ne s'entendront pas sur la définition de la structure de la canopée, car les échelles spatiales et temporelles changent en fonction des questions qui sont posées. Dans mes travaux de doctorat, le choix de la définition a été orienté par celle proposée par Purves et coll. (2007) qui définissent la structure de la canopée comme l'association de la forme, de la taille et de l'emplacement de chacun des houppiers des individus qui la composent. Cette définition est choisie, car elle intègre à la fois la dimension individuelle de l'arbre et l'interaction avec son environnement proche qui se trouve être l'échelle d'analyse de ma thèse de doctorat. En effet nous allons ici nous intéresser à la structure des arbres individuels de façon fine et à leurs interactions avec l'environnement local. Avec une telle approche du couvert forestier, il convient de commencer par poser les bases de la croissance des arbres et des facteurs qui l'influencent.

1.2 CROISSANCE DES ARBRES

Les arbres se développent grâce à plusieurs processus parmi lesquels on peut compter la croissance primaire (*c.-à-d.* élongation des axes caulinaires ou racinaires), la croissance secondaire (*c.-à-d.* croissance en épaisseur du tronc, des branches et des racines) et la floraison. La structure d'un arbre à un temps donné résulte de l'expression de ces processus et de son histoire de vie. Le développement morphologique d'un arbre dépend donc de facteurs déterminés génétiquement d'une part et de contraintes environnementales d'autre part (Barthelemy et Caraglio, 2007).

Afin d'identifier la partie déterministe de la croissance des arbres, Hallé et Oldeman (1978) ont caractérisé plusieurs modèles architecturaux répondant à des règles dans l'expression des processus de croissance de ramification et de floraison. Un même modèle se répète entre les individus d'une même espèce, mais peut également se répéter entre plusieurs espèces.

Le développement des arbres répond également à l'environnement. La plasticité phénotypique est définie comme la capacité d'un génotype à moduler son phénotype en fonction des contraintes environnementales (Bradshaw, 1965). Elle peut s'exprimer à tous les niveaux et pour plusieurs traits de l'individu (du génotype) considéré et, ainsi, lui permettre de croître dans des habitats divers. Par exemple, en considérant des traits fonctionnels liés à l'acquisition de la ressource, les plantes vont allouer plus de biomasse aux racines en condition pauvre de sol ou faire de grandes feuilles dans des conditions ombragées (Sultan, 2000). La plasticité est également observable à une échelle anatomique. La taille et la structure des vaisseaux ou des trachéides du bois des arbres varient en réponse à des contraintes hydrauliques, thermiques ou biomécaniques (Pittermann et coll., 2006; Rigling et coll., 2002; Schneuwly et coll., 2009). Bien que l'effet de l'environnement sur les organismes végétaux soit largement connu, beaucoup de questions demeurent quant à la gamme de variabilité des traits étudiés, l'interaction

des facteurs influençant cette variabilité et le rapport coût/bénéfice de la plasticité (Sultan, 2000; Valladares et coll., 2007). Dans le cas des arbres de la canopée, on sait que les caractéristiques du houppier peuvent être influencées par différents facteurs tels que le vent, la neige, la pente, et surtout par la compétition.

1.3   REPONSE DES HOUPPIERS A L'ENVIRONNEMENT.

La compétition entre des arbres détermine leurs capacités à croitre et à survivre en occupant l'espace et en accédant à la lumière. Les indices de compétition utilisant les dimensions du houppier d'un arbre-cible et de ses compétiteurs sont les mieux corrélées à l'accroissement en surface terrière (Biging et Dobbertin, 1992; Canham et coll., 2004; Pretzsch, 2009). Ce type d'indice met bien en évidence l'importance du houppier des arbres dans la compétition et la croissance du peuplement, mais ne renseigne pas quant à l'influence de cette compétition sur les caractéristiques des houppiers eux-mêmes.

Il a été montré au travers de mesures simples ou de l'étude de relations allométriques que la forme des houppiers peut être influencée par les conditions de compétition. Par exemple, l'investissement dans la croissance en hauteur en comparaison avec la croissance latérale du houppier varie avec la densité du peuplement (Pretzsch et Dieler, 2012). Les arbres vont en effet privilégier la croissance en hauteur au détriment de l'expansion latérale si la pression de compétition est importante pour atteindre la lumière. En revanche en condition de compétition moins importante (*p. ex.* densité de peuplement faible ou position de l'arbre dominant), ils investiront plus dans la croissance latérale (Antin et coll., 2013; Muller-Landau et coll., 2006). La variabilité des réponses du houppier à son environnement compétitif dépend également de l'espèce. Par exemple, les espèces les plus tolérantes à l'ombre vont généralement présenter une distribution du feuillage et des branches plus basses dans le houppier (Garber et Maguire, 2005; Horn, 1971). Les branches basses survivant mieux à l'auto-ombrage et à des conditions de lumière généralement plus faible.

Les arbres présentent très fréquemment une asymétrie du houppier (distance projetée au sol séparant le centre du houppier de la base du tronc) du fait d'une croissance privilégiée dans la direction opposée à leurs voisins et là où l'espace et la ressource lumineuse sont disponibles. Cette mesure est souvent utilisée pour quantifier la plasticité des houppiers. Plusieurs études ont été publiées à ce sujet, notamment pour essayer de comprendre quels sont les facteurs relatifs au voisinage influençant cette asymétrie (Brisson, 2001; Longuetaud et coll., 2013; Muth et Bazzaz, 2003; D. Seidel et coll., 2011). Chez l'érable à sucre, la direction de l'asymétrie est très corrélée au diamètre et à la distance des plus gros voisins (Brisson, 2001). D'autres travaux trouvent le même type de résultats chez plusieurs espèces de zones climatiques tempérée et tropicale (Schröter et coll., 2012; D. Seidel et coll., 2011; Young et Hubbell, 1991). Il semble donc généralement admis que l'asymétrie soit fortement influencée par les dimensions des compétiteurs.

D'autres facteurs que la compétition peuvent aussi entrainer une asymétrie. Getzin et Wiegand (2007) ont trouvé que les asymétries moyennes à l'échelle du peuplement étaient plus corrélées à la direction de la pente qu'à la dimension des voisins. La tolérance à l'ombre est également un facteur déterminant la capacité d'asymétrie du houppier. Les espèces tolérantes ont une asymétrie généralement plus faible en comparaison aux espèces intolérantes du fait de stratégies de croissance différentes (Canham, 1988; Muth et Bazzaz, 2002; Petriţan et coll., 2009). En outre, le stade de développement apparait aussi être un paramètre important. La plupart des études s'intéressant à l'asymétrie soulignent que l'intensité du déplacement du centre du houppier est plus forte pour des arbres plus petits indépendamment de la position dans la canopée (Muth et Bazzaz, 2003; Young et Hubbell, 1991).

1.4   LE ROLE DES HOUPPIERS DANS LA DYNAMIQUE DES TROUEES

La dynamique des trouées est un sujet qui a largement été étudié et documenté du fait de son importance sur la régénération et son rôle dans la dynamique naturelle des forêts (McCarthy, 2001; Oliver et Larson, 1990). Il est surprenant de constater à quel point le rôle des arbres en bordure de trouées et leur plasticité semblent négligés dans la littérature sur la dynamique des trouées alors que leurs impacts peuvent s'avérer en être un facteur déterminant (Pedersen et Howard, 2004; Vepakomma et coll., 2011). Brisson (2001) suggère d'ailleurs que l'avantage de l'asymétrie est lié à la rapidité à conquérir une ouverture nouvellement formée. Muth et Bazzaz (2002) ont caractérisé l'asymétrie en direction de la trouée pour plusieurs espèces. Ils mettent notamment en évidence des différences entre conifères et feuillus, ces derniers semblent avoir une meilleure capacité à croitre asymétriquement dans la direction de la trouée que les conifères grâce à leur mode de développement plus flexible. Toutefois, très peu d'études ont été menées sur le temps de réponse des arbres en bordure suite à l'ouverture de la canopée (Runkle, 1998; Runkle et Yetter, 1987). La croissance latérale des arbres en bordure peut contribuer fortement à la fermeture du couvert en limitant ainsi le temps pendant lequel le sous-étage reçoit une quantité importante de lumière. Ce phénomène est particulièrement marqué dans le cas de trouées de petite taille qui peuvent jouer un rôle dans les processus de régénération en forêt boréale et mixte (de Römer et coll., 2007).

À la lumière des informations sur le comportement des arbres en fonction des trouées et de la compétition, on comprend que la plasticité des houppiers varie en fonction des espèces et du stade ontogénétique. Par ailleurs, elle s'exprime à tous les niveaux du houppier en réponse aux conditions du peuplement, à la position dans la canopée ainsi qu'à d'autres facteurs abiotiques. Une meilleure connaissance des mécanismes qui gouvernent la plasticité du houppier des arbres semble donc centrale en écologie

forestière, notamment pour comprendre les déterminants de la relation entre la diversité et la productivité des écosystèmes forestiers.

1.5 LA DIVERSITE ET LA STRUCTURE DES HOUPPIERS

La relation entre la diversité spécifique et fonctionnelle et la productivité dans les peuplements forestiers est un sujet de plus en plus étudié. Dans un contexte de changements globaux qui peut résulter dans la perte de diversité à l'échelle de la planète, la nécessité de changer nos modes de gestion des écosystèmes forestiers devient une urgence. En 2016, une meta-analyse étudiant la relation entre la diversité spécifique et la productivité de forêts naturelle et plantée montrait que les forêts diversifiées étaient en moyenne 23,9 % plus productive que les monocultures (Liang et coll., 2016). Une analyse économique parallèle faite dans la même étude montrait que la valeur commerciale des forêts diversifiées se chiffrait entre 166 et 490 milliards de dollars par an contre un coût de 76,1 milliards pour la protection de tous les écosystèmes terrestres. Cette étude suggère donc que le ratio coût-bénéfice de la conservation de la biodiversité pourrait être très avantageux. Malgré cela, la déforestation d'écosystèmes diversifiés continue de sévir au profit des monocultures.

La relation entre diversité et productivité est dû à la complémentarité des traits des espèces présente dans un peuplement pour l'exploitation d'une ou plusieurs ressources (Forrester et Bauhus, 2016). La complémentarité dans les forêts mixtes entraîne une facilitation entre les espèces ou une diminution de la compétition en comparaison avec une monoculture. Cette facilitation ou diminution de la compétition peut provoquer l'expression de traits pour une espèce qui sortent de la gamme de variation de ces mêmes traits observés en peuplement pur (Pretzsch, 2014). Il est très difficile en milieux forestiers d'isoler un effet de facilitation d'un effet de diminution de la compétition, c'est pourquoi le terme de complémentarité a été choisi pour prendre en compte ces deux effets (Jucker et coll., 2015). Un exemple simple de complémentarité

est l'association d'une espèce capable de fixer l'azote atmosphérique avec une qui ne peut pas. La première rendant l'azote disponible pour la seconde, on est ici typiquement dans le cas d'une facilitation. Les expériences de Tilman et coll. (1996) sur des espèces herbacées en prairie ont montré que la complémentarité des traits pour l'acquisition de l'azote permettait de réduire les pertes de cet élément par lessivage dans ces écosystèmes. La complémentarité et son effet sur la productivité a également été mise en évidence en peuplement forestier pour plusieurs type de ressources (Forrester et Bauhus, 2016).

Dans beaucoup d'écosystèmes forestiers, la compétition pour la lumière est souvent avancée comme un des facteurs limitant la croissance des arbres. La complémentarité des traits d'exploitation de cette ressource semble donc être déterminante dans la compréhension de la relation entre la diversité et la productivité en forêt (Williams et coll., 2017). Le terme de remplissage de la canopée (de l'anglais « *canopy packing* ») a alors été introduit et défini dans plusieurs études récentes comme étant le remplissage de l'espace aérien par la végétation (Morin, 2015; Pretzsch, 2014). Des espèces ayant des traits architecturaux du houppier ou des stratégies d'exploitation de la lumière complémentaires vont augmenter le remplissage de la canopée. Deux mécanismes sont proposés comme étant à l'origine du remplissage de la canopée: (i) la stratification et (ii) la plasticité des houppiers (Jucker et coll., 2015).

La stratification est observée lorsque deux espèces aux stratégies d'acquisition de la lumière différentes occupent des strates verticales différentes dans la canopée. Un exemple est lorsqu'une espèce intolérante à l'ombre est mixée avec une espèce tolérante à l'ombre. La première occupe la strate supérieure de la végétation alors que la seconde occupe la strate inférieure. Ces deux espèces vont ainsi exploiter la lumière sans être en compétition, ou tout au moins en limitant la compétition en comparaison avec un peuplement pur. La plasticité des houppiers en revanche va induire une meilleure exploitation de l'espace en modifiant la forme et ainsi l'emboitement des houppiers. Dans un cas comme dans l'autre, l'augmentation de la diversité spécifique

ou fonctionnelle dans un peuplement augmente l'exploitation de l'espace disponible et, par conséquent, de la ressource lumineuse.

Plusieurs études récentes ont suggéré que la plasticité des houppiers était probablement l'élément le plus important dans le remplissage de la canopée et expliquerait ainsi en grande partie la relation entre la diversité et la productivité (Jucker et coll., 2015; Niklaus et coll., 2017). Cette hypothèse a notamment été avancée au vu de plusieurs études démontrant que les houppiers des arbres sont généralement plus profonds et occupent plus d'espace dans des peuplements mixte que dans des peuplements purs (Bayer et coll., 2013; Dieler et Pretzsch, 2013; Jucker et coll., 2015). Toutefois, il est nécessaire de multiplier les études dans divers écosystèmes pour confirmer cette hypothèse récente. Par ailleurs, des précautions sont à prendre lorsqu'on étudie l'effet de la mixité pour arriver à séparer l'effet des différents facteurs et surtout comprendre comment elle varie dans le temps avec le changement des disponibilités des ressources (Forrester et Bauhus, 2016; Forrester et Pretzsch, 2015). Finalement, il est absolument nécessaire de préciser les données quant à la structure des houppiers et comment ils interagissent avec leur environnement proche. La plupart des études à grande échelle sur la relation entre la diversité et la productivité utilisent des relations allométriques ou des représentations de houppier très simplifiées (Jucker et coll., 2015; Liang et coll., 2016; Zhang et coll., 2012). Afin d'étudier de façon plus précise et robuste la plasticité des houppiers, des approches 3D traitant l'arbre dans son ensemble et non limitées à un plan vertical ou horizontal sont nécessaires. Considérant la disponibilité de plus en plus importante de données obtenues à partir d'outils de télédétection précis (LiDAR et imagerie), il devient nécessaire de développer les méthodes de traitement et de multiplier les études sur la structure de la canopée à partir de ces données.

1.6   UTILISATION DU LIDAR EN FORESTERIE

Les capteurs LiDAR peuvent être divisés en deux types de technologies. La technologie de « décalage de phase » consiste à analyser les changements de phase d'un signal sinusoïdal produit par un laser qui émet en continu. Ces changements de phases sont ensuite transformés en retour discret (c'est-à-dire des points avec des coordonnées cartésiennes) et permettent d'obtenir la coordonnée du premier retour. La technologie « temps de vol » est un capteur actif qui émet des impulsions lasers qui sont réfléchies vers l'appareil après le contact avec un objet. La mesure du temps de retour de l'impulsion laser permet de calculer la distance précise entre l'appareil et l'objet ayant intercepté le rayon. Cette seconde technologie permet d'obtenir le premier, le dernier et les retours intermédiaires. Chaque point a donc une valeur de position (x,y,z) et une intensité de retour. Puisqu'un miroir permet de déplacer la direction de visée du faisceau laser et qu'un très grand nombre d'impulsions est envoyé, cela permet au LiDAR de balayer las cene pour couvrir différents angles de vues. Chaque type de capteur peut donc produire un nuage de points distribué dans l'espace balayé par l'appareil. Les patrons du signal peuvent également être analysés de façon plus précise à partir de l'onde complète (full waveform).

Depuis les années 2000, la technologie LiDAR aéroportée a fait son apparition opérationnelle dans le monde de la foresterie. Cette technologie s'avère intéressante pour évaluer de façon précise des attributs du couvert forestier (Lefsky et coll., 2002; Naesset et coll., 2011; Wulder et coll., 2012). Bien qu'elles ne puissent être utilisées sur des étendues aussi importantes que pour les images satellitaires à cause du coût d'acquisition, les données de LiDAR aérien apportent de nouvelles informations à une échelle plus fine. Elles offrent une représentation 3D détaillée de la canopée informant notamment sur sa hauteur et sa densité. Elle permet aussi d'individualiser les houppiers des arbres de façon plus précise que d'autres systèmes de télédétection (Wulder et coll., 2008). Cependant, pour des études à l'échelle de l'arbre, ces données peuvent ne pas

être assez précises à moins d'avoir des données avec une grande densité de points (> 12 points.m^{-2}). Par ailleurs, la vue de dessus offert par le LiDAR aéroporté limite l'information de la partie inférieure de la canopée.

Il existe également une version terrestre du LiDAR (LiDAR-t) permettant une prise de données sous la canopée. Le LiDAR-t procède à un balayage hémisphérique et utilise des faisceaux plus fins et moins puissants. La portée de l'instrument est de l'ordre de 100 à 1000 m selon les instruments. Considérant le grand nombre d'impulsions mesurées (plusieurs millions), les données LiDAR-t procurent une caractérisation 3D plus précise et plus locale par rapport au LiDAR aéroporté. Le détail de l'information acquise ouvre un grand nombre de possibilités pour améliorer, automatiser et obtenir de nouvelles mesures structurelles de la canopée. En revanche, le traitement de cette information implique de grands défis liés à leurs volumes et à l'usage d'algorithmes souvent complexes.

1.7   CHAMPS D'APPLICATION DU LIDAR-T EN FORESTERIE.

Les premières applications du LiDAR-t dans le domaine forestier consistaient à estimer les données dendrométriques et la localisation des arbres pour les inventaires forestiers (Othmani et coll., 2011; Simonse et coll., 2003; Thies et Spiecker, 2004). En employant les résultats de 4 études, Dassot et coll. (2012) ont montré qu'ils détectaient entre 87 et 100 % des arbres avec une erreur du diamètre à hauteur de poitrine (DHP) variant de 1 à 3 cm et une erreur de la hauteur variant de 0,3 à 1,5 m par rapport à des données d'inventaires classiques. Dans une optique d'estimation de caractéristiques plus précises que les mesures classiques d'inventaire forestier, il a été montré qu'il est possible d'obtenir de façon précise le volume d'un arbre sans passer par des mesures destructives en employant des algorithmes d'ajustement de cylindres le long des axes (Calders et coll., 2015; Dassot et coll., 2012; Hildebrandt et Iost, 2012). Par ailleurs, le potentiel du LiDAR-t pour détecter les défauts et les tailles de billons exploitables a été

révélé (Schütt et coll., 2004). Le principe des approches développées repose sur la détection de paramètres extérieurs tels que la présence de cicatrice de branche, la texture de l'écorce, ou la forme du billon influençant la qualité du bois. L'analyse des textures d'écorces permettrait également d'utiliser le LiDAR-t pour l'identification des espèces en forêt et ainsi compléter les données d'inventaires avec des informations de composition (Lin et Herold, 2016; Othmani et coll., 2013; Reulke et Haala, 2005). Ces études ont largement mis en évidence le potentiel d'utilisation de cet outil et les efforts de traitement des données 3D qui doivent continuer à être faits pour son développement en foresterie.

1.8   ÉTUDE DES HOUPPIERS A PARTIR DE DONNEES DE LIDAR-t

Dans le contexte d'étudier les houppiers des arbres, la grande précision de l'information et la caractérisation 3D de l'environnement qu'offre le LiDAR-t sont particulièrement pertinentes. Par exemple, la quantité et la distribution du feuillage dans le houppier sont des informations largement utilisées comme intrants dans des modèles de croissance (Coates et coll., 2003; Medlyn, 2004). Ces caractéristiques du houppier sont souvent estimées à partir de mesures telles que le LAI (*leaf area index :* surface de feuille par unité de surface de sol) ou LAD (*leaf area density :* Surface de feuille par unité de volume) (Bréda, 2003; Lin et West, 2016). Plusieurs méthodes telles que des relations allométriques, la récolte de litière, des appareillages comme le LAI-2000 (LiCor ©) ou la photo hémisphérique sont utilisées pour estimer ces indices. Ces mesures comportent toutefois des biais et limites importantes, soit par leur imprécision, par le temps d'acquisition ou par la nécessité de recourir à des méthodes destructives (Bréda, 2003; Fournier et coll., 2003; Jonckheere et coll., 2004; Weiss et coll., 2004).

Plusieurs études ont testé des approches pour quantifier le LAI et le LAD à partir de données de LiDAR-t (Ashcroft et coll., 2014; Béland et coll., 2011; Grau et coll., 2017). Ces méthodes passent souvent par l'utilisation de voxels. Un voxel est une sous-unité

de l'espace généralement représentée par un cube. De la même façon qu'un ensemble de pixels forme une image bidimensionnelle, un ensemble de voxels forme un espace tridimensionnel. Cette approche présente l'avantage de simplifier un nuage de points tridimensionnels en regroupant l'information. La scène « voxelisée » peut ensuite être divisée en plusieurs couches de hauteur fixe. Enfin, pour chaque couche, un calcul de la fréquence des points correspondant à du feuillage dans chaque voxel est réalisé. Ceci permet de dresser un profil vertical de surface de feuilles qui donne l'information de la distribution du feuillage dans l'arbre. Ces expérimentations révèlent que la représentation par voxel permet d'estimer de façon précise le LAD et le LAI sur des céréales (blé), sur de petits arbres, sur des arbres de canopée (Hosoi et Omasa, 2006, 2009) et sur des arbres de savane (Béland et coll., 2011).

Dans une étude de réponse des houppiers à la compétition, Seidel et coll. (2011) ont quantifié plusieurs métriques de houppier et des indices de compétition à partir de données LiDAR-t. Ils mettent notamment en évidence que ces métriques permettent une prédiction plus précise de l'asymétrie des houppiers que les études classiques. D'autres études montrent que les métriques de houppier et de compétition obtenue à partir de LiDAR-t permettent de mieux prédire la croissance des arbres que des métriques obtenues à partir d'inventaires classiques (Pedersen et coll., 2012; Seidel et coll., 2015).

1.9 LIMITES DU LIDAR-T

L'utilisation du LiDAR-t en science forestière a toutefois révélé certaines limites dont trois ressortent par leur importance : la grande quantité et la complexité des données à traiter, le problème d'occlusion et la reconnaissance feuillage/bois. Premièrement, la précision de l'information s'avère être à la fois une force et une faiblesse du LiDAR-t. Des compromis doivent alors être faits entre le niveau de résolution des scans, la capacité de stockage et la performance des outils informatiques pour traiter

l'information. Deuxièmement, lors du scan, des objets peuvent être cachés par d'autres, ce qui engendre des espaces avec peu ou pas de points. Dans des environnements aussi complexes que le sous-bois, ce phénomène d'occlusion est très courant et pose des problèmes à l'analyse des données. Le scan multiple consiste à balayer sous plusieurs angles de vue l'objet d'intérêt afin de limiter le problème d'occlusion. La géoréférence fine des différents scans est possible grâce au positionnement de repères posés dans la scène et vues sur plusieurs scans. Cette approche multiplie en revanche la taille des données et implique d'autres problèmes comme l'échantillonnage multiple. L'utilisation de voxels est une autre piste permettant de s'affranchir de ce genre de problèmes (Fournier et coll., 2015; Dominik Seidel et coll., 2011). Troisièmement, la séparation des points appartenant aux feuillages de ceux appartenant aux parties ligneuses (bois) lorsqu'on s'intéresse aux houppiers peut s'avérer difficile. Plusieurs techniques ont été explorés pour dissocier les retours liés au feuillage et au bois, mais elles ont toutes des contraintes importantes (Béland et coll., 2011; Côté et coll., 2011; Hosoi et Omasa, 2006; Oshio et coll., 2015). Bien que l'usage du LiDAR-t en milieu forestier présente encore des limites importantes, l'amélioration continue des technologies, des performances informatiques et des méthodes d'utilisation permettent de les surmonter progressivement.

1.10 OBJECTIFS ET HYPOTHESES DU DOCTORAT

L'objectif général de mon doctorat est d'étudier l'effet de la mixité sur la structure et la dynamique des houppiers chez le sapin baumier (*Abies balsamea* Mill.) et l'érable à sucre (*Acer saccharum* Marsh.) à partir de données de LiDAR-t. Le corps de cette thèse est composé de trois chapitres qui ont été ou seront soumis pour publication. Étant donné les défis méthodologiques liés à l'utilisation des données de LiDAR-t, chacun des chapitres est décliné en objectifs méthodologiques et écologiques. Les deux premiers chapitres ont été réalisés à l'aide d'une approche statique où la structure des

arbres est observée à un temps donné. Le troisième chapitre a été réalisé avec une approche dynamique grâce à un suivi temporel de la structure du houppier des arbres.

Chapitre 1 Réponse de la structure du houppier de L'érable à sucre (*Acer saccharum,* Marsh) en peuplement pur et mixte

Objectif méthodologique : Utiliser des données de LiDAR-t pour mettre en place des indices de compétition basés sur l'arrangement de la végétation autour d'arbres cibles et de proposer de nouvelles métriques 3D d'occupation de l'espace par les arbres.

Objectifs écologiques : (1) Quantifier la variabilité des indices de compétition et des métriques de houppier de l'érable à sucre en peuplement pur et mixte et à deux stades de développement. (2) Étudier le potentiel des indices de compétition développés pour expliquer la plasticité du houppier de l'érable à sucre.

Hypothèses : (1) La compétition est moins forte et plus hétérogène en peuplement mixte qu'en peuplement pur. (2) L'érable à sucre présente une grande plasticité de houppier lui permettant une meilleure exploitation de l'espace en peuplement mixte qu'en peuplement pur. (3) L'effet du type de peuplement sur la structure du houppier d'un arbre est principalement dû à la structure de la végétation qui l'entoure.

Chapitre 2 Comparer les profils verticaux de matière de l'érable à sucre (*Acer saccharum,* Marsh) et du sapin baumier (*Abies balsamea* Mill.) entre peuplement pur et mixte à partir de données de LiDAR-t

Objectifs méthodologiques : (1) Développer une méthode de séparation du bois et des feuilles à partir de donnée de LIDAR-t pour bâtir des profils verticaux de distribution de la matière dans le houppier. (2) Utiliser une approche par voxel pour limiter l'effet de l'occlusion sur la distribution verticale de la matière.

Objectif écologique : Quantifier l'effet de la mixité du peuplement et du stade de développement sur la distribution verticale de la matière pour l'érable à sucre et le sapin baumier.

Hypothèses : (1) La distribution verticale de la matière (totale, feuille, bois) est concentrée dans la partie supérieure et inférieure du houppier pour l'érable à sucre et le sapin baumier respectivement. (2) En peuplement mixte, les deux espèces montrent une distribution de la matière plus basse sur le houppier en comparaison aux peuplements purs.

Chapitre 3 Une méthode pour quantifier les changements de la canopée à partir de données multi temporelles de LiDAR terrestre : la réponse des arbres aux trouées environnantes

Objectif méthodologique : Mettre en place une méthode pour quantifier le développement du houppier du sapin baumier et de l'érable à sucre.

Objectif écologique : Quantifier la réponse des houppiers des deux espèces deux ans après le dégagement des compétiteurs en peuplements pur et mixte.

Hypothèses : (1) L'érable à sucre montre une réponse à la suppression des compétiteurs plus forte que le sapin baumier. (2) Aucune différence de réponse n'est observée entre peuplement pur et mixte puisque la compétition pour la lumière a été supprimée. (3) les deux espèces montrent une réponse plus importante en direction du sud où le rayonnement est plus important.

1.11 PRESENTATION DES ESPECES

Le choix du sapin baumier et de l'érable à sucre a été basé sur le fait que ce sont deux espèces à l'architecture et au mode de développement contrasté. Par ailleurs, elles appartiennent à deux grands groupes très différents (résineux et feuillu) mais ont une

stratégie d'exploitation de la lumière semblable, car ce sont des espèces tolérantes à l'ombre. Ainsi, des conclusions quant à ceux deux groupes et leurs architectures très contrastées peuvent être discutées en s'affranchissant des différences de stratégie d'exploitation de la lumière. Finalement, ces deux espèces sont largement présentes dans la région d'étude et ont un grand intérêt économique.

Le sapin baumier se retrouve dans les forêts nordiques de l'Est jusqu'au centre du Canada. La limite sud de son aire de répartition se situe dans les états du nord des États-Unis, de l'est jusqu'au Minnesota. Il croît sur une grande variété de sols, mais préférentiellement sur des sols humides et acides (pH entre 5.1 et 6) et est associé à un climat frais. Les arbres sont matures et fertiles à environ 30 ans et les bonnes années semencières se succèdent tous les 2 à 4 ans. La viabilité des graines est très variable, de 4 à 62 % avec une moyenne de 26 % (Burns et Honkala, 1990). C'est une espèce tolérante à l'ombre, capable de s'établir en condition pauvre de lumière en attendant de profiter d'une ouverture de canopée. Le sapin baumier est particulièrement sensible à la tordeuse du bourgeon de l'épinette. Son système racinaire superficiel augmente la probabilité d'attaque fongique et de déracinement par le vent. Son bois est peu résistant aux chocs et à la pourriture (Beaudet et Messier, 1997). Il est généralement utilisé pour la pâte à papier ou pour des ouvrages ne nécessitant pas une grande résistance. Il se développe suivant le modèle architectural de Massart (Hallé et coll., 1978). Le fonctionnement du méristème apical est indéfini et l'arbre présente alors un tronc unique (monopodial) à direction verticale (orthotrope). Les branches sont également monopodiales, mais poussent en direction horizontale (plagiotrope). Cette mise en place du houppier est généralisable à tous les stades de développement de l'arbre. Toutefois, une perte de la dominance apicale chez l'arbre sénescent arrive fréquemment et mène à la formation d'un sympode dichasial (une fourche) dans la partie terminale du tronc (Millet, 2012).

Au Canada, l'érable à sucre se situe dans les Maritimes et dans les forêts feuillues du sud de l'Ontario et du Québec. Aux États-Unis, il est présent dans tous les états de la

côte est jusqu'au milieu du New Jersey ainsi que dans les états de New York et de Pennsylvanie. Plus au sud, il est retrouvé dans les Appalaches jusqu'à la frontière Nord de la Caroline du Nord qui détermine la limite sud de son aire de répartition (Godman et coll., 1990). Il croit mieux là où le climat est frais et humide (Beaudet et Messier, 1997). Il pousse sur une grande variété de types de sol, mais sa croissance est optimale sur des sols dont le pH varie entre 5.5 et 7.3. Les arbres sont matures et fertiles entre 40 et 60 ans. Le taux de germination des graines est très élevé, environ 95 % (Godman et coll., 1990). C'est une espèce très tolérante à l'ombre. Les semis peuvent survivre longtemps en condition ombragée, tout en gardant leurs capacités à répondre à une ouverture du milieu (Canham, 1988). L'érable à sucre est peu sensible aux insectes et les épidémies sont plutôt rares. Il est recherché pour le bois d'œuvre et pour la production de sirop d'érable. L'érable à sucre présente un développement architectural beaucoup plus complexe que le sapin baumier. Il répond à l'emboitement de plusieurs modèles architecturaux : Leeuwenberg, de Koriba, de Rauh (Hallé et coll., 1978). À la différence du sapin, le fonctionnement du méristème apical change au cours de son développement. Un début de perte de la dominance apicale est observé très tôt dans le développement. Ainsi, au stade jeune plant, le développement des méristèmes latéraux (branches) est déjà favorisé. Au stade jeune arbre (environ 13 m), l'arrêt du méristème terminal est si important qu'il mène invariablement à la formation d'une fourche, dont une partie prend le relais du tronc et l'autre s'affaisse un peu et forme une branche maîtresse. Au stade adulte, la mortalité de l'apex mène à une cime composée d'une grande fourche dont chacune des parties reproduit la structure du jeune arbre avec 4 catégories d'axes (Millet, 2012).

1.12 ZONE D'ETUDE.

La zone d'étude se situe dans la région du Bas-Saint-Laurent au Québec (Figure 1.1). Cette région est à la transition entre la forêt feuillue mixte et la forêt boréale et se trouve dans le domaine bioclimatique de la sapinière à bouleau jaune de l'est et dans la région

écologique des collines des moyennes Appalaches (Robitaille et Saucier, 1998). Les sites mésiques sont caractérisés par la dominance du bouleau jaune, du sapin baumier, de l'épinette blanche et du cèdre (Grondin et coll., 1999).

Il existe plusieurs espèces compagnes comme l'érable à sucre, l'érable rouge, le peuplier faux-tremble ou le bouleau à papier qui peuvent constituer localement une partie dominante du couvert. Le dépôt de surface de cette région est majoritairement composé de till. Les températures annuelles moyennes depuis 1971 sont respectivement de 3.9°C et 2.8°C pour Rimouski et Squatec, et les précipitations de 915 mm et 1083 mm, dont 271 mm et 292 mm sous forme de neige (Environnement Canada).

1.13 SELECTION DES SITES

Nous avons retenu six sites en se basant sur des prospections effectuées à l'été 2012 et sur l'information des cartes écoforestières (Figure 1.1) : trois sites de stade de développement qui est qualifié d'intermédiaire (hauteur moyenne et âge moyen des arbres codominants de 15,3 m et 33,1 ans, respectivement); trois sites de stade de développement qui est qualifié de mature (hauteur moyenne et âge moyen des arbres codominants de 19,5 m et 57,6 ans, respectivement). Afin de pouvoir échantillonner nos arbres dans différentes conditions de compétition, chaque site choisi est composé de 3 types de peuplement : une sapinière, une érablière et une zone mélangée. En plus des critères de proximité entre eux, les sites sélectionnés devaient être semblables en termes de :

- caractéristiques géographiques et édaphiques (exposition, pente, drainage, type de dépôt, etc.)
- indice de qualité de station (Buda et Wang, 2006; Pothier et Savard, 1998)
- contraintes reliées à l'abattage.
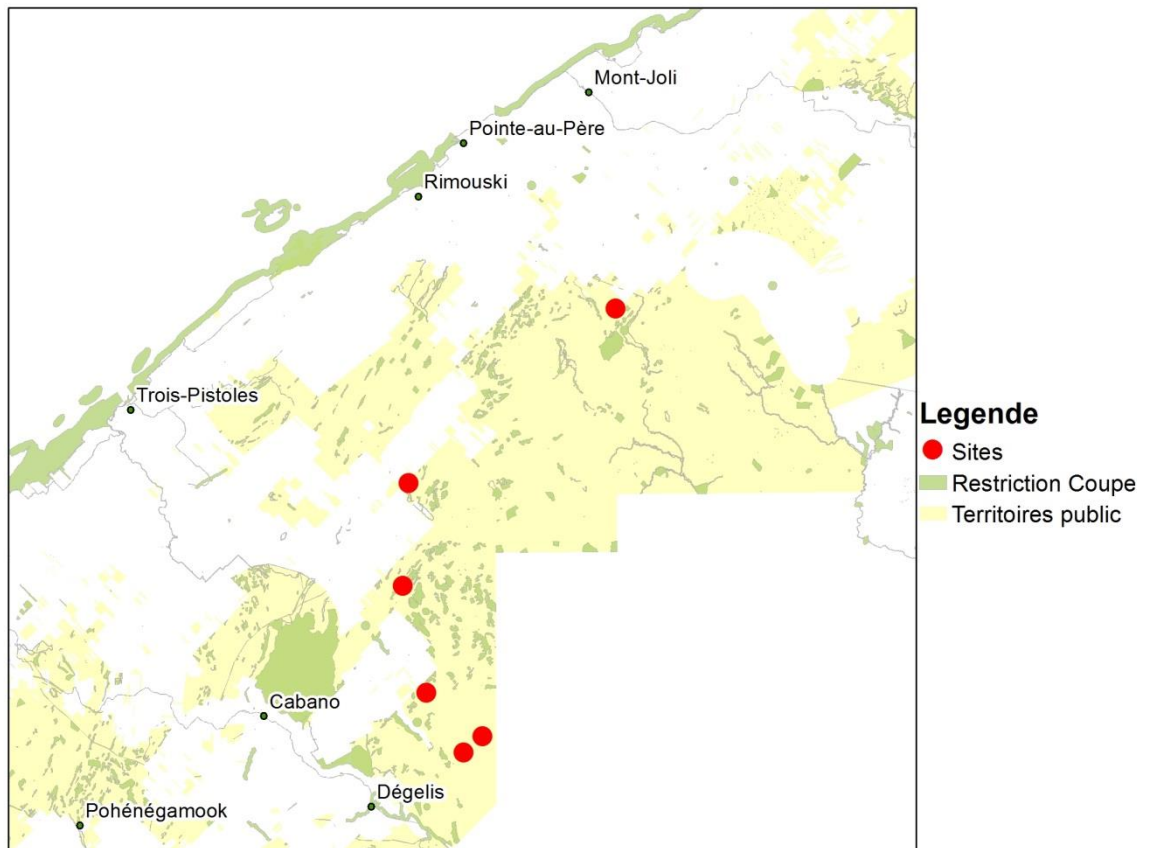
Figure 1-1: Carte de la zone d'étude et localisation des sites

1.14 SELECTION DES ARBRES

Pour chaque site retenu, des arbres-cibles ont été identifiés. Au total, 36 arbres par site (6 sapins dans la sapinière, 6 sapins dans la zone mixte, 6 érables dans la zone mixte, 6 érables dans l'érablière) ont été échantillonnés pour un total de 144 arbres sur l'ensemble des sites. La moitié de ces arbres ont été dégagés de la compétition en abattant les arbres voisins (houppier directement en contact avec l'arbre-cible) au mois d'août 2013 pour répondre aux objectifs du deuxième chapitre. Pour être sélectionné comme arbre-cible, l'arbre devait:

- être un codominant,

- ne pas être blessé ou avoir un houppier dépérissant,

- être situé sur un microsite représentatif de l'ensemble du peuplement (p.ex. ne pas être dans une forte pente alors que les autres arbres ne le sont pas),

- être entouré d'autres arbres, par conséquent, ne pas être en bordure d'une trouée

- pour le sapin, ne pas avoir de fourche,

- pour l'érable, ne pas provenir d'une régénération végétative (c.-à-d. pas de rejets de souche) ou être en groupe.

- Les caractéristiques moyennes des arbres par site et par espèce sont fournies dans le tableau 0.1.

1.15 PRISE DE DONNEES AVEC UN LIDAR-T

Les arbres-cibles ont été scannés avec un FARO Focus 3d (Faro technologies inc.) avec une résolution angulaire de 0.036° (un faisceau laser tous les 3 mm à 10 m). Les angles de rotation sont de 360° à l'horizontale et 152,5° à la verticale. Les prises de mesures ont été effectuées lorsque les érables à sucre avaient des feuilles complètes (mois de juin). Un suivi a été effectué en scannant les mêmes arbres chaque année entre 2013 et 2015. Lors de la première campagne de mesures (été 2013), les arbres dégagés de leurs compétiteurs ont été scannés avant et après le dégagement. Chaque arbre a été scanné dans 4 directions afin de limiter l'occlusion et d'obtenir le maximum d'informations sur le houppier. Les différents scans étaient géoréférencés à l'aide de sphères blanches de 7 cm de diamètre afin de pouvoir aligner les quatre scans ensemble. Finalement, les prises de mesures à l'aide du LiDAR-t ont été faites lorsqu'il n'y avait pas ou peu de vent afin de réduire les mouvements des houppiers.

Tableau 1-1: Caractéristique moyenne des arbres par site et par espèce (écart type)

	Sites intermédiaire			Sites mature		
	Site 1	Site 2	Site 3	Site 4	Site 5	Site 6
Érable à sucre						
DHP (mm)	220 (65)	260 (68)	250 (53)	150 (25)	140 (27)	130 (25)
Âge	48 (8.3)	62 (10.0)	64 (10.0)	30 (3.5)	32 (8.9)	31 (10.0)
Hauteur (m)	18 (0.91)	20 (2.20)	19 (1.70)	15 (1.20)	16 (1.40)	15 (1.40)
Sapin baumier						
DHP (mm)	220 (45)	240 (45)	250 (31)	160 (22)	150 (25)	140 (30)
Âge	50 (6.3)	58 (9.7)	64 (13.0)	32 (2.7)	31 (10.0)	43 (16.0)
Hauteur (m)	19 (2.10)	21 (1.80)	20 (1.60)	16 (0.92)	14 (1.40)	16 (1.40)

CHAPITRE II : REPONSE DE LA STRUCTURE DU HOUPPIER DE L'ERABLE A SUCRE (*ACER SACCHARUM*, MARSH) EN PEUPLEMENT PUR ET MIXTE

2.1 RESUME

Ce premier article, intitulé « *Response of sugar maple (Acer saccharum, Marsh.) tree crown structure to competition in pure versus mixed stands* », fut rédigé par moi-même avec l'aide des professeurs Robert Schneider et Richard Fournier. Il fut accepté pour publication dans sa version finale en 2016 par les éditeurs de la revue *Forest Ecology and Management*. En tant que premier auteur, ma contribution à ce travail fut les travaux de terrain, l'essentiel de la recherche sur l'état de l'art, le développement de la méthode, les analyses statistiques et la rédaction de l'article. Le professeur Robert Schneider, second auteur, a fourni l'idée originale. Il a aidé au développement de la méthode et aux analyses statistiques ainsi qu'à la révision de l'article. Richard Fournier, troisième auteur, a contribué à la révision de l'article. De façon générale, les deux coauteurs ont activement participé aux réflexions dans toutes les étapes de la mise en place du manuscrit qui ont mené à sa publication. Ceci est valable pour ce premier chapitre, mais également pour le deuxième et troisième chapitre. Une version abrégée de cet article a été présentée à la conférence *Silvilaser* à La grande motte (France) à l'automne 2015.

La caractérisation de la structure du houppier et son interaction avec l'environnement local sont capitales en écologie et en aménagement des forêts. Cette interaction dépend de la plasticité de l'espèce considérée et de la compétition locale exercée sur l'individu.

24

Cependant, il est difficile de caractériser cette partie de la forêt à cause de son inaccessibilité et de sa complexité. Dans ce premier chapitre, nous avons utilisé des données de LiDAR-t pour surmonter ces difficultés liées à l'étude de la canopée. L'objectif était de quantifier les différences de structure de houppier de l'érable à sucre entre peuplement pur et mixte et entre les stades de développement intermédiaire et mature. 72 érables à sucre ainsi que leur environnement local ont été scannés avec un LiDAR-t. Nous avons développé huit métriques de houppier et trois indices de compétition. Les résultats révèlent que la pression de compétition est plus importante en peuplement pur qu'en peuplement mixte. Aussi, les érables à sucre ont un houppier qui occupe en moyenne plus de place, qui est moins dense, qui est plus ouvert et plus asymétrique en peuplement mixte qu'en peuplement pur. Cela suggère qu'ils ont une meilleure occupation de l'espace en termes d'interception de la lumière. Ces différences entre peuplement pur et mixte sont plus marquées pour les arbres matures que pour des arbres en stade de développement intermédiaire. Finalement, nos indices de compétition développés à partir de données TLS sont de meilleurs prédicteurs de la variabilité de structure des houppiers que le type de peuplement. Cela suggère qu'ils sont de bons descripteurs de la structure de la canopée et ont un potentiel important pour quantifier la compétition pour la lumière.

2.2 RESPONSE OF SUGAR MAPLE (ACER SACCHARUM, MARSH.) TREE CROWN STRUCTURE TO COMPETITION IN PURE VERSUS MIXED STANDS

2.3 ABSTRACT

Characterizing tree crown structure and quantifying its relationships with the surrounding environment is of critical importance in forest ecology and management.

These relationships depend heavily on species plasticity and local competition for light. It is however difficult to study forest canopies due to their inaccessibility and complexity. The objective of this study was thus to use terrestrial laser scanning (TLS) data to overcome the limits of traditional canopy studies and to quantify the differences in sugar maple (Acer saccharum, Marsh.) tree crowns between stands with different composition and developmental stage. A total of 72 sugar maple trees and their immediate surroundings were scanned using a TLS. We developed eight crown structure metrics and three competition indices using TLS data. We found that competitive pressure is higher in pure stands, when compared to mixed ones. Sugar maple crowns were bigger, less dense, and more sinuous and open in mixed stands. Moreover, differences between trees were generally more pronounced for trees in mature stands. Finally, TLS competition indices are better predictors of crown metric variability than stand type, highlighting the potential of TLS data to quantify tree competition and space occupancy. Our competition indices are good proxies of the canopy structure and thus seem promising to predict tree growth.

2.4   KEY WORDS

Crown plasticity, competition index, crown volume, alpha shape, convex hull, structure-environment loop.

2.5   INTRODUCTION

The forest canopy is the interface between the vegetation and the atmosphere, actively participates in gas exchange and is locally responsible for water availability due to water interception and transpiration (Marin et al., 2000; Oliver and Larson, 1990).

Moreover, it determines light interception and transmission (Hardiman et al., 2013; Canham et al., 1994). Canopy structure thus plays a central role in forest dynamics (Hardiman et al., 2011).

Canopy structure can be defined as the position, size and shape of each tree crown (Purves et al., 2007). It is thus necessary to study changes in individual tree crowns in order to understand canopy structure and dynamics. Barthelemy and Caraglio (2007) defined tree architecture as the spatial arrangement of the different parts of a tree at a given time. They suggest that it is the result of a complex interaction between the intrinsic constraints of an individual (e.g., its genome) and its environmental constraints. Morphological plasticity is the capacity of a given genotype (intrinsic constraints) to modulate its morphological characteristics under different environmental conditions (extrinsic constraints) (Sultan, 2000; Valladares et al., 2007).

The range of variability in crown morphology and ability to grow towards an area with high light availability could thus be considered as plasticity and is mostly species dependent. For example, angiosperm species show more crown asymmetry than gymnosperms (Getzin and Wiegand, 2007). Species' shade tolerance can also determine the degree of crown plasticity. For instance, even if shade tolerant species usually have poor plastic responses for many traits (particularly leaf traits), they have high crown plastic responses in order to maximize light interception in many conditions (Valladares and Niinemets, 2008). Tree developmental stage is also an important determinant of crown plasticity. Small trees usually show a greater crown plasticity due to their needs to respond quickly to changes in the light environment and their low biomechanical constraints which enable higher crown displacements (Delagrange et al., 2004; Muth and Bazzaz, 2002; Young and Hubbell, 1991).

Furthermore, crown plasticity is influenced by abiotic factors such as slope or wind (Brüchert and Gardiner, 2006; Getzin and Wiegand, 2007). Competition is however the most important factor that determines crown plasticity (Brisson, 2001; Schröter et

al., 2012; Seidel et al., 2011-a). Generally, tree crowns grow opposite to the largest and/or the closest competitor, or towards gaps in order to optimize light interception (Brisson, 2001; Muth and Bazzaz, 2003).

Changes in crown structure of a given species can also be influenced by the competitor species. For example, subalpine fir (*Abies lasiocarpa* (Hook.) Nutt.) is an efficient competitor in the forests of western Canada, as it has a very high crown extinction coefficient (Coates et al., 2009). However, its effect on neighboring trees is species dependent, where the development of lodgepole pine (*Pinus contorta* Douglas ex Loudon) is less hindered by subalpine fir than interior spruce (*Picea glauca engelmannii* Parry ex Engelm.) (Thorpe et al., 2010). Likewise, European beech (*Fagus sylvatica* L.) grown in pure stands have less developed crowns than when mixed with Norway spruce (*Picea abies* L.) (Bayer et al., 2013). No differences in crown structure were, however, observed when European beech was in mixed stands with sycamore maple (*Acer pseudoplatanus* L.) (Barbeito et al., 2014). This variability in the competitive relationships between species in a stand is commonly explained by the complementarity of crown traits and differences in light acquisition strategies (Forrester et al., 2013; Le Maire et al., 2013; Pretzsch, 2014). It has been shown that the complementarity between species could lead to higher productivity in forests composed of mixed stands (Forrester, 2014; Morin et al., 2011). Furthermore, a "close-to-nature" management system should favor stands with more species diversity and/or more heterogeneous structure by integrating the concept of complementarity into management practices in order to maintain or increase ecosystem services (Messier et al., 2013).

Crown plasticity remains poorly understood as it is hard to quantify from the forest floor. Many authors have tried to quantify the competitive pressure suffered by a tree with conventional methods. Distance dependent or distance independent competition indices (CI) have been developed (Bachmann, 1998; Biging and Dobbertin, 1995; Pretzsch, 2009). Distance independent indices are based on the density of the stand

and/or the relative size of a target tree compared to other trees within the stand. Distance dependent indices need competitor tree locations in order to quantify competition based on their size and distance to the target tree. The CI are generally used to predict tree growth (Alemdag, 1978; Biging and Dobbertin, 1995; Canham et al., 2004; Tome and Burkhart, 1989). Some studies have used CI to understand or predict crown plasticity (Brisson, 2001; Muth and Bazzaz, 2003; Young and Hubbell, 1991). Such studies remain marginal and often characterize crowns with two-dimensional projected crown metrics (e.g., crown projected area (CPA), eight crown radii).

Terrestrial laser scanning (TLS) provide a very accurate three-dimensional (3D) representation of a forest and overcome some limitations of traditional canopy studies. The popularity of TLS in forest ecology and forestry has therefore increased in the last few years. Canopy occupancy by trees and within-crown tree structure (branch number, branch size and topology) can now be accurately described (Bayer et al., 2013; Béland et al., 2011; Côté et al., 2011; Dassot et al., 2012; Seidel, 2011). Recently, new CI based on information extracted from 3D point clouds obtained from airborne laser scanning (ALS) (Pedersen et al., 2012) and TLS (Metz et al., 2013; Seidel et al., 2015) have been proposed. These TLS and ALS derived indices better explain tree growth than the traditional indices computed from DBH, height or CPA. They quantify the crown structure of competitor trees or the amount and the spatial distribution of woody and leafy materials that intercept light around a target tree.

Our study focused on quantifying the interaction between the sugar maple (*Acer saccharum*, Marsh.) tree crown structure and its environment. A first objective was to compare the structure of the immediate surrounding of trees in pure and mixed stands at different developmental stages. A second objective was to highlight variations in tree crown structure with stand type and developmental stage. A third objective was to link individual crown structure with its local environment. TLS based metrics were developed to achieve these objectives. The tested hypotheses were that (1) competition

in mixed stands is lower and more heterogeneous compared to pure stands, since the crown structure variability and the potential complementarity of crown traits is higher in multi-species forests; (2) sugar maple tree crowns are highly plastic as inter-species competition forces niche partitioning and thus induces changes in crown metrics between mixed and pure stands; (3) sugar maple tree crown plasticity is higher in intermediate aged-stands than in mature ones as younger trees are usually more plastic; and (4) the effect of stand type (e.g., mixed or pure) on crown characteristics is mostly due to the structure of the competitive environment, and therefore TLS derived indices should be sufficient to explain crown structure variability.

2.6   MATERIAL

2.6.1   Study site

The data were obtained from forest stands located in eastern Quebec, Canada. Mesic sites in this region are characterized by mixed stands of yellow birch *(Betula alleghaniensis* Britton*)*, balsam fir *(Abies balsamea (L.)* Mill.*)*, white spruce *(Picea glauca* (Moench) Voss*)* and eastern white cedar *(Thuja occidentalis* L.*)* (Grondin et al., 1998). Other species such as trembling aspen *(Populus tremuloides* Michx.*)*, paper birch *(Betula papyrifera* Marshall*)*, as well as sugar and red maple *(Acer rubrum* L.*)* are also observed locally, with sugar maple often found in pure stands. A total of six sites were identified from the eco-forest map developed by the Quebec Ministry of Forests, Fauna and Parks (MFFP, 2007). The information used from the maps were stand composition, age class and dominant height class. Each site is composed of two stand types which are on the same geomorphological deposit: a pure sugar maple stand and a mixed stand generally composed of sugar maple and balsam fir. Stand composition for each site was determined using four wedge prism plots (Table 2.1). The six sites can be further divided into two forest development stages: intermediate

(approx. 30 years old) and mature (approx. 55 years old) stages with three sites per developmental stage. Developmental stages were identified according to architectural stage in Millet (2012). Moreover, no indications were found that management activities had taken place in the last 30 years.

2.6.2   Target-tree measurements

In July 2013, a total of 72 sugar maples were sampled as Target Trees (TTs) with twelve sampled trees from each site: six in mono-specific and six in mixed conditions. We ensured that TTs in mixed conditions were mostly surrounded by trees of other species, and by at least one conifer competitor. All the TTs were co-dominant and did not have major injuries or defects such as dead or pruned large branches. The diameter at breast height (DBH) of each TT was recorded using a measuring tape at a height of 1.30 m. Trees were scanned with a Faro Focus 3D set with a resolution angle of 0.036° in both the horizontal and vertical directions and scanner rotation angles from 0 to 360° in the horizontal direction (a full turn) and from - 60 to 90° in the vertical direction. Each TT was scanned from four viewpoints to minimize occlusion and maximize visible details of the TT crown and of the surrounding canopy. These viewpoints were not exactly located at 90 degrees from each other as they were determined visually in the field in order to have the best visibility of the TT crown. Each individual scan was aligned using six spherical targets, with a minimum of three targets seen from each scan. General characteristics of all TT per site are given in Table 2.2.

2.6.3   Data preparation

Multi-scan alignments were preprocessed with Faro Scene 5.0.1 (Faro, 2012). Target sphere detection and subsequent alignment are automatic if at least three spheres shared between the four scans are detected. Manual identification of the target spheres was necessary if less than three shared spheres were detected. Noise points were removed with two filters available in Faro Scene: (i) the dark scan points filter to remove points with a very low reflectance (less than 300) which correspond to false returns or sky points and (ii) the stray filter. The latter filter validates that the return is due to an object by comparing the distance with the scanner with the distance of the surrounding points (grid size of 3×3×3 points). The return is retained as a scan point if 50% of the differences in distance with the surrounding points is smaller than 0.02 m.

2.7   METHODS

To quantify the effect of competition on tree crown structure, several steps were carried out in order to transform the TLS point-clouds into biologically and ecologically meaningful data (i.e., metrics of crown and inter-tree competition). First, sub-point clouds were created to discriminate TT data from its surroundings (see the "Point cloud processing" section). Then, algorithms were developed and applied to the sub-point clouds in order to extract (i) crown metrics (see "Tree crown metrics" section) and (ii) competition indices (see "Competition metrics" section). All algorithms were developed in the R statistical and programming language (R Development Core Team, 2011).

2.7.1 Point cloud processing

The TTs were isolated from the point clouds using a semi-automatic procedure in the Computree platform (Computree, n.d.; Othmani et al., 2011). Three point clouds were then exported from Computree:

(1) The points belonging to the TT (TT-PC for Target-Tree Point Cloud);
(2) The points belonging only to the crown of the target tree (Cr-PC for Crown Point Cloud) (Fig. 2.1A). Height to crown base coordinates (x, y, z) were obtained from visual inspection of each TT in Faro Scene;
(3) The entire scene in a cylinder with a radius of 8 m around the TT. For this point cloud, the TT-PC was withdrawn in order to only have points from the immediate surroundings of the TT (STT-PC for Surrounding Target Tree Point Cloud). The STT-PC was used to characterize competition (see below).
(4)

2.7.2 Tree crown metrics

Several steps were applied to the Cr-PC in order to measure a total of eight crown metrics in the point cloud. These metrics were calculated using volumes, surfaces, point coordinates manually recorded, distance between objects or based on a theoretical representation of the crown. In this section, all the metrics and the algorithm applied to obtain them are described with the studied metrics written in bold.

(1) **Crown length to tree height ratio:** On the raw point cloud the maximum height (Z coordinate) of the tree was visually estimated. The crown base height was manually recorded (see 3.1) (Fig. 2.1A).
(2) **Crown length to crown width ratio:** The crown width was estimated as the diameter of the circle of area equal to the CPA of the crown. The CPA of the

crown was computed using a convex-hull algorithm available in the geometry package (Barber et al., 2014) on the XY coordinates of all Cr-PC points.

(3) **Crown volume:** This metric is the volume of the 3D alpha-shape which was fitted to the Cr-PC with the "alphashape3d" package (Lafarge and Pateiro-Lopez, 2014). The alpha value was set at 0.5 as this value provides an accurate hull of the crown without creating holes (Fig. 2.1B).

(4) **Crown density:** The metric was estimated by dividing the volume of the non-empty 10-cm edged voxels of the Cr-PC ("voxR" library , Lecigne and Messier, 2014) by the crown volume (Fig. 2.1B).

(5) **Sinuosity:** This metric was computed by dividing the crown into several volumes. First, the symmetry axis of the crown was identified as the vector passing through the crown base (the center of the stem at the base of the crown) and the center of the alpha-shape 3D volume (Fig. 2.1B). The alpha-shape 3D center was calculated as the mean of the vertice coordinates used to build it. Second, the Cr-PC was then divided into 10-cm slices along the symmetry axis, from the base to the top of the crown. Third, a 3D polygon was fitted to each slice using a convex-hull algorithm (Fig. 2.1C). The sinuosity is the deviation of the 3D polygons center with regard to crown symmetry axis, calculated as the sum of the distance between the symmetry axis and the center of the 3D polygon for each slice, and divided by crown length.

The three remaining metrics (crown openness, crown roughness, and shade crown length to crown length ratio) are based on a theoretical crown computed with the 10-cm slices previously described. The theoretical crown is composed of two sections: the sun-exposed and the shaded sections (Pretzsch, 2009). The shaded section was defined as an inverted truncated cone, with the smallest base being at crown base, and the largest base at the junction between the shaded and sun-exposed section. The sun-exposed section was assumed to be hemispherical. The outer limits of the theoretical crown were obtained by calculating the mean distance between the center of mass of

the polygon of a slice and all of its vertices (d_{mean} in Fig. 2.1C). The theoretical crown model was obtained with a linear-log segmented regression, with the lower segment relating d_{mean} to height, and the second segment d_{mean} to $\ln(height)$. Parameter estimates where obtained by optimizing the log-likelihood of the segmented regression (Toms and Lesperance, 2003). The transition height between the shaded and sun-exposed sections of the crown is given by the breakpoint. The resulting smoothed theoretical crown corresponds to the surface of revolution of the segmented regression around the symmetry axes (Fig. 2.1D) and was used to quantify the three remaining metrics:

(6) **Crown openness:** It was defined as the angle between the axis of symmetry of the crown and the outer limit of the shade crown as given by the linear segment of the regression (Fig. 2.1D).

(7) **Crown roughness:** This metric is the ratio between the surface of the theoretical crown (Fig. 2.1D) and the surface of the 3D alpha-shape (Fig. 2.1B), similar to the rumple index for canopy roughness (Parker et al., 2004).

(8) **Shade crown length to crown length ratio:** This metric is the ratio between the length of the shade crown section given by the break point of the segmented regression (Fig. 2.1D) and the total crown length (Fig. 2.1A).

These eight metrics quantify some structural aspects of a whole tree crown. To study local asymmetry, the crown was also divided into six equal parts of 60° around the axis of symmetry, corresponding to the six cardinals directions zones: northeast (NE), north (N), northwest (NW), southwest (SW), south (S) and southeast (SE). The percentage of crown volume in each zone (sum of the 10-cm-high convex-hull volumes in a given zone divided by the sum of total 10 cm high convex-hull volumes) was calculated for the whole crown, the shade section and for the sun-exposed section (Fig. 2.1E). This percentage is proportional to crown asymmetry. We arbitrary decided to use six zones to quantify the asymmetry, but the method can easily be applied to user-divided zones or other systematic divisions.

2.7.3 Competition metrics

Competition was quantified using the STT-PC. This involved extracting any returns from the point cloud that could contribute to shading of the TT. To identify these points we used the so-called search cone method to detect all plant material in an upside-down cone with a 60° angle placed at the TT crown base height that potentially enforces competition on a TT (a similar method was used in Seidel et al. (2015)) (Fig. 2.2A). The symmetry axis of the truncated cone is the same as that of the crown. The radius of the small base of the truncated cone (i.e., the base with the lowest Z) is equal to the radius of the crown base. The resulting point cloud was also voxelized with voxels of the same size as those used on the TT-PC (i.e., 10-cm edges), yielding to a point cloud grid (Seidel et al., 2011-b) called the competition cone point cloud (CC-PC). Finally we computed three metrics to characterize the competition of a tree. A competition pressure index (CPI), a competition heterogeneity index (CHI) and a competition density index (CDI).

A 10-cm raster projection of the CC-PC on the XY plane ("VoxR" library, Lecigne and Messier, 2014) was used to calculate the CPI (Fig. 2.2B):

$$CPI = \frac{1}{n}\sum_{i=1}^{n}\frac{H_i * V_i}{d_i} \tag{1}$$

where n is the number of cells in the raster, V_i the number of non-empty cells in the Z direction above the raster cell i, d_i the distance between cell i and the projected center of the crown and H_i is the mean height of the voxels of the cell i (e.g., the mean height of the voxel was divided by the height of the TT in order to have a relative height and

therefore avoid a tree size effect). This metric was also computed for each of the cardinal zones (Fig. 2.2D).

The CHI is the Clark and Evans aggregation index (Clark and Evans, 1954), which was calculated based on the XY position of each cell of the raster (Fig. 2.2B).

Finally, canopy density index (CDI) was estimated by the ratio between the volume occupied by non-empty voxels and the total volume of the truncated cone without the TT-PC (Fig. 2.2C).

2.7.4   Data analysis

The data analysis concentrated on three aspects: (i) differences in crown metrics and competition indices between stand types (mixed vs pure) and developmental stages (intermediate vs mature); (ii) links between crown metrics and competition indices; (iii) changes in crown asymmetry with competition.

First, two-way analysis of variances (ANOVA) was used to study the differences in crown structure and competition environments with stand type and developmental stage. Simple (development stage, stand type) and interaction effects (development stage X stand type) were tested for each crown metric and each competition index.

Second, the effects of the competition indices on target tree crown metrics were studied using linear mixed-effect models. The fixed components of the models were composed of competition indices and stand types (e.g., CPI, CHI, CDI, stand type). All possible combinations of presence/absence of each variable (CPI, CHI, CDI, stand type) in the fixed components led to 15 models being calibrated for each crown metric, with the full model having the four variables and the reduced models having only one of the four variables. Developmental Stage (DS) of the TT was used as a co-variable in all

models in order to account for differences in tree size and age. A site random effect was added to all models to account for within-site TT correlation. The resulting full model is:

$$Y_{ijk} = a_0 + a_1 CPI_{ijk} + a_2 CHI_{ijk} + a_3 CDI_{ijk} + a_4 ST_{ij} + a_5 DS_i + a_6\, ST_{ij}\, DS_i + u_i + \varepsilon_{ijk}$$

(2)

where Y_{ijk} is one of the crown metrics of tree k in stand type j of site i, a_0 to a_6 the fixed effect parameters, ST_{ij} a binary variable to indicate stand type ($ST_{ij} = 0$ for *pure* stands, $ST_{ij} = 1$ for *mixed* stands), DS_i a binary variable to indicate developmental stage ($DS_i = 0$ for intermediate stage and $DS_i = 1$ for mature stage), u_i the normally distributed site random effect parameter ($u_i \sim N(0, \sigma_i^2)$) and ε the residual error ($\varepsilon_{ijk} \sim N(0, \sigma^2)$). The full and all the reduced models were then compared using Akaike's Information Criteria (AIC) to identify the best model for each crown metric (e.g., crown volume, length to width ratio, crown length to crown width ratio, openness, roughness, shade crown length to crown length ratio, sinuosity, crown density). Homoscedasticity and normality of the residuals were evaluated visually. Natural-logarithm or square root transformations were applied when needed to the response variables in order to reduce the heteroscedasticity. Whenever an interaction effect was significant, the Tukey HSD (honest significant differences) test was used.

Finally, linear regressions were used to study the relationship between CPI inside the zone and percentage of crown volume inside the zone. These relationships were studied for the whole, shaded and sun-exposed crown. The CPIs computed in each zone were scaled by TT since the CPI of a TT is size-dependant.

2.8   RESULTS

2.8.1   Effect of stand type and developmental stage

Effect on tree crown metrics

Tree crown metrics highlighted differences between pure and mixed stands and between developmental stages (Fig. 2.4). Crown volume, crown length to tree height ratio, crown openness and sinuosity were significantly higher in mixed stands whereas crown length to width ratio, shade crown length to crown length ratio and crown density were significantly lower. Crown roughness was the only crown metric without statistical differences between the two stand types. Crown volume and sinuosity were significantly higher for trees in mature sites whereas crown roughness and crown density were lower. The four remaining variables showed non-significant differences between the intermediate and mature sites. Interaction effects were found to be statistically significant for crown volume only, where the Tukey HSD test revealed that crown volume was higher for mixed stands in mature sites. The interaction effects were non-significant for all the remaining crown metrics. However, differences between mixed and pure stands for Crown length to width ratio, crown openness and shade crown length to crown length ratio seem to be more important in mature sites. It should be noted that this trend was also observed for CDI and CHI.

Effect on competition indices

The three indices describing the immediate surroundings of the TT (CDI, CHI and CPI) also behaved differently between trees in pure and mixed stands (Fig. 2.3). Statistically significant differences were observed between mixed and pure stands as well as between intermediate and mature sites (simple effects) for the CPI only, with a higher value in pure stands and in intermediate sites. No significant differences were observed for the CDI and CHI. Moreover, interactions between stand type and developmental

stage were also found to be non-significant for all three indices. Nevertheless, certain trends can be observed for CDI and CHI: differences between mixed and pure stands seem to be more important for mature sites.

2.8.2   Effect of competition indices on tree crown metrics

Effect at the scale of the whole crown

For each of the eight studied crown metrics, 15 candidate models were compared using the AIC (Table 2.4). The best model (i.e., lowest AIC) for six of the eight crown metrics studied contained the CPI (Table 2.3). CHI was retained in four models and was always statistically significant. Finally, the least important competition index was the CDI, as it was retained for only two crown metrics and was only statistically significant for crown sinuosity. Stand type was retained for three of the best crown metric models, even though the effects were statistically non-significant. However, the interaction effects between stand type and developmental stage were significant for crown volume and crown length to tree height ratio (Table 2.3).

Effect at the scale of the crown zones

Fig. 2.5 shows the relationships between the CPI computed inside a zone (i.e., northeast (NE), north (N), northwest (NW), southwest (SW), south (S) and southeast (SE)) and the percentage of tree crown volume in that zone. For the whole crown, the slope was found to be negative for intermediate stage trees in mixed stands only, whereas the slope was found to be non-significant for trees in pure stands and those in mixed stands that were mature (Fig. 2.5A). For the shaded part of the crown, the slope was statistically significant and negative for each combination of stand type and developmental stage (Fig. 2.5B). Finally, when the light crown was considered, the relationship was positive, but only statistically significant for mature trees in pure stands (Fig. 2.5C).

2.9   DISCUSSION

In certain jurisdictions, "close-to-nature" management systems are being developed, with the objective to favor more complex stand structures and composition in order to maintain or increase ecosystem services (Messier et al., 2013). For example, many studies have shown that forests composed of mixed stands can be more productive compared to those with pure stands (Morin et al., 2011; Paquette and Messier, 2011). However, the complexity of the arrangement of trees belonging to different species in mixed stands makes the quantification of the tree crown response to its surroundings particularly difficult. Our study aimed to quantify these relationships in pure and mixed stands in order to better understand forest dynamics.

2.9.1   Pure vs mixed stands

Our first hypothesis stated that competition is stronger and more homogeneous in pure stands compared to mixed ones. Our results partially confirm this hypothesis since substantial differences between mixed and pure stand canopies were found for CPI. This index integrates the density, the distance to the TT crown and the height of the woody and leafy material around the TT. In other words, it summarizes the shading potential from the immediate surroundings on a TT crown. Our results thus suggest that this effect is more important in pure stands than in mixed ones. These results are also in agreement with those of Metz et al. (2013) for European beech. They found that the KKL index (Pretzsch, 1995) and their own TLS-based index of competition was higher for intra-specific competition when compared to inter-specific competition.

They suggested that it could be due to the high shade tolerance of European beech. Similar results were found here for sugar maple.

Light interception efficiency has been shown to be related to species shade tolerance (Canham et al., 1994). Sugar maple is, along with balsam fir, the most shade tolerant species in our sites (Humbert et al., 2007). Thus, the higher CPI observed in pure sugar maple stands was probably due to its ability to deal with increased light interception due to its shade tolerance. Moreover, sugar maple crown density was found to be higher in pure stands, substantiating the hypothesis suggesting that we should observe higher CPI in pure stands.

Vegetative material arrangement within the competition cone, which directly hinders a TT, is lower in the mixed stands tested here. However following the theory of higher resource acquisition trait complementarity in diversified environments (Hooper et al., 2002; Pretzsch, 2014; Tilman et al., 2001), one would expect a higher total space occupation in mixed stands due to niche partitioning. This is not supported by our results. Furthermore, Seidel et al. (2013) have found comparable results by studying the canopy space occupation in a species richness stand gradient in Europe. Their main conclusions were that the relation between species diversity and canopy space occupation is not evident and that the increase in space occupation is mostly due to the presence of certain species with specific crown traits leading to a better occupation of certain canopy layers. However, in our case we focused on the material around a TT and not on individual competitors per se, whereas in Seidel et al. (2013), they focused on the material in the canopy for a group of trees. In other words, in our study as well as in the study of Seidel et al. (2013), the space occupancy by individual crowns within the canopy was not quantified. Therefore, tree crown volume (defined by its hull) in mixed stands could be larger, with less woody and leafy material within these crowns, similar to what is observed for our sugar maple trees in mixed stands. This could decrease the total vegetative material space occupation but increase the space occupation of the volume occupied by a single tree crown hull. The contrary was

however observed for European beech in Bayer et al. (2013) where the crown density was higher in mixed rather than in pure stands. Finally, in our study, the way we quantified competition for a TT did not take into account all of the vertical canopy structure, but only the part of the canopy interacting directly with the TT crown. In conclusion, our results are difficult to use to study niche partitioning, or at the very least yield indications of the partitioning in the upper part of the canopy.

2.9.2   Tree crown plasticity

<u>Crown metrics variability</u>

Our second hypothesis stating that sugar maple crowns are highly plastic regarding changes in crown metrics between pure and mixed stands is confirmed with our results. Indeed, differences were observed between mixed and pure stands for seven out of the eight crown metrics studied. These results are also compatible with several studies showing the importance of tree crown plasticity in response to neighborhood species (Jucker et al., 2015; Lintunen and Kaitaniemi, 2010; Pretzsch, 2014; Thorpe et al., 2010). For some metrics (e.g., crown volume and crown openness), similar results were observed with TLS data for European beech and Norway spruce (Bayer et al., 2013). They observed larger crown volumes in mixed stands, which may be due to more horizontal branches. Even though individual branch angles were not measured, the larger crown openness of sugar maple trees in mixed conditions suggests similar behavior in the present study.

Bayer et al. (2013) also found that European beech had much more ramified branches in mixed stands, contributing to a denser canopy. In the present study, a lower crown density in mixed stands was observed. Sugar maple tree foliage is mostly found on the outside part of the crown (Horn, 1971). Crown density could thus be high in the periphery, with large gaps in the inner parts of the crown due to lower order branches

that do not support twigs and leaves. Such a situation could lead to a lower total crown density for trees in mixed stands due to their high crown volume.

<u>Horizontal crown growth</u>

Tree crowns are more sinuous in mixed stands with considerable variations observed when compared to pure stands. This supports the results of the study by Brisson (2001) showing the ability of sugar maple to grow horizontally, away from the stem base position, depending on competition pressure.

Several authors have shown that this ability is partly explained by the position of the bigger and closer competitor using competition indices based on individual competitor tree metrics (DBH, height, CPA) (Brisson, 2001; Muth and Bazzaz, 2003; Schröter et al., 2012; D. Seidel et al., 2011-a). Our results showed that competition indices based on the amount and the distribution of the material in the canopy surrounding the TT could also explain this ability.

We studied crown attributes in six zones that face different compass direction and at different height levels (i.e., whole crown, shade crown and light crown). We observed a negative relationship between the percentage of volume occupied and the CPI inside the geographically oriented zones for the shade crown, which confirms the horizontal growth plasticity of sugar maple in response to neighborhood pressure. It is more surprising to observe the inverse relationship for the sun-exposed part. This could be explained by a compensation effect to limit biomechanical risks (e.g., tree buckling, branch breakage). The shaded part of the crown is by definition more exposed to the shade, while the sun-exposed part is less hindered by the surroundings. The asymmetry of the shaded part could generate important biomechanical risks (Young and Hubbell, 1991). Therefore, the lateral growth of the sun exposed part could be oriented towards the opposite direction to readjust the trade-off between light acquisition and biomechanical risks. In addition, the shaded part has been under the effects of competition for much longer than the sun-exposed part. This ability of sugar maple to

grow horizontally away from the most competitive zones and adapt at different crown heights shows the sugar maple's considerable crown plasticity.

Structure/environment feedback loop

The variability we observed for crown structure between stand types is probably a consequence of the compensatory feedback loop "Structure -> Environment -> Growth -> Structure" operating in the forest ecosystem. Species "A" is mixed with others species ("B", "C", "D"…), with each species having their own crown morphological traits. The presence of other species induces a modification in the surrounding structure of "A", when compared to the "A" in pure stand conditions. This modification of the growth environment can trigger crown morphological traits variability of species "A", which go beyond the known range of these traits in pure stands (Bayer et al., 2013; Pretzsch, 2009b). Our result suggests that this mixing effect is beneficial to sugar maple with, for example, higher crown volume, a longer crown or higher crown openness in mixed stands which should optimize light interception. These results supports the idea of potential benefits of mixed stands on canopy space filling by trees for certain species (Pretzsch, 2014).

2.9.3   Intermediate vs mature developmental stage sites

Our third hypothesis stated that sugar maple tree crown plasticity is higher in intermediate aged-stands than in mature ones. Contrary to our expectations, differences in crown metrics between pure and mixed stands were more pronounced in the mature sites. This could be explained by the fact that intermediate developmental stage sites are probably too young to observe substantial differences in environmental structure between these two types of stands. The processes leading to structural heterogeneity in a stand and differentiation between stands include generally gap dynamics (e.g., tree mortality), competitive exclusion or self-thinning. These processes do not dominate

young or intermediate stands whereas they characterize the later stages of stand development (Franklin et al., 2002). High variation of the TLS-based competition indices between mixed and pure stands for trees in mature sites, compared to younger sites, supports this explanation.

2.9.4   Competition indices explain crown variability

Our fourth hypothesis stated that the differences in canopy structure between pure and mixed stands should be accounted for by the proposed competition indices (CPI, CHI and CDI) and that when used, stand type is not needed to quantify crown metric variability. This hypothesis was not completely supported as stand type (i.e., pure or mixed) was retained in the best models for three of the eight metrics. However, stand type, even if it was retained, was not statistically significant. Furthermore, our TLS-based competition indices were sufficient to explain crown metrics variability (five of the eight). We conclude that our competition indices (and particularly CPI and CHI) are good quantifiable descriptors of the structural environment surrounding the TT and can provide a numerical support to explain the variability of crown structure.

2.10   CONCLUSION

We quantified space occupation by trees and tree competition using TLS-data. We showed the high plasticity of sugar maple tree crown structures. The competition indices we developed help to quantify the relationship between tree crowns and their immediate surroundings at different crown levels. Results suggest that our TLS-based competition indices are good proxies to quantify stand structure in forest ecosystems since they are better determinants of tree crown structure than the composition of the stand. In future studies, these indices should be used to predict tree growth as they seem

46

to accurately quantify the shading potential of the surroundings of target trees. Moreover, our TLS-based TT crown metrics could be integrated in light interception models to quantify their importance in terms of light interception, which is a key process in forest ecology and management. Finally, considering the increasing use of TLS and ALS data in forest research and forest management, our competition indices and crown metrics should be a valuable addition to classical dendrometrics obtained in forest inventories. Indeed, those metrics are computationally easy and generalizable to any species and stand once TLS and/or ALS data are acquired.

2.11 ACKNOWLEDGEMENT

2.12 APPENDIX

See table 2.4

2.13 REFERENCES

Alemdag, 1978. Evaluation of some competition indexes for the prediction of

diameter increment in planted white spruce. Inf. Rep. For. Manag. Inst. Can. No FMR-X-108 39.

Bachmann, M., 1998. Indizes zur Erfassung der Konkurrenz von Einzelbaumen.Methodische Untersuchung in Bergmischwaldern, Forslt Forschungsber München. ed. Forslt Forschungsber München.

Barbeito, I., Collet, C., Ningre, F., 2014. Crown responses to neighbor density and species identity in a young mixed deciduous stand. Trees 28, 1751–1765. doi:10.1007/s00468-014-1082-2

Barber, C.B., Habel, K., Grasman, R., Stahel, A., Stahel, A., Sterratt, D.C., 2014. geometry: Mesh generation and surface tesselation.

Barthelemy, D., Caraglio, Y., 2007. Plant architecture: A dynamic, multilevel and comprehensive approach to plant form, structure and ontogeny. Ann. Bot. 99, 375–407. doi:10.1093/aob/mcl260

Bayer, D., Seifert, S., Pretzsch, H., 2013. Structural crown properties of Norway spruce (Picea abies [L.] Karst.) and European beech (Fagus sylvatica [L.]) in mixed versus pure stands revealed by terrestrial laser scanning. Trees 27, 1035–1047. doi:10.1007/s00468-013-0854-4

Béland, M., Widlowski, J.L., Fournier, R.A., Côté, J.F., Verstraete, M.M., 2011. Estimating leaf area distribution in savanna trees from terrestrial LiDAR measurements. Agric. For. Meteorol. 151, 1252–1266.

Biging, G.S., Dobbertin, M., 1995. Evaluation of Competition Indices in Individual Tree Growth Models. For. Sci. 41, 360–377.

Boucher, Y., Arseneault, D., Sirois, L., 2006. Logging-induced change (1930-2002) of a preindustrial landscape at the northern range limit of northern hardwoods, eastern Canada. Can. J. For. Res. 36, 505–517. doi:10.1139/x05-252

Boucher, Y., Arseneault, D., Sirois, L., Blais, L., 2008. Logging pattern and landscape changes over the last century at the boreal and deciduous forest transition in Eastern Canada. Landsc. Ecol. 24, 171–184. doi:10.1007/s10980-008-9294-8

Boulanger, Y., Arseneault, D., 2004. Spruce budworm outbreaks in eastern Quebec over the last 450 years. Can. J. For. Res. 34, 1035–1043. doi:10.1139/x03-269

Brisson, J., 2001. Neighborhood competition and crown asymmetry in Acer saccharum. Can. J. For. Res. 31, 2151–2159.

Brüchert, F., Gardiner, B., 2006. The effect of wind exposure on the tree aerial architecture and biomechanics of Sitka spruce (Picea sitchensis, Pinaceae). Am. J. Bot. 93, 1512–1521. doi:10.3732/ajb.93.10.1512

Canham, C.D., Finzi, A.C., Pacala, S.W., Burbank, D.H., 1994. Causes and consequences of resource heterogeneity in forests: interspecific variation in light transmission by canopy trees. Can. J. For. Res. 24, 337–349.

Canham, C.D., LePage, P.T., Coates, K.D., 2004. A neighborhood analysis of canopy tree competition: effects of shading versus crowding. Can. J. For. Res. 34, 778–787.

Clark, P.J., Evans, F.C., 1954. Distance to Nearest Neighbor as a Measure of Spatial

Relationships in Populations. Ecology 35, 445–453.

Coates, K.D., Canham, C.D., LePage, P.T., 2009. Above-versus below-ground competitive effects and responses of a guild of temperate tree species. J. Ecol. 97, 118–130.

Computree, n.d. Computree [WWW Document]. RD Innov. ONF. URL http://computree.onf.fr

Côté, J.F., Fournier, R.A., Egli, R., 2011. An architectural model of trees to estimate forest structural attributes using terrestrial LiDAR. Environ. Model. Softw. 26, 761–777.

Dassot, M., Colin, A., Santenoise, P., Fournier, M., Constant, T., 2012. Terrestrial laser scanning for measuring the solid wood volume, including branches, of adult standing trees in the forest environment. Comput. Electron. Agric. 89, 86–93. doi:10.1016/j.compag.2012.08.005

Delagrange, S., Messier, C., Lechowicz, M.J., Dizengremel, P., 2004. Physiological, morphological and allocational plasticity in understory deciduous trees: importance of plant size and light availability. Tree Physiol. 24, 775–784. doi:10.1093/treephys/24.7.775

Faro, 2012. Faro Scene 5.0 [WWW Document]. Httpwwwfarocomproductsfaro-Softwaresceneoverview.

Forrester, D.I., Kohnle, U., Albrecht, A.T., Bauhus, J., 2013. Complementarity in mixed-species stands of Abies alba and Picea abies varies with climate, site quality and stand density. For. Ecol. Manag. 304, 233–242. doi:10.1016/j.foreco.2013.04.038

Forrester, D.I., 2014. The spatial and temporal dynamics of species interactions in mixed-species forests: From pattern to process. For. Ecol. Manag. 312, 282–292. doi:10.1016/j.foreco.2013.10.003

Franklin, J.F., Spies, T.A., Pelt, R.V., Carey, A.B., Thornburgh, D.A., Berg, D.R., Lindenmayer, D.B., Harmon, M.E., Keeton, W.S., Shaw, D.C., Bible, K., Chen, J., 2002. Disturbances and structural development of natural forest ecosystems with silvicultural implications, using Douglas-fir forests as an example. For. Ecol. Manag., Forest Ecology in the next Millennium : Putting the long view into Practice 155, 399–423. doi:10.1016/S0378-1127(01)00575-8

Getzin, S., Wiegand, K., 2007. Asymmetric tree growth at the stand level: Random crown patterns and the response to slope. For. Ecol. Manag. 242, 165–174. doi:10.1016/j.foreco.2007.01.009

Grondin, P., Blouin, J., Racine, P., 1998. Rapport de classification écologique: sapinière à bouleau jaune de l'Est (No. RN99-3046.). Direction des inventaires forestiers. Ministère des Ressources naturelles du Québec., Québec Canada.

Hardiman, B.S., Bohrer, G., Gough, C.M., Vogel, C.S., Curtis, P.S., 2011. The role of canopy structural complexity in wood net primary production of a maturing northern deciduous forest. Ecology 92, 1818–1827. doi:10.1890/10-2192.1

Hardiman, B.S., Gough, C.M., Halperin, A., Hofmeister, K.L., Nave, L.E., Bohrer, G., Curtis, P.S., 2013. Maintaining high rates of carbon storage in old forests: A mechanism linking canopy structure to forest function. For. Ecol. Manag. 298, 111–119. doi:10.1016/j.foreco.2013.02.031

Hooper, D.U., Solan, M., Symstad, A., Diaz, S., Gessner, M.O., Buchmann, N., Degrange, V., Grime, P., Hulot, F., Mermillod-Blondin, F., others, 2002. Species diversity, functional diversity and ecosystem functioning. Biodivers. Ecosyst. Funct. Synth. Perspect. 195–208.

Horn, H.S., 1971. The adaptive geometry of trees. Princeton University Press.

Humbert, L., Gagnon, D., Kneeshaw, D., Messier, C., 2007. A shade tolerance index for common understory species of northeastern North America. Ecol. Indic. 7, 195–207. doi:10.1016/j.ecolind.2005.12.002

Jucker, T., Bouriaud, O., Coomes, D.A., 2015. Crown plasticity enables trees to optimize canopy packing in mixed-species forests. Funct. Ecol. 29, 1078–1086.

Lafarge, T., Pateiro-Lopez, B., 2014. alphashape3d: Implementation of the 3D alpha-shape for the reconstruction of 3D sets from a point cloud.

Lecigne, B., Messier, S.D. and C., 2014. VoxR: Metrics extraction of trees from T-LiDAR data.

Le Maire, G., Nouvellon, Y., Christina, M., Ponzoni, F.J., Gonçalves, J.L.M., Bouillet, J.-P., Laclau, J.-P., 2013. Tree and stand light use efficiencies over a full rotation of single- and mixed-species Eucalyptus grandis and Acacia mangium plantations. For. Ecol. Manag. 288, 31–42. doi:10.1016/j.foreco.2012.03.005

Lintunen, A., Kaitaniemi, P., 2010. Responses of crown architecture in Betula pendula to competition are dependent on the species of neighbouring. Trees 24, 411–424. doi:10.1007/s00468-010-0409-x

Marin, C.T., Bouten, W., Sevink, J., 2000. Gross rainfall and its partitioning into throughfall, stemflow and evaporation of intercepted water in four forest ecosystems in western Amazonia. J. Hydrol. 237, 40–57. doi:10.1016/S0022-1694(00)00301-2

Messier, C., Puettmann, K.J., Coates, K.D., 2013. Managing forests as complex adaptive systems: building resilience to the challenge of global change, Routledge. ed. Routledge.

Metz, J., Seidel, D., Schall, P., Scheffer, D., Schulze, E.-D., Ammer, C., 2013. Crown modeling by terrestrial laser scanning as an approach to assess the effect of aboveground intra- and interspecific competition on tree growth. For. Ecol. Manag. 310, 275–288. doi:10.1016/j.foreco.2013.08.014

MFFP, 2007. Normes d'inventaire forestier, placettes- échantillons temporaires. Direction des inventaires forestiers, Forêt Québec. Gouvernement du Québec, Québec, CA.

Morin, X., Fahse, L., Scherer-Lorenzen, M., Bugmann, H., 2011. Tree species richness promotes productivity in temperate forests through strong

complementarity between species: Species richness promotes forest productivity. Ecol. Lett. 14, 1211–1219. doi:10.1111/j.1461-0248.2011.01691.x

Muth, C.C., Bazzaz, F.A., 2002. Tree canopy displacement at forest gap edges. Can. J. For. Res. 32, 247–254. doi:10.1139/x01-196

Muth, C.C., Bazzaz, F.A., 2003. Tree canopy displacement and neighborhood interactions. Can. J. For. Res. 33, 1323–1330.

Oliver, C.D., Larson, B.C., 1990. Forest stand dynamics. McGraw-Hill, Inc.

Othmani, A., Piboule, A., Krebs, M., Stolz, C., Voon, L.F.C.L.Y., 2011. Towards automated and operational forest inventories with T-Lidar. Presented at the 1th International Conference on LiDAR Applications for Assessing Forest Ecosystems (SilviLaser 2011), Hobart, Australia.

Paquette, A., Messier, C., 2011. The effect of biodiversity on tree productivity: from temperate to boreal forests. Glob. Ecol. Biogeogr. 20, 170–180. doi:10.1111/j.1466-8238.2010.00592.x

Parker, G.G., Harmon, M.E., Lefsky, M.A., Chen, J., Van Pelt, R., Weis, S.B., Thomas, S.C., Winner, W.E., Shaw, D.C., Frankling, J.F., 2004. Three-dimensional structure of an old-growth Pseudotsuga-Tsuga canopy and its implications for radiation balance, microclimate, and gas exchange. Ecosystems 7, 440–453.

Pedersen, R.Ø., Bollandsås, O.M., Gobakken, T., Næsset, E., 2012. Deriving individual tree competition indices from airborne laser scanning. For. Ecol. Manag. 280, 150–165. doi:10.1016/j.foreco.2012.05.043

Pretzsch, H., 1995. Zum Einfluß des Baumverteilungsmusters auf den Bestandeszuwachs. Allg. Forst- Jagdztg. 190–201.

Pretzsch, H., 2009. Forest dynamics, growth and yield: from measurement to model. Springer.

Pretzsch, H., 2014. Canopy space filling and tree crown morphology in mixed-species stands compared with monocultures. For. Ecol. Manag. 327, 251–264. doi:10.1016/j.foreco.2014.04.027

Purves, D.W., Lichstein, J.W., Pacala, S.W., 2007. Crown Plasticity and Competition for Canopy Space: A New Spatially Implicit Model Parameterized for 250 North American Tree Species. PLoS ONE 2, e870. doi:10.1371/journal.pone.0000870

R Development Core Team, 2011. R Development Core Team.

Schröter, M., Härdtle, W., Oheimb, G. von, 2012. Crown plasticity and neighborhood interactions of European beech (Fagus sylvatica L.) in an old-growth forest. Eur. J. For. Res. 131, 787–798. doi:10.1007/s10342-011-0552-y

Seidel, D., Leuschner, C., Müller, A., Krause, B., 2011-a. Crown plasticity in mixed forests—Quantifying asymmetry as a measure of competition using terrestrial laser scanning. For. Ecol. Manag. 261, 2123–2132.

Seidel, D., Beyer, F., Hertel, D., Fleck, S., Leuschner, C., 2011-b. 3D-laser scanning: A non-destructive method for studying above- ground biomass and growth of

juvenile trees. Agric. For. Meteorol. 151, 1305–1311. doi:10.1016/j.agrformet.2011.05.013

Seidel, D., Leuschner, C., Scherber, C., Beyer, F., Wommelsdorf, T., Cashman, M.J., Fehrmann, L., 2013. The relationship between tree species richness, canopy space exploration and productivity in a temperate broad-leaf mixed forest. For. Ecol. Manag. 310, 366–374.

Seidel, D., Hoffmann, N., Ehbrecht, M., Juchheim, J., Ammer, C., 2015. How neighborhood affects tree diameter increment – New insights from terrestrial laser scanning and some methodical considerations. For. Ecol. Manag. 336, 119–128. doi:10.1016/j.foreco.2014.10.020

Sultan, S.E., 2000. Phenotypic plasticity for plant development, function and life history. Trends Plant Sci. 5, 537–542.

Thorpe, H.C., Astrup, R., Trowbridge, A., Coates, K.D., 2010. Competition and tree crowns: A neighborhood analysis of three boreal tree species. For. Ecol. Manag. 259, 1586–1596. doi:10.1016/j.foreco.2010.01.035

Tilman, D., Reich, P.B., Knops, J., Wedin, D., Mielke, T., Lehman, C., 2001. Diversity and productivity in a long-term grassland experiment. Science 294, 843–845.

Tome, M., Burkhart, H.E., 1989. Distance-dependent competition measures for predicting growth of individual trees. For. Sci. 35, 816–831.

Toms, J.D., Lesperance, M.L., 2003. Piecewise regression: a tool for identifying ecological thresholds. Ecology 84, 2034–2041. doi:10.1890/02-0472

Valladares, F., Gianoli, E., Gómez, J.M., 2007. Ecological limits to plant phenotypic plasticity. New Phytol. 176, 749–763.

Valladares, F., Niinemets, Ü., 2008. Shade tolerance, a key plant feature of complex nature and consequences. Annu. Rev. Ecol. Evol. Syst. 39, 237.

Young, T.P., Hubbell, S.P., 1991. Crown Asymmetry, Treefalls, and Repeat Disturbance of Broad-Leaved Forest Gaps. Ecology 72, 1464–1471. doi:10.2307/1941119

2.14 TABLES

Table 2-1Stand basal area for each stand of each site (m²/ha)

	Bal. fir	Whi. spr.	Whi. ced.	Yel. bir.	Pap. bir.	Sug. map.	Red map.	Tre. asp.	Fir. che.	Total BA
Site 1										
Pure stand	0	0	0	2	0	19	0	0	1	22
Mixed stand	13	1.5	0	2	0	9.5	0.5	0.5	1.5	28.5
Site 2										
Pure stand	2.5	0.5	0	0	0	14.5	10	0	0	27.5
Mixed stand	22	3	0	1.5	0	5.5	3.5	0.5	0	36
Site 3										
Pure stand	0	0	0	4.5	0	17.5	0.5	1.5	0	24
Mixed stand	11.5	2.5	0	5	0.5	9	0.5	3.5	0	32.5
Site 4										
Pure stand	0.5	1.5	0	6	0.5	21.5	0	0.5	0	30.5
Mixed stand	5.5	7	0	3	4.5	4.5	0	3	0.5	28
Site 5										
Pure stand	0.5	0	0	0	0	26.5	0	0	0	27
Mixed stand	18	2	3.33	2.67	2.67	6	0	0	0	34.67
Site 6										
Pure stand	0	1	0	0	0	28	0	0	0	29
Mixed stand	15.5	8	0	4.5	1	4.5	0	1	0	34.5

Bal. fir: Balsam fir (Abies balsamea (L.) Mill.); Whi. spr.: White spruce (Picea glauca (Moench) Voss); Whi. ced.: White cedar (Thuja occidentalis L.); Yel. bir.: Yellow birch (Betula alleghaniensis Britton); Pap. bir.: Paper birch (Betula papyrifera Marshall); Sug. map.: Sugar maple (Acer saccharum Marshall); Red map.: Red maple (Acer rubrum L.); Tre. asp: Trembling aspen (Populus tremuloides Michx.); Fir. che.: Fire cherry (Prunus pensylvanica L. f.); Total BA: Total basal area

Table 2-2: Tree characteristics by site. Mean (Standard deviation)

	Early stage site						Mature stage site					
	Site 1		Site 2		Site 3		Site 4		Site 5		Site 6	
	Pure	**Mixed**	**Pure**	**Mixed**	**Pure**	**Mixed**	**Pure**	**Mixed**	**Pure**	**Mixed**	**Pure**	**Mixed**
General metrics												
n	6	6	6	6	6	6	6	6	6	6	6	6
Height (m)	16.1 (1)	13.8 (0.6)	15.8 (1.1)	15.1 (1.4)	15.9 (1.1)	15.2 (1.6)	18.2 (0.6)	18.3 (1.2)	20.4 (1.1)	17.6 (0.9)	21.5 (0.7)	17.8 (1.3)
DBH (mm)	146 (12)	123.8 (31.2)	134 (19.5)	163.5 (22.9)	144 (26.7)	145.2 (29.3)	178.9 (33.9)	264.3 (54)	259 (45.3)	249.3 (58.7)	266.7 (68.4)	241.4 (49)
Age	32.5 (5)	30.3 (10)	30.2 (1)	29.2 (5)	28.8 (5)	35.2 (10)	45 (10)	50.3 (4)	66.8 (8)	61.2 (10)	66.8 (7)	56.3 (10)
Competitive environment metrics												
CPI	1.4 (0.4)	1.3 (0.2)	1.5 (0.4)	1.2 (0.3)	1.7 (0.4)	1.5 (0.2)	1.3 (0.2)	0.9 (0.2)	0.9 (0.2)	0.8 (0.1)	0.8 (0.3)	0.8 (0.1)
CHI	1.6 (0.1)	1.6 (0.2)	1.5 (0.1)	1.6 (0.1)	1.7 (0.1)	1.6 (0.1)	1.6 (0.1)	1.6 (0.2)	1.5 (0.2)	1.4 (0.2)	1.5 (0.1)	1.3 (0.2)
CDI	0.06 (0.03)	0.07 (0.03)	0.06 (0.02)	0.05 (0.02)	0.07 (0.02)	0.07 (0.02)	0.06 (0.03)	0.05 (0.03)	0.04 (0.02)	0.03 (0.01)	0.03 (0.01)	0.02 (0.01)
Crown structure metrics												
Crown volume (m³)	43.3 (14.9)	31.3 (6.5)	42.1 (18.2)	61.5 (27.6)	32.8 (18.3)	47.8 (6.6)	32.6 (17.1)	99 (38)	59.5 (25.7)	91.6 (36)	82.3 (48)	121.8 (19.2)
Crown length:Crown width	2.4 (0.6)	2.5 (0.6)	2.6 (1)	2.7 (0.8)	3.3 (0.7)	2.6 (0.7)	2.9 (0.5)	2.4 (0.5)	2.7 (0.8)	2.2 (0.5)	2.8 (1.1)	2 (0.4)
Crown length:Tree height	0.6 (0.1)	0.6 (0.1)	0.6 (0.2)	0.8 (0.1)	0.7 (0.1)	0.7 (0.1)	0.5 (0.1)	0.8 (0)	0.6 (0.1)	0.7 (0.1)	0.6 (0.1)	0.7 (0.1)
Crown openness (°)	18.1 (5)	17.4 (9.9)	17 (4.5)	18.3 (6.5)	13.7 (4)	17.8 (9.2)	16.4 (4.6)	20.2 (6.4)	17.6 (5.6)	30.4 (21)	20.9 (8.2)	29.4 (10.7)
Crown roughness	0.6 (0.1)	0.6 (0.1)	0.6 (0.2)	0.5 (0)	0.6 (0.1)	0.6 (0.1)	0.6 (0.1)	0.5 (0.1)	0.5 (0.2)	0.5 (0.1)	0.4 (0.1)	0.4 (0.1)
Shade crown length:Crown length	0.7 (0.1)	0.7 (0.2)	0.7 (0.2)	0.6 (0.1)	0.7 (0.2)	0.7 (0.2)	0.7 (0.2)	0.5 (0.3)	0.7 (0.2)	0.5 (0.2)	0.6 (0.3)	0.5 (0.2)
Sinuosity	4.7 (1.4)	5.8 (1.1)	5.6 (1.2)	5.7 (1.3)	4.1 (0.91)	5.8 (2.1)	3.9 (0.67)	10.1 (5.2)	7 (1.7)	9.2 (1.7)	8.2 (2.1)	9.3 (2)
Crown density	0.3 (0.034)	0.3 (0.045)	0.3 (0.046)	0.2 (0.025)	0.3 (0.049)	0.3 (0.033)	0.3 (0.037)	0.2 (0.026)	0.2 (0.026)	0.2 (0.0093)	0.2 (0.019)	0.2 (0.018)

Table 2-3 Estimates and standard error[1] for the variables of the best models (with lower AIC) for each crown metric. Developmental stage (DS) is considered in all models. When stand type was considered in a model its interaction with developmental stage was systematically considered. − means that the environment variable was not retained in the best model.

	CPI	CHI	CDI	ST	DS	ST:DS
	Est (Std.Er)	Est (Std.Er)	Est (Std.Er)	Est (Std.Er)	Est (Std.Er)	Est (Std.Er)
Crown volume (m³)	-60 (9.1)***	–	–	-6 (7.2)	-12 (10)	40 (9.7)***
Crown length:Crown width	0.19 (0.07)**	0.69 (0.14)***	–	–	0.14 (0.053)*	–
Crown length:Tree height	-0.12 (0.044)**	0.33 (0.087)***	–	0.052 (0.035)	-0.095 (0.04)*	0.11 (0.048)*
Crown openness (°)	–	-1.5 (0.25)***	–	–	0.03 (0.084)	–
Crown roughness	0.11 (0.045)*	–	–	–	-0.056 (0.035)	–
Shade crown length:Crown length	–	0.43 (0.15)**	–	–	-0.033 (0.05)	–
Sinuosity	-0.56 (0.11)***	–	-3.3 (1.4)*	0.055 (0.085)	-0.1 (0.096)	0.21 (0.12)
Crown density	0.08 (0.012)***	–	-0.29 (0.16)	–	-0.017 (0.009)	–

[1]P<0.05*; <0.01**; <0.001***

Table 2-4: Model comparison details for each crown metric.

ΔAIC gives the difference between the AIC value of the model and the lowest AIC value among the 15 models

Formula's models[1]	CPI	CHI	CDI	Stand type	AIC	ΔAIC
Crown volume						
CPI + Stand type	-60 (9.1)***	–	–	-6 (7.2)	658.92	0
CPI + CHI + Stand type	-58 (9.3)***	-12 (18)	–	-5.7 (7.2)	660.47	1.55
CPI + CDI + Stand type	-61 (9.7)***	–	50 (120)	-6.2 (7.2)	660.76	1.83
CPI + CHI + CDI + Stand type	-61 (9.6)***	-30 (24)	180 (160)	-6.4 (7.1)	661.2	2.28
CPI + CHI	-64 (10)***	-33 (20)	–	–	674.61	15.69
CPI	-68 (9.7)***	–	–	–	675.22	16.3
CPI + CHI + CDI	-66 (10)***	-53 (27)	190 (180)	–	675.49	16.57
CPI + CDI	-67 (10)***	–	-43 (140)	–	677.13	18.2
CHI + Stand type	–	-38 (22)	–	7.3 (8.6)	689.64	30.72
CDI + Stand type	–	–	-210 (140)	7.4 (8.6)	690.28	31.36
CHI + CDI + Stand type	–	-29 (30)	-94 (190)	7.3 (8.6)	691.41	32.49
Stand type	–	–	–	27 (6.5)***	697.58	38.66
CHI	–	-74 (24)**	–	–	704.38	45.45
CHI + CDI	–	-60 (35)	-120 (220)	–	706.07	47.14
CDI	–	–	-400 (160)*	–	707.04	48.12
Crown length:Crown width						
CPI + CHI	0.19 (0.07)**	0.69 (0.14)***	–	–	-38.14	0
CPI + CHI + CDI	0.19 (0.073)*	0.71 (0.2)***	-0.19 (1.3)	–	-36.17	1.98
CPI + CHI + Stand type	0.17 (0.074)*	0.66 (0.15)***	–	0.0044 (0.059)	-35.51	2.63
CPI + CHI + CDI + Stand type	0.18 (0.077)*	0.67 (0.2)**	-0.13 (1.3)	0.0049 (0.059)	-33.52	4.62
CHI	–	0.81 (0.14)***	–	–	-33.41	4.73

	CPI	CHI	CDI	Stand type		
CHI + Stand type	–	0.75 (0.15)***	–	-0.034 (0.059)	-32.16	5.98
CHI + CDI	–	0.73 (0.21)***	0.71 (1.3)	–	-31.7	6.45
CHI + CDI + Stand type	–	0.67 (0.21)**	0.72 (1.3)	-0.035 (0.058)	-30.47	7.68
CPI + CDI	0.2 (0.079)*	–	3.1 (1)**	–	-26.12	12.03
CPI + CDI + Stand type	0.17 (0.083)*	–	2.9 (1)**	0.0025 (0.063)	-24.98	13.17
CDI + Stand type	–	–	3.7 (0.99)***	-0.037 (0.063)	-22.65	15.49
CDI	–	–	4.1 (1)***	–	-22.09	16.06
CPI	0.29 (0.077)***	–	–	–	-19.86	18.29
CPI + Stand type	0.26 (0.081)**	–	–	0.021 (0.066)	-19.56	18.58
Stand type	–	–	–	-0.11 (0.049)*	-11.53	26.61
Crown length:Tree height						
CPI + CHI + Stand type	-0.12 (0.044)**	0.33 (0.087)***	–	0.052 (0.035)	-110.39	0
CPI + CHI + CDI + Stand type	-0.13 (0.046)**	0.27 (0.12)*	0.6 (0.77)	0.049 (0.035)	-108.99	1.41
CPI + CDI + Stand type	-0.13 (0.047)**	–	1.8 (0.59)**	0.049 (0.036)	-105.92	4.47
CHI + Stand type	–	0.27 (0.088)**	–	0.078 (0.035)*	-105.4	4.99
CHI + CDI + Stand type	–	0.27 (0.12)*	-0.026 (0.79)	0.078 (0.035)*	-103.4	6.99
CDI + Stand type	–	–	1.2 (0.57)*	0.078 (0.036)*	-100.85	9.54
CPI + Stand type	-0.075 (0.046)	–	–	0.06 (0.038)	-99.38	11.02
Stand type	–	–	–	0.11 (0.027)***	-99	11.39
CPI + CHI	-0.17 (0.048)***	0.25 (0.097)*	–	–	-94.98	15.41
CPI + CDI	-0.18 (0.049)***	–	1.6 (0.65)*	–	-94.32	16.07
CPI + CHI + CDI	-0.18 (0.049)***	0.17 (0.13)	0.85 (0.88)	–	-93.89	16.5
CPI	-0.13 (0.047)**	–	–	–	-90.43	19.96
CHI	–	0.15 (0.1)	–	–	-85.16	25.23
CDI	–	–	0.67 (0.65)	–	-84.1	26.3

CHI + CDI	−	0.15 (0.14)	-0.027 (0.93)	−	-83.16	27.23
Crown openness						
CHI	−	-1.5 (0.25)***	−	−	49.83	0
CPI + CHI	-0.13 (0.13)	-1.4 (0.27)***	−	−	50.9	1.07
CHI + Stand type	−	-1.4 (0.26)***	−	0.046 (0.1)	50.94	1.11
CHI + CDI	−	-1.3 (0.37)***	-1.5 (2.4)	−	51.41	1.59
CHI + CDI + Stand type	−	-1.2 (0.37)**	-1.5 (2.3)	0.046 (0.1)	52.5	2.67
CPI + CHI + Stand type	-0.082 (0.14)	-1.3 (0.27)***	−	0.028 (0.11)	52.58	2.75
CPI + CHI + CDI	-0.11 (0.14)	-1.3 (0.37)***	-1 (2.4)	−	52.73	2.91
CPI + CHI + CDI + Stand type	-0.061 (0.14)	-1.2 (0.37)**	-1.2 (2.4)	0.033 (0.11)	54.31	4.49
CDI + Stand type	−	−	-6.9 (1.8)***	0.05 (0.11)	60.34	10.51
CDI	−	−	-7.6 (1.8)***	−	61.12	11.3
CPI + CDI + Stand type	-0.059 (0.15)	−	-6.6 (1.9)***	0.037 (0.12)	62.19	12.36
CPI + CDI	-0.13 (0.15)	−	-7 (1.9)***	−	62.37	12.54
CPI + Stand type	-0.26 (0.15)	−	−	-0.0064 (0.12)	71.42	21.59
CPI	-0.34 (0.15)*	−	−	−	72.34	22.52
Stand type	−	−	−	0.19 (0.088)*	72.87	23.05
Crown roughness						
CPI	0.11 (0.045)*	−	−	−	-97.92	0
CPI + CDI	0.093 (0.049)	−	0.64 (0.64)	−	-96.92	1
CPI + CHI	0.1 (0.047)*	0.05 (0.096)	−	−	-96.19	1.73
CPI + Stand type	0.093 (0.048)	−	−	-0.014 (0.039)	-95.58	2.34
Stand type	−	−	−	-0.052 (0.027)	-95.46	2.46
CDI	−	−	1.1 (0.6)	−	-95.37	2.55
CPI + CHI + CDI	0.093 (0.049)	-0.029 (0.13)	0.77 (0.88)	−	-94.97	2.95
CPI + CDI + Stand type	0.075 (0.051)	−	0.59 (0.64)	-0.018 (0.039)	-94.44	3.48
CDI + Stand type	−	−	0.95 (0.6)	-0.035 (0.038)	-94.3	3.62
CPI + CHI + Stand type	0.09 (0.049)	0.029 (0.097)	−	-0.015 (0.039)	-93.67	4.25

	CPI	CHI	CDI	Stand type		
CHI	−	0.12 (0.094)	−	−	-93.44	4.48
CHI + CDI	−	-0.021 (0.13)	1.2 (0.87)	−	-93.39	4.53
CPI + CHI + CDI + Stand type	0.075 (0.051)	-0.06 (0.13)	0.86 (0.87)	-0.018 (0.039)	-92.64	5.28
CHI + CDI + Stand type	−	-0.061 (0.13)	1.2 (0.85)	-0.035 (0.038)	-92.5	5.42
CHI + Stand type	−	0.076 (0.096)	−	-0.035 (0.039)	-92.45	5.47
Shade crown length:Crown length						
CHI	−	0.43 (0.15)**	−	−	-24.17	0
CHI + Stand type	−	0.36 (0.15)*	−	-0.052 (0.062)	-23.37	0.8
CPI + CHI	0.017 (0.079)	0.42 (0.16)*	−	−	-22.22	1.96
CHI + CDI	−	0.42 (0.22)	0.094 (1.4)	−	-22.18	2
CPI + CHI + Stand type	-0.026 (0.081)	0.37 (0.16)*	−	-0.057 (0.065)	-21.47	2.71
CHI + CDI + Stand type	−	0.35 (0.22)	0.1 (1.4)	-0.052 (0.062)	-21.37	2.8
Stand type	−	−	−	-0.099 (0.046)*	-21.23	2.94
CDI + Stand type	−	−	1.7 (1)	-0.053 (0.063)	-20.93	3.25
CDI	−	−	2 (1)*	−	-20.7	3.48
CPI + CHI + CDI	0.016 (0.082)	0.41 (0.22)	0.015 (1.5)	−	-20.22	3.96
CPI + CHI + CDI + Stand type	-0.03 (0.085)	0.35 (0.22)	0.25 (1.4)	-0.058 (0.065)	-19.5	4.68
CPI + CDI + Stand type	-0.03 (0.086)	−	1.8 (1.1)	-0.06 (0.066)	-19.05	5.12
CPI + CDI	0.022 (0.084)	−	1.9 (1.1)	−	-18.76	5.41
CPI + Stand type	0.025 (0.081)	−	−	-0.048 (0.067)	-18.31	5.86
CPI	0.08 (0.078)	−	−	−	-17.77	6.4
Sinuosity						
CPI + CDI + Stand type	-0.56 (0.11)***	−	-3.3 (1.4)*	0.055 (0.085)	16.7	0
CPI + CHI + CDI + Stand type	-0.56 (0.11)***	0.041 (0.29)	-3.5 (1.9)	0.055 (0.085)	18.68	1.98
CPI + CHI + Stand type	-0.62 (0.11)***	-0.32 (0.21)	−	0.042 (0.086)	20.01	3.3
CPI + Stand type	-0.66 (0.11)***	−	−	0.034 (0.088)	20.19	3.48
CPI + CDI	-0.65 (0.11)***	−	-3.7 (1.5)*	−	22.31	5.61
CPI + CHI + CDI	-0.64 (0.11)***	-0.13 (0.3)	-3.1 (2)	−	24.13	7.42
CPI + CHI	-0.69 (0.11)***	-0.44 (0.22)*	−	−	24.45	7.74
CPI	-0.76 (0.11)***	−	−	−	26.37	9.67
CDI + Stand type	−	−	-6 (1.5)***	0.18 (0.095)	36.81	20.11
CHI + CDI + Stand type	−	0.048 (0.33)	-6.2 (2.1)**	0.18 (0.094)	38.79	22.09

	CPI	CHI	CDI	Stand type		
CHI + Stand type	−	-0.63 (0.25)*	−	0.18 (0.1)	44.89	28.19
CDI	−	−	-7 (1.6)***	−	48	31.3
Stand type	−	−	−	0.3 (0.073)***	48.53	31.82
CHI + CDI	−	-0.19 (0.36)	-6.2 (2.3)*	−	49.73	33.03
CHI	−	-0.88 (0.26)**	−	−	54.32	37.62
Crown density ~						
CPI + CDI	0.08 (0.012)***	−	-0.29 (0.16)	−	-298.05	0
CPI + CHI	0.077 (0.012)***	-0.04 (0.024)	−	−	-297.65	0.4
CPI	0.071 (0.011)***	−	−	−	-296.82	1.23
CPI + CHI + CDI	0.08 (0.012)***	-0.02 (0.032)	-0.19 (0.22)	−	-296.44	1.61
CPI + CHI + Stand type	0.072 (0.012)***	-0.042 (0.024)	−	-0.011 (0.0097)	-295.6	2.45
CPI + CDI + Stand type	0.075 (0.013)***	−	-0.28 (0.16)	-0.011 (0.0097)	-295.58	2.47
CPI + Stand type	0.066 (0.012)***	−	−	-0.012 (0.0098)	-294.54	3.51
CPI + CHI + CDI + Stand type	0.075 (0.013)***	-0.025 (0.033)	-0.16 (0.22)	-0.011 (0.0097)	-294.18	3.87
Stand type	−	−	−	-0.023 (0.008)**	-272.7	25.35
CDI + Stand type	−	−	0.076 (0.18)	-0.027 (0.011)*	-269.19	28.86
CHI + Stand type	−	-0.0046 (0.028)	−	-0.027 (0.011)*	-269.04	29.01
CHI + CDI + Stand type	−	-0.026 (0.04)	0.19 (0.25)	-0.027 (0.011)*	-267.63	30.42
CDI	−	−	0.13 (0.18)	−	-265.49	32.56
CHI	−	0.0084 (0.029)	−	−	-265.08	32.97
CHI + CDI	−	-0.013 (0.041)	0.19 (0.27)	−	-263.59	34.46

[1]The site random effect and the TT developmental stage fixed effect were not include in formulas as they were present in all models

$P < 0.05$*; < 0.01**; < 0.001***
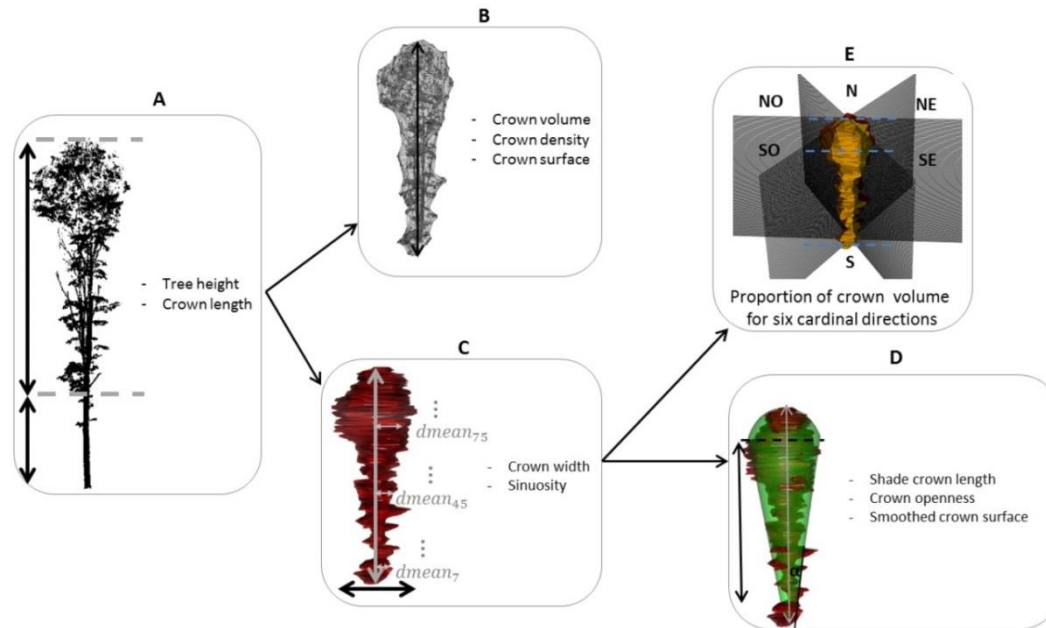
Figure 2-1: Steps to obtain crown metrics . A. Three dimensional point cloud of a TT-PC. Grey dashed line shows the vertical boundary of the crown. B. Alpha-shape 3D adjusted on the Cr-PC. Black arrow shows the axis of symmetry. C. Convex-hulls polygons adjusted on 10-cm vertical slices on the Cr-PC. Vertical grey arrows show the axis of symmetry of the crown, horizontal grey arrows are examples of d_{mean} at three heights (70 cm, 450 cm, 750 cm) D. Theoretical "smoothed" crown in green fitted from the segmented regression on all d_{mean}. E. Crown divided into 6 oriented zones; the proportion of volume in each zone is calculated for the shaded and sun-exposed parts. Blue dashed lines show limits of different crown parts
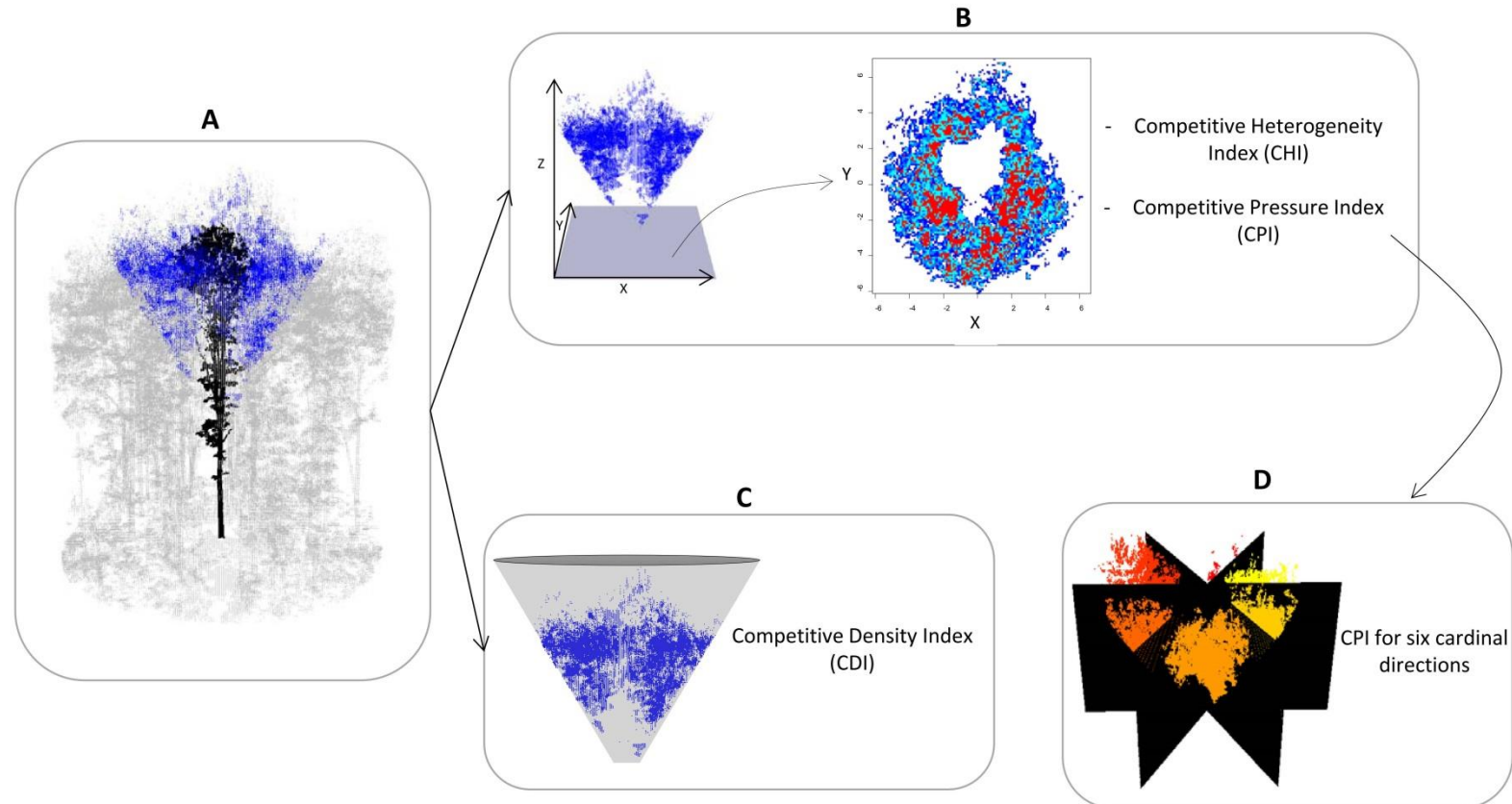
Figure 2-2: Steps to obtain competition indices. A. Three dimensional point cloud of the whole scene with the TT-PC in black. Radius of eight meters around the target tree in grey, and the CC-PC in blue. B. Projection of the CC-PC on the XY plane resulting in a raster used to compute CPI and CHI. Dark-blue and red cells correspond to low and high values of cumulated voxels in Z, respectively. C. Upside down truncated cone volume containing the CC-PC used to compute CDI. D. CPI computed by oriented zone and scaled by tree.
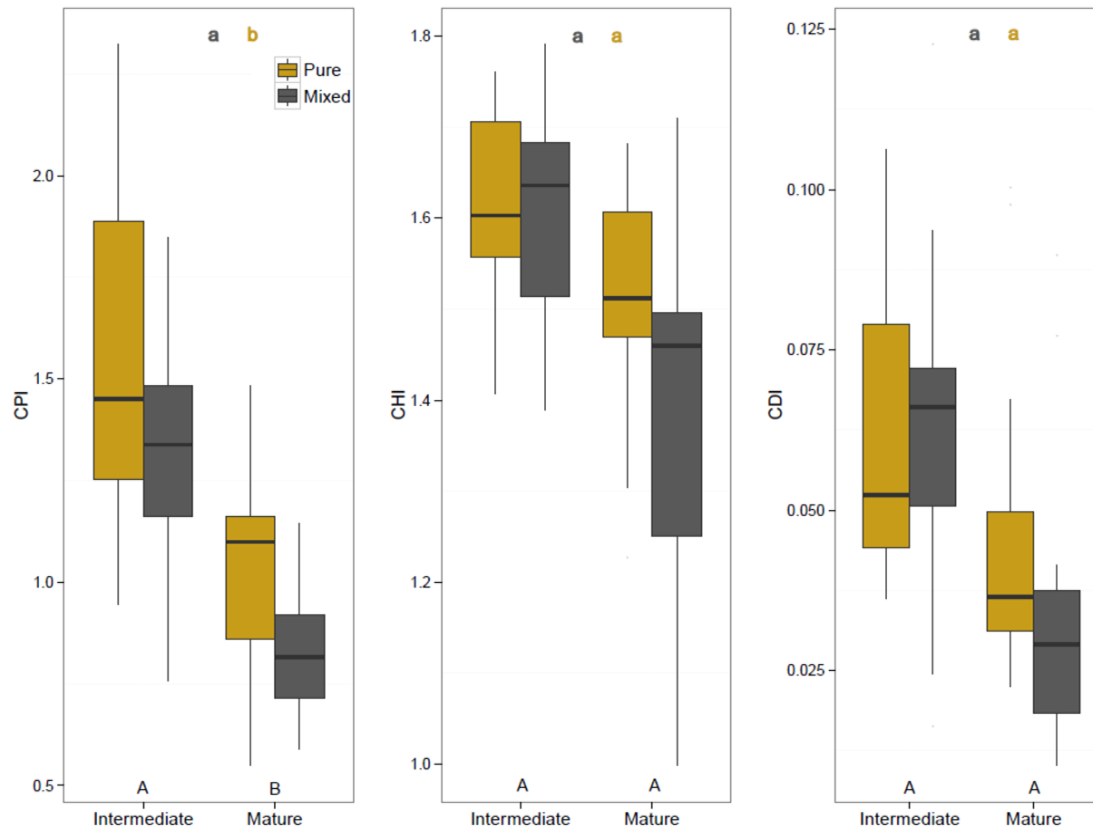
Figure 2-3 Differences in the competitive environment (CPI), heterogeneity (CHI) and density (CDI) indices with stand type and developmental stage. Developmental stage statistical differences are given by different capital letters at the bottom of the graphs. Stand type statistical differences are given by different small colored letters at the top of the figures (pure stand in orange and mixed stand in black). Interaction (stand type X developmental stage) was statistically non-significant.
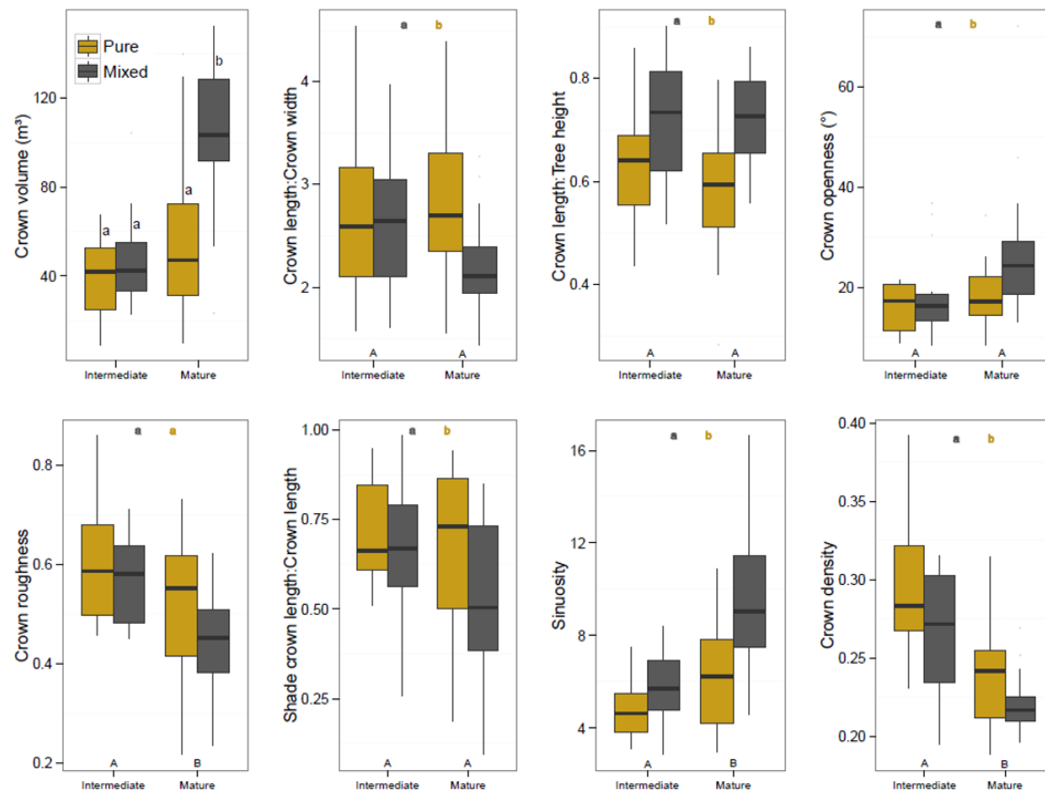
Figure 2-4: Variations in crown metrics with developmental stage and stand type Developmental stage statistical differences are given by different capital letters at the bottom of the graphs. Stand type statistical differences are given by different small colored letters at the top of the graphs (pure stand in orange and mixed stand in black). Statistical differences are given directly above the boxplots for the crown volume metric as the interaction effect between developmental stage and stand type was found to be statistically significant (Tukey HSD test).
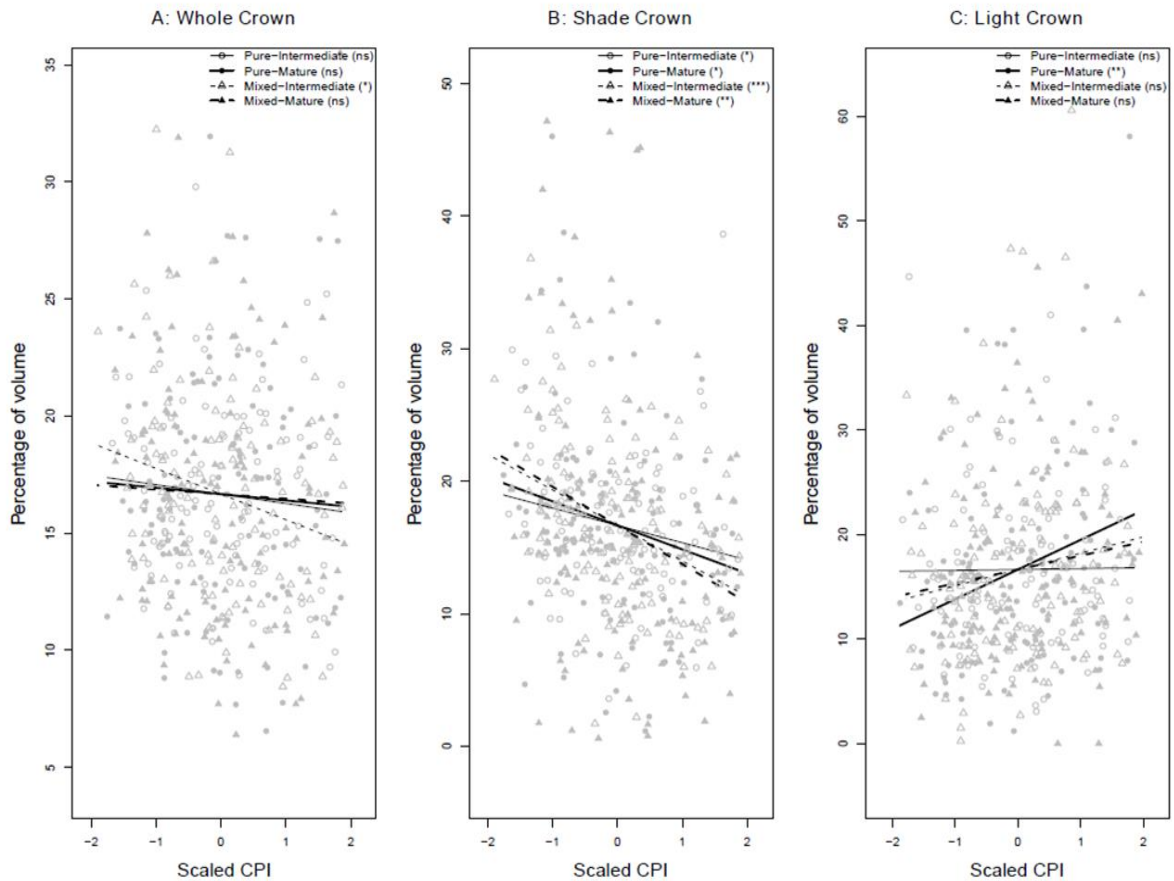
Figure 2-5 Percentage of volume as a function of CPI at the crown zone scale. Relationships are given for different crown parts: A, the whole crown; B, the shade crown and; C, the light crown. Grey empty circles, grey full circles, grey empty triangles and grey full triangles are respectively zones for intermediate and mature stage trees in pure stands, and intermediate and mature stage trees in mixed stands. Plain black line, plain bold black line, dashed black line and dashed bold black line represent respectively linear regressions for zones of intermediate and mature stage trees in pure stands, and intermediate and mature stage trees in mixed stands. The statistical tests on the slope are given in the legend (P <0.05*; <0.01**; <0.001***).

◼CHAPITRE III : ETUDE DE LA DISTRIBUTION VERTICALE DE LA MATIERE DANS LE HOUPPIER A PARTIR DE DONNEES DE LIDAR-T

3.1 RESUME

Ce deuxième article, intitulé « *Studying crown vertical distribution with terrestrial laser scanner* », fut rédigé par moi-même ainsi que par les professeurs Robert Schneider et Richard Fournier. Cet article a été préparé pour une soumission prochaine dans la revue « *Forests* ».

En aménagement et en écologie forestière, il est très important d'être capable de quantifier la distribution du matériel dans le houppier des arbres. Dans ce deuxième chapitre, nous avons développé une approche pour quantifier des profils de distribution totale, de feuillage et de bois à l'échelle du houppier à partir de données de LiDAR-t. Ces profils ont été séparés entre bois et feuilles grâce à une approche géométrique. Les distributions Beta des profils ont ensuite été comparées entre les deux espèces (l'érable à sucre et le sapin baumier) et deux stades de développement (intermédiaire et mature). Nous avons également testé le potentiel de métriques de houppier simples comme indicateur de la forme des distributions. Les résultats montrent que les profils de distribution totale et de feuille étaient similaires alors que les profils de bois étaient différents. L'érable à sucre a une distribution concentrée dans la partie supérieure du houppier alors que pour le sapin baumier, la matière est concentrée dans la partie inférieure. Ces différences s'expliquent par le développement architectural contrasté de ces deux espèces. En réponse au type de peuplement, l'érable présente une distribution de la matière plus basse dans le houppier en peuplement mixte qu'en

66

peuplement pur. Le comportement inverse est observé pour le sapin baumier. Ces résultats suggèrent que l'érable à sucre a une distribution du feuillage plus efficace en terme d'interception de la lumière en peuplement mixte qu'en peuplement pur. Ce n'est cependant pas le cas pour le sapin. Parmi les cinq métriques de houppier quantifiées, la proportion et la densité du houppier semblent les plus prometteuses pour prédire la forme de la distribution verticale de la matière. Finalement les avantages et limites de la méthode mise en place sont discutés.

3.2 STUDYING CROWN VERTICAL DISTRIBUTIONS WITH TERRESTRIAL LASER SCANNERS

3.3 ABSTRACT

Quantifying the vertical distribution of material inside the tree crown has great implications in forest ecology and management. In the present study we have developed an approach to quantify vertical profiles of the total, woody and leafy material at the crown scale using a geometrical approach with terrestrial laser scanning (TLS) data. Using data from two species (sugar maple and balsam fir) and two types of stands (pure and mixed), Beta distributions were compared between two species (sugar maple and balsam fir) and between two types of stands (pure and mixed). Moreover, the potential of simple crown metrics to explain the vertical distributions was explored. Results show that total and leafy profiles are similar while woody profiles are different. Sugar maple (*Acer saccharum* Marsh.) and balsam fir (*Abies balsamea* Mill.) have respectively a top heavy and a bottom heavy distributions. These differences are explained in terms of architectural development constraints. Moreover, sugar maple shows that the foliage distribution is lower in mixed stands than in pure ones. The opposite behaviour is observed for balsam fir. These results suggest that

sugar has a more efficient crown foliage distribution in term of light interception in mixed than in pure stands. This is, however, not the case for balsam firs. Among the five crown metrics quantified, crown proportion and crown density are the most promising to explain vertical distribution variability. Finally, advantages and limitations of the developed method were discussed.

3.4   KEY WORDS

Vertical profile; beta distribution; Lvox; wood leaf separation; coniferous; broadleaved; tree architecture

3.5   INTRODUCTION

The importance of the vertical distribution of foliage on light interception at the tree crown scale has largely been highlighted (Niinemets 2007, 2010) and the subsequent linear relationship with individual tree growth is now generally accepted (Monteith 1972; Medlyn 1998; Binkley et al. 2013). This relationship is used in several process based models to understand and predict tree and stand growth and is largely used in forest management growth and yield models (Wang and Jarvis 1990; Landsberg and Waring 1997; Coates et al. 2003).

The vertical distribution of material inside the crown is influenced by the surrounding environment and especially the level of competition. Several studies on coniferous species have shown that suppressed trees or trees growing in dense stands usually have a concentration of foliage higher in the crown than dominant trees or trees growing in low density stands (Maguire and Bennett 1996; Gilmore and Seymour 1997; Garber

and Maguire 2005; Weiskittel et al. 2009). Inter-species variations have also been highlighted, such as the changes in the foliage distribution with species shade tolerance (Horn 1971; Garber and Maguire 2005). Few studies have however reported results for the material distribution of broadleaved species (Nelson et al. 2014; Guisasola et al. 2015). Most of these studies are conducted in managed and monospecific stands. In order to better understand mechanisms driving the vertical arrangement of material in forest ecosystems, studies on more complex stands and on broadleaved species are needed.

Some emphasis has been recently placed on mixed forests (Messier et al. 2013; Pretzsch and Rais 2016), as their productivity can, under certain circumstances, be greater than monospecific forests. Crown space occupation in mixed versus pure stands through simple crown metric has recently been compared (Seidel et al. 2013; Bayer et al. 2013; Pretzsch 2014; Forrester et al. 2016; Martin-Ducup et al. 2016). Few studies have however studied the vertical distribution material in the crown between trees growing in pure versus mixed stands. Moreover, most studies on vertical distributions face important limiting factors: the methods used to obtain the distributions are both labor intensive and destructive.

Light Detection And Ranging (LiDAR) technology has been increasingly used to quantify the amount of plant material (leaf and wood separated or not) and its 3D distribution at the stand and tree scale (Hosoi and Omasa 2006; Coops et al. 2007; Béland et al. 2014). However many limitations come with the use of LiDAR data. There are three types of returns a LiDAR sensor can record (i.e., single or multiple returns, full waveform), and the algorithms must be developed accordingly. Other limitations of the LiDAR data are signal occlusion and the presence of noise returns which both affect the ability to detect the exact distribution of canopy components.

Among the different challenges for processing LiDAR data, two seem to be particularly important for quantifying the vertical density profiles. The first one is to separate wood

from leaf returns where different methods have been explored. A simple and intuitive method is to scan leaf-on and leaf-off trees to obtain the leaf returns by subtracting the two point clouds (Hosoi and Omasa 2006; Li et al. 2016). This approach needs bi-temporal scans and it is obviously impossible on evergreen species. Another approach is to use an intensity return threshold but the wave length of the impulsion needed for such an approach must have a minimum of 1535 nm and is not available for all types of scanners (Béland et al. 2011; Douglas et al. 2015). Dual wave-length devices seems also to offer promising solutions but are not well developed (Li et al. 2013; Danson et al. 2014). Oshio et al. (2015) separated manually woody and leafy returns in airborne laser scanner point clouds. The manual method is however too time consuming and subjective to be applicable over large areas or complex datasets. The methods that can be the most generalizable seem to be the geometrical based approaches, which rely solely on the xyz coordinates of the point cloud. It is thus not limited by sensor quality (wavelength or multispectral). Different approaches have been explored and tested in the last few years using geometrical feature extraction and machine learning (Belton et al. 2013; Wahabzada et al. 2015; Hétroy-Wheeler et al. 2016; Ma et al. 2016). Tao et al. (2015) have shown that circle and line fitting on 2D projections of the 3D point cloud allowed a better wood/leaf separation than approaches based on intensity returns.

A second important limitation of LiDAR data is occlusion, which appears when part of the scene is hidden by objects between the scanner and the area of interest in the point cloud. This limitation depends on vegetation density, scanner resolution, and in the case of TLS, on the number of scans used from different positions in a plot (Ashcroft et al. 2014). With TLS data, occlusions are particularly pronounced in the upper part of the canopy because the scans are taken from the ground. As for Airborne Laser Scanners (ALS), occlusions are more pronounced in the lower part of the canopy. Several studies have tried to address the problem of occlusion by using voxels (e.g.

volumetric pixels) (Seidel et al. 2011; Fournier et al. 2015; Kükenbrink et al. 2016; Martin-Ducup et al. 2016).

The first main objective of our study was to propose a method to estimate the vertical distribution of a trees' material using TLS data. More specifically, this first general objective will be reached through two sub-objectives: (1) propose a method to separate woody and leafy material and (2) deal with the limitations of signal occlusion. The second objective was to analyse the variability of the three types of material distributions (total, leaves, wood) between a coniferous (Balsam fir) and a broadleaved (Sugar maple) species in pure and mixed stands at two developmental stages. We make the assumptions that (i) the Balsam fir distribution will be bottom heavy when compared to Sugar maple, (ii) the vertical distributions of trees in pure stands will be top heavy compared to trees in mixed stand and (iii) the distributions of mature trees will be top heavy for sugar maple and bottom heavy for balsam fir when compared to younger trees since their architectural topology differ. Finally we tested the hypothesis that simple crown attributes explain the differences in vertical distributions between species, stand type and developmental stage.

3.6   MATERIAL AND METHODS

3.6.1   Sites and tree sampling

A total of 36 Balsam fir (*Abies Balsamea* Mill.) and 36 Sugar maple (*Acer saccharum* Marsh.) target trees were sampled among six sites located in eastern Quebec, Canada (i.e., six target trees per species per site), as described in Martin-Ducup et al. (2017). The provincial eco-forest maps developed by the Quebec Ministry of Forests, Wildlife and Parks (MFFP 2007) were used to select the sites based on homogenous edaphic

and slope characteristics. Each site was composed of three stand types: a pure Balsam fir stand, a pure Sugar maple stand, and a mixed stand where both species were found. Sites differed from each other by the developmental stage of the co-dominant trees and can be divided into two groups: intermediate and mature stage sites. Tree characteristics by site and by species are given in Table 3.1. Basal areas were estimated using four wedge prism plots per stand type. Mean basal area for by species for each condition and developmental stage are given in Table 3.2.

Target trees (TT) were scanned with a TLS, the Faro Focus 3D, during the summer of 2013 at four opposite viewpoints after the closest neighbours were felled. The TTs were scanned with a TLS with a resolution angle of 0.036° in both the horizontal and vertical directions. The scanner rotation angles ranged from 0 to 360° in the horizontal direction and from -60 to 90° in the vertical direction. The Faro Focus 3D is a single return instrument. Scan alignment was required to create one global point cloud from the four scans. It was done by using six spherical targets placed around the TT, with a minimum of three targets visible in each scan. No filters were activated on the Faro instrument during the scans but two filters were applied during data preprocessing using the software Faro Scene 5.0: (i) the dark scan points filter to remove points with a very low reflectance (less than 300) which correspond to false returns or sky points and (ii) the stray filter. The latter filter validates that the return is due to an object by comparing the distance with the scanner with the distance of the surrounding points (grid size of 3×3×3 points). The return is retained as a scan point if 50% of the differences in distance with the surrounding points is smaller than 0.02 m.

Files were prepared for wood/leaf separation and the correction of signal occlusion. For the wood/leaf discrimination algorithm, an ascii file containing the four aligned and filtered point clouds were exported from Faro Scene, with the TT previously manually isolated using the Computree software (http://rdinnovation.onf.fr/, consulted on March 14th 2017). Tree isolation was easy since the TT neighbours had been felled before the scans were taken and the TT were thus left clearly isolated in the middle of

a gap (Figure 3.1a). Filtered point clouds were necessary for this step as raw point cloud contained too much noise points which could bias the geometrical approach. For the occlusion correction algorithm, a raw ".xyb" file without filters was extracted for each scanning position. Raw point clouds were necessary for this step as they were compared with simulated scans with the same scanner settings.

3.6.2   Wood and leaf separation

A cylinder fitting algorithm available in the Computree software initially developed to detect stems was used to determine which returns were tied to a wood structure and which ones were from a leaf. This algorithm consists of five steps: (1) clustering of the point cloud by two cm horizontal slices in order to obtain small trunk arcs and branches. In order for two points to be considered part of the same cluster, they had to be separated by no more than 3 cm; (2) merge clusters vertically to form logs following two constraints: i) the vertical distance between clusters has to be less than 10 cm and ii) the bounding box of two clusters intersect each other in the XY plan. This step was originally designed to detect trunks but a continuous branch which is not vertical will also meet the two conditions. (3) Merge parallel logs to form the trunk and branches. The XY distance threshold to merge logs was large enough to merge non vertical branches (50 cm). (4) Adjust cylinders on logs from vertical to horizontal angle in order to fit a cylinder on the trunk and on the branches which are not vertical. (5) Export all the cylinders fitted with a cylinder identity and a value of linearity error (error of the three dimensional regression). The point cloud with the cylinder ID associated to each point was also extracted. More details on each step are given in the Computree software documentation (http://rdinnovation.onf.fr/, consulted on March 14th 2017).

Returns from wood (WR) and leaves (LR) were then identified in R (R Development Core Team 2011) based on the cylinder fitting output. A 3D linear regression is

performed on each point cluster of a given cylinder (Jacquelin 2010). Cylinders with a linearity error value lower than 0.001 were considered as trunk or branches, and the corresponding points were labeled as WR. The rest of the points were considered as LR. The 0.001 threshold was established by visual observation. Finally, the point cloud was divided into 10 cm edged voxels to calculate the proportion of WR and LR in each voxel (Figure 3.1).

3.6.3 Lidar data bias reduction with the L-vox algorithm

The number of returns in the point cloud of a forest scene is not an exact representation of the 3D distribution of the canopy components because the TLS data includes bias due to signal occlusion and variable sampling rates. An algorithm called L-vox, available in Computree, reduces this bias for an accurate estimation of the 3D distribution of material density in the canopy (Fournier et al. 2015). The general idea of the L-vox algorithm is to divide the space of the point cloud in voxels and calculate a relative density index (RDI) for each voxel using the number of laser beams that crosses the voxel and the number of returns from within the voxel. The number of laser beams crossing a target voxel depends on the theoretical number of beams launched by the TLS but subtracted by the beams intercepted (stopped) between the scanner and the target voxel. The algorithm assumes that the TLS is a single return instrument. The theoretical beams are calculated using a ray tracing model set with the scan parameters (angular resolution, scanner position, and vertical and horizontal openness angle). The RDI is thus calculated as follows:

$$RDI = \frac{n_r}{n_t - n_b} \tag{1}$$

with n_r the number of observed returns in the voxel, n_t the number of theoretical beams passing through the voxel obtained from the ray-tracing algorithm and n_b the number

of beams intercepted before the voxel. The algorithm was applied to each individual scan, but the four voxel grids of each TT were combined for analysis. This implies that each voxel has four RDI values, each corresponding to a scan. The retained RDI value is the one corresponding to the scan that has the least occlusion (i.e., the highest $n_t - n_b$ value). The voxel edge size used was 10 cm as recommended in Béland et al. (2014) and Fournier et al. (2015), corresponding to a voxel volume ($VoxV$) of 0.001 m^3.

In order to extract the voxel belonging to the TT, the isolated TT point cloud previously described was used to "clip" the voxels from the L-vox grid. The crown boundaries of the isolated TT point cloud were identified using 2D convex hull every 10-cm height slice with the package "geometry" in R (Barber et al. 2014). The resulting polygons were used to identify all the voxels of the L-vox grid inside those polygons. These voxels were considered as voxels belonging to the TT.

At this stage, two voxel grids of the TT are available, (1) the WR/LR voxel grid where each voxel has the proportion values of WR and of LR and (2) the L-vox grid where each voxel has the RDI value. The RDI of the voxel in the L-vox grid was then divided into wood RDI (WRDI) and leaf RDI (LRDI) by multiplying the RDI and the proportion of WR and LR values of the closest voxels in the WR/LR voxel grid (Figure 3.2). The resulting three voxel grids (i.e. RDI, LRDI and WRDI) were used to make vertical profiles. Only the voxels above the crown base were used to make the three profiles as the aim of study is to analyse the crown material distribution. Cumulative relative RDI at each vertical height step ($\Delta z = 10$ cm) were used to make the profiles:

$$y_z = \frac{\sum RDI_z}{\sum RDI_{tree}} \tag{2}$$

The shape of the profile was modeled using a two parameter (r,s) beta distribution. This distribution was chosen because it is highly flexible and defined in an interval with fixed endpoints (Maguire and Bennett 1996; Garber and Maguire 2005). The beta

distribution (Eq. 3) was fitted to each tree and density distribution (RDI, WRDI, LRDI) individually using the nls function in R (Bates and Watts 1988):

$$y = x^r(1 - x)^s \tag{3}$$

The RDI voxel grid was also used to quantify the following six crown metrics:

- Crown length (CrL): The highest Z coordinate was used to determine the height of the tree. The Z position of the crown base was recorded manually (in Faro Scene) by using the aligned point clouds for each tree.
- Projected area of the crown (PACr): area of the polygon calculated on the XY plane using the 2D convex hull algorithm of the package "geometry" (Barber et al. 2014).
- Crown volume (CrV): Volume calculated from the hull generated by the 3D alpha shape with the package "alphashape3d" (Lafarge and Pateiro-Lopez 2014).
- Crown density (CrD): Proportion of crown volume occupied by material:

$$CrD = \frac{CrV}{\sum RDI \times VoxV} \tag{4}$$

- Crown width to length ratio (CrW:CrL): Crown width estimation comes from the diameter of a circle of area equal to crown projected area
- Crown proportion (Cr%): Crown length to tree height ratio

3.6.4 Data analysis

Data analysis was divided into two parts. First, the effect of species, type of stand and developmental stage on the *r* and *s* parameters of the beta distribution was analyzed using mixed effect models. Second, each parameter was linearly related to the different crown metrics as well as with the stand characteristics, and the models compared.

The effect of stand type, developmental stage and species on *r* and *s* parameters were analysed using the following model for the three types of profile (i.e., RDI, LRDI, WRDI):

$$Y_{ijk} = \mu + ST_{ij} + DS_{ij} + SP_{ijl} + ST_{ij}SP_{ijk} + DS_{ij}SP_{ijk} + DS_{ij}ST_{ij} + u_i + \varepsilon_{ijk} \tag{5}$$

where Y_{ijk} is the *r* or *s* beta distribution parameter (of RDI, LRDI or WRDI) estimated for a species (k) of stand type (j) in the site (i), and μ the overall mean. The variable ST_{ij} is a binary variable indicating stand type ($ST_{ij} = 0$ for mixed stand, $ST_{ij} = 1$ for pure stand), DS_{ij} a binary variable to indicate developmental stage ($DS_i = 0$ for intermediate stage and $DS_i = 1$ for mature stage), SP_{ijk} indicating the species ($SP_{ijk} = 0$ for Sugar maple and $SP_{ijk} = 1$ for Balsam fir), u_i is the site random effects ($u_i \sim N(0, \sigma_i^2)$) and ε the residual error ($\varepsilon_{ijk} \sim N(0, \sigma_i^2)$).

All possible combinations of presence/absence of the crown metrics and stand characteristics (i.e., SC that could be SP, ST or SP) were then calibrated (Eq. 6), and a total of 479 models compared. Among the 6 metrics initially calculated, crown projected area (PACr) was dropped as it was found to be collinear with other variable (especially with CrV) as indicated by a high variance inflation factor (vif > 5) (Heiberger and Holland 2015). Once the PACr dropped, the vif values of the remaining variables were below five. Interaction effects between the stand characteristics were also considered when two or the three stand characteristics (SC) were in the same model:

$$Y_i = \mu + a_1 CM_1 + a_2 CM_2 + a_3 CM_3 + \cdots SC_1 + SC_2 + \cdots + SC_1:SC_2 + u_i + \varepsilon_i \tag{6}$$

where a_x are the fixed effect parameters for the crown metric x (CM_x); SC_x is a stand characteristic variable x among the three characteristics tested in the first step (ST, DS and SP), u_i is the site random effects parameters $u_i \sim N(0, \sigma_i^2)$).

3.7   RESULTS

3.7.1   Profile comparisons

Important differences in the vertical distribution between both species were observed (Table 3.3). The material is preferentially distributed in the upper part of crown (mode around 75% of height) for Sugar maple and in the lower part (mode around 30% of height) for Balsam fir (Figures 3.3 and 3.4).

We observed that in all conditions (type of stand and developmental stage) results for LRDI and RDI are very similar whereas WRDI profiles differ (Table 3.3 and Figure 2.3 and 2.4). For Sugar maple, the WRDI distribution has a higher variance and the mode is located lower in the crown than for RDI or LRDI (Figure 3.3). For Balsam fir, the WRDI mode is higher in the crown with a higher variance than for the RDI or LRDI distributions. The only significant effect on WRDI parameters other than differences between the species ($p < 0.0001$ for both parameters, Table 3.3) is the interaction between stand type and species for the parameter r ($p = 0.032$, Table 3.3). The effect of stand type seems to be stronger for Sugar maple than for Balsam fir, with a lower mode in mixed than in pure stands (Figure 3.3 and 3.4). This effect is more pronounced for mature trees (Figure 3.3) although there is no significant effect of the interaction between developmental stage and stand type ($p = 0.088$ and 0.43 for r and s respectively, Table 3.3).

Differences in profile shapes between mixed and pure stands are also observed. The effect of stand type is significant for the s parameter ($p = 0.043$ and 0.03 for LRDI, Table 3.3). However, the two species behave differently in response to stand type as indicated by a strong interaction effect between species and stand type on both parameters ($p = 0.0012$ and 0.00095 for r and s respectively for RDI and $p = 0.0011$ and 0.0012 for LRDI, Table 3.3). For sugar maple, the mode is located closer to the

base of the crown and the variance of the distribution is higher in mixed than in pure stands (Figure 3.3). This result is only observed for mature trees. The interaction effect between stand type and developmental stage is non-significant ($p = 0.084$ and 0.28 for r and s respectively for RDI and $p = 0.11$ and 0.34 for LRDI, Table 3.3). For the balsam fir, trees growing in mixed stands have a mode located higher in the crown than in pure stands for both mature and intermediate developmental stage (Figure 3.4).

The two species present differences in developmental stage and show opposite responses. The effect of developmental stage is significant for the s parameter ($p = 0.047$ for RDI and 0.045 for LRDI, Table 3.3). Moreover, there is an interaction effect between species and developmental stage on the r parameter for RDI ($p = 0.041$) and r and s parameters for LRDI ($p = 0.044$ and 0.029 for r and s respectively, Table 3.3). For sugar maple, mature trees have a mode located higher in the crown than intermediate trees (Figure 3.3). However, balsam fir mature trees have a mode lower in the crown than intermediate trees contrary to Sugar maple (Figure 3.3).

3.7.2 Model comparison

Results of the model comparisons generally show that the crown metrics were not sufficient to explain alone the variability of the distribution profiles. Nevertheless, two crown metrics, the crown density and the crown proportion, were retained in all the best models (Table 3.4). The best models for both r and s parameters are the same no matter what distribution is considered (i.e., RDI, LRDI or WRDI) (Table 3.4). Crown density is only significant for the s parameters of RDI and LRDI distribution ($p < 0.0001$) although crown proportion was significant for all parameters of all distributions (p ranged between <0.0001 and 0.026, Table 3.4) except for s parameters of WRDI distribution ($p = 0.46$, Table 3.4). All stand characteristic variables (species, stand type and developmental stage) as well as their interactions were retained for the

r parameters. All interaction terms were found to be statistically significant for RDI and LRDI (p ranged between <0.0001 and 0.0059, Table 3.4). For WRDI, only the interaction between stand type and species (p = 0.03, Table 3.4) and stand type and developmental stage (p = 0.019) were statistically significant. For *s* parameter, the only stand characteristic variable that remained in the models is the species which is still significant in all models (p ranged between <0.0001 and 0.0012).

3.8   DISCUSSION

3.8.1   Differences between species

Sugar maple has top-heavy distributions and Balsam fir bottom heavy ones, no matter what kind of return is considered (total, wood or leaves). These differences are not surprising because of the contrasted architectural development of the two species. Balsam fir follows the architectural model of Massart, where a strong apical dominance with a well-defined unique trunk and close to horizontal branches is observed (Millet. 2012). This architectural development is constant across the ontogeny and leads to a conical, bottom heavy crown (Hallé et al. 1978; Millet 2012). Sugar maple however generally has multiple forks due to the loss of the apical dominance early in its ontogeny. Co-dominant trees generally present an inverted cone shape with a high proportion of material towards the top of the crown (Tucker et al. 1993). Moreover, the difference in the architectural development of these two species also explains the opposite response to developmental stage we observed. The high insertion angle on the trunk (i.e horizontal) of balsam fir's first order branches lead to an increase in material low in the crown. On the other hand, the low insertion angle (i.e vertical) of sugar maple's first order branches lead to an accumulation of material higher in the crown. This becomes more pronounced in older Sugar maple trees.

Our results are in accordance with the literature on coniferous species. Gilmore and Seymour (1997) found that co-dominant Balsam fir trees have their leaf area concentrated in the first 40% of the crown. Weiskittel et al. 2009 found similar results for Balsam fir and three other coniferous species in the state of Maine, USA. Our results are very close to these findings On the other hand, Schneider et al. (2011) observed a concentration of foliage in the upper part of the crown for jack pine (*Pinus banksiana* Lamb.) and Mäkela and Vanninen (2001) reported that Scots pine *(Pinus sylvestris* L.) have a maximum density very close to the midpoint. These studies highlight an interspecific variability of material distribution which is often related to species shade tolerance while the intraspecific variability is influenced by the position of the tree in the canopy (Maguire and Bennett 1996; Garber and Maguire 2005).

Few studies have been conducted on broadleaved species vertical distribution of foliage, and nearly none compare broadleaved and coniferous. As with conifers, the foliage distribution of broadleaved species is strongly correlated to shade tolerance. Shade tolerant species have bottom heavy distributions when compared to shade intolerant (Forrester et al. 2012; Nelson et al. 2014; Guisasola et al. 2015). Considering that Sugar maple is a very shade tolerant species, it is surprising to observe such a top heavy material distribution. An explanation could be the fact that in this study we defined the crown base as the insertion height of the first fork or main branch that has leaves. Therefore, the bottom part of the crown is generally composed by two main branches with few twigs and leaves. Higher in the crown, the branching topology is more complex, with more twigs and leaves. This translates to in an increase in the amount of material that is intercepted by the LiDAR-t. The differences of wood distribution shape when compared to total (or leaf) distribution confirm these results. The distribution peak for wood returns is located lower on the crown than the total (or leaf) returns. This is consistent with the hypothesis that big branches with very few twigs and leaves mostly occupy the bottom of the crown. Finally, these differences between wood and total (or leaf) distributions are more important for mature trees than

for intermediate ones. This is in accordance with the fact that young developmental stage Sugar maple trees have generally smaller branches low in the crown (Millet 2012).

3.8.2 Differences between mixed and pure stands

Our results show that Sugar maples in mixed stands have more homogeneously distributed material (i.e., higher variance) that is lower in the crown when compared with maples in pure stands. A downward shift of the material is often associated with trees under less competition and is advantageous in terms of light interception because this minimizes self-shading, thus increasing light interception (Horn 1971; Gilmore and Seymour 1997; Garber and Maguire 2005). This in accordance with the results of Martin-Ducup et al. (2016) on the same sites, where they showed that the competitive pressure of Sugar maples is lower and space occupancy higher in mixed stands than in pure ones. Metz et al. (2013) has also shown that the competition is lower in mixed stands which in turn explains the higher growth of European beech. This effect of stand composition is however observable only for mature trees in both Martin-Ducup et al. (2016) and the present study. The potential benefit of increased diversity varies with developmental stage due to temporal modification in resource capture and utilization and could explain our results (Forrester 2014; Guisasola et al. 2015).

It is interesting to observe that stand density is higher in the mixed stands than in pure ones for sugar maple (Table 3.2). The advantage of mixture seems to overcome the potential negative effect of density (i.e. competition). Garber and Maguire (2005) have observed that the positive effect of diversity on vertical distribution was more important in high density stands. As stand density increases, the interaction between the different individuals is stronger. This increased interaction thus underlines the importance of trait complementarity in mixed stands (Condés et al. 2013; Forrester et

al. 2013; Forrester and Bauhus 2016). One could thus argue that the stronger effect of mixture on mature trees is confounded with the effect of stand density. However, the densities of intermediate and mature trees in mixed stands are very close (Table 3.2). It would have been interesting to test the interaction effect of density and type of stand (i.e. pure/mixed). The present dataset was however not set up for testing such hypotheses.

Balsam firs have a concentration of foliage higher in the crown in mixed stands than in pure ones. This suggests that in mixed stands, they experience more competition and have less efficient crowns in order to intercept light. These results are true for both mature and intermediate developmental stages. Here again these differences could not be attributed to stand density because for balsam fir basal area is higher in pure than in mixed stands contrary to sugar maple (Table 3.2). By considering the stem density only, one would have expected an inverse response. But here the stand composition seems to be in cause.

When balsam fir and Sugar maple are found in the same stand, it appears that one species takes advantage of the mixture to the detriment of the other. Both species have indeed opposite reactions to mixture, with balsam fir shifting its foliage up towards the middle of the crown and sugar maple down towards the bottom of the crown. Thus, mixture seems to be advantageous for sugar maple but not for balsam fir. However, the distribution is generally more homogenous along the crown height (i.e., higher variance) in mixed stands for both species and could result in a better total space occupation with an optimal sharing of the available space in mixed stands. Our stands are however composed of many other species. An analysis of the response of all species is needed to clarify the effect of mixture on space occupation at the stand scale.

3.8.3   Does crown metrics explain material distribution?

Crown density and crown proportion were the crown variables that best explained the variability of the beta distribution parameters. The crown proportion is present and significant in almost all models. This suggests that it might be not necessary to quantify complex metrics that need TLS data such as crown area, crown volume or crow density to obtain the vertical distribution of material. Although crown density is present in all models, it is often non-significant, or has an F-value that is lower than the one observed for the crown proportion. However, contrary to our expectations, the crown metrics are not sufficient to explain the variability in the distribution parameters. In other words, the differences between the distributions in stand type, species and developmental stage cannot be solely explained with crown metrics such as crown shape, dimension or density. The local competition for light prior to release might better explain the variability of material distribution, as it has been shown on space occupation crown metrics for Sugar maple in Martin-Ducup et al. (2016).

3.8.4   Differences between material types

There are important differences between wood and total/leaf distribution, regardless of species. As explained earlier, the development mode of Sugar maple leads to more wood returns lower in the crown and inversely for foliage returns. The wood distribution has its mode lower in the crown for trees in mixed stands, when compared to trees in pure stands. This is in accordance with the results of Martin-Ducup et al. (2016), where crowns were more open at their base for trees in mixed stands, and leading to more branches close to the base of the crown. Bayer et al. (2013) also showed that European beech in mixed stands had more branches with shallower angles when

compared to beech in pure stands. This probably increases the amount of woody material in the lower part of the crown.

Balsam firs have the opposite behaviour with an upward shift in wood distribution when compared to leaf or total material. This result is surprising as one could expect that the wood distribution should be more concentrated on the lower part of the crown where branches are thicker and longer with less leaves due to self-shading. However, our approach to separate wood and leaves using TLS data needs to be validated.

Finally, it is interesting to observe that the leaves and total material distributions are very similar, regardless of species. It suggests that the total material distribution (i.e., without separating wood and leaves) could be a good proxy of the leafy material. It has important implications considering the uncertainties, the algorithm complexity and the time cost associated with wood and leaf separation. Indeed, at least for the stands studied in the present paper, the gain of the wood-leaf separation to study material distribution stay open to discussion. Moreover, with ALS data, occlusion from above and the lower return density do not allow accurate branch representations (Kükenbrink et al. 2016). It seems thus impossible to use the present geometrical method at large scale using ALS data. However, if our results are confirmed by other studies for different stand and species, characterizing the shape of the vertical material profiles using all the return would be sufficient to characterize the leaf profile at large scale.

3.8.5   Method's advantages and limitations

The separation using geometrical shape (i.e., cylinder fitting) presents a major advantage over other methods as it can be applied to a point cloud with x,y,z coordinates information without any additional data of return intensity or color. Geometrical-based methods are more generalizable (i.e. they can be applied to any sensor) and have already been proved to be efficient on adult trees (Belton et al. 2013; Tao et al. 2015). Moreover, in the present study, the cylinder fitting algorithms used

are already developed and operational to detect stems in Computree, an open software (http://rdinnovation.onf.fr/, consulted on March 14th 2017).

We did not validate the wood/leaf separation as no leaf data were available for the experimental trees in our study. Therefore, results on leaves and wood have to be interpreted carefully. This method should theoretically provide a good approximation and is a good starting point for wood/leaf separation using an easy to use geometrical approach on TLS data. However, in a further step, validation with leaf data should be performed to optimize certain parameters of the algorithm steps for each species. For example, species-specific thresholds should probably be established for the cylinder fitting steps (e.g., cylinder angle; size; error, etc). Moreover, the cylinder-fitting algorithm has been developed to detect trunk and is optimized for more or less vertical structures. It can detect horizontal branches, but is less efficiently and thus could induce large bias for species such as balsam fir. A complementary approach performing clusters on vertical slices (step 1 of the algorithm) could improve the efficiency of the algorithm to detect horizontal branches.

Signal occlusion and the variable sampling density are known biases for TLS data, and lead to two major limitations. The first is the underestimation of the material density. Using the L-vox algorithm, we are able to limit this problem to the point where the RDI value of the voxel was assumed to provide the exact 3D distribution of material (Fournier et al. 2015). The second limitation is the detection of cylinders in zones with strong occlusion. Although L-vox algorithm is able to re-estimate the density in a voxel by correcting the occlusion, the spatial arrangement of points is unpredictable. We supposed that this problem should not be important for Sugar maple but could induce important biases for Balsam fir. Indeed, Balsam fir has denser crowns and the branch occlusion could be much more important than for Sugar maple.

Finally, we used TLS data to quantify the vertical distribution of the relative density of material. It has important applications in forest management and forest ecology. This

innovative method provides new valuable data to the forest science community that could be used in order to predict tree growth and other processes regulating forest dynamics. However, if tree growth and photosynthesis have to be simulated using leaf surface area and transform TLS return to area, a thorough validation of the algorithm is needed to establish if any bias remains. A transformation from the LRDI to the leaf area is possible at the voxel scale using methods such as those developed by Hosoi and Osama (2006), Van der Zande et al (2011) or Béland et al (2011). It is also possible to use the total leaf area index at the tree or stand scale obtained by other methods (e.g. field data, allometric relationship), and redistribute it proportionally to LRDI values in order to obtain leaf area at the voxel scale.

3.9   CONCLUSION

A method to analyse vertical distribution of total, wood and leaf material using TLS data is proposed. The separation between wood and leave material is done using a geometrical approach based on cylinder fitting using an open software specialized in TLS data analysis (Computree). Although the approach needs to be validated for an operational use, it offers a very good starting point for a generalizable method of wood/leave separation using LiDAR technologies. Moreover, the correction of the signal occlusion biases answer is an important step forward in the TLS user community in forest sciences. No differences were found between total and leaf material distribution suggesting that for our two species the total distribution could be sufficient to estimate the leaf distribution. This is an important outcome of the study considering the time cost, the uncertainties and the impossibility to use this method at large scale with ALS data. Moreover, simple crown metrics seem to be insufficient to explain the important variability in profile shapes between species, stand type and developmental stage. Results show that Sugar maple and Balsam fir have very different vertical

distributions that is in accordance with their architectural development. Their responses to the stand composition are also opposite and suggest that the Sugar maple benefits more from mixtures than Balsam fir. The present study has brought important results on the material distribution response to mixture for the two species studied. It is however necessary to analyse all the species present to draw space occupancy conclusions at the stand scale.

3.10 REFERENCES

Ashcroft MB, Gollan JR, Ramp D (2014) Creating vegetation density profiles for a diverse range of ecological habitats using terrestrial laser scanning. Methods Ecol Evol 5:263–272. doi: 10.1111/2041-210X.12157

Barber CB, Habel K, Grasman R, et al (2014) geometry: Mesh generation and surface tesselation.

Bates DM, Watts DG (1988) Nonlinear regression analysis and its applications. Wiley

Bayer D, Seifert S, Pretzsch H (2013) Structural crown properties of Norway spruce (Picea abies [L.] Karst.) and European beech (Fagus sylvatica [L.]) in mixed versus pure stands revealed by terrestrial laser scanning. Trees 27:1035–1047. doi: 10.1007/s00468-013-0854-4

Béland M, Widlowski JL, Fournier RA, et al (2011) Estimating leaf area distribution in savanna trees from terrestrial LiDAR measurements. Agric For Meteorol 151:1252–1266.

Béland M, Widlowski J-L, Fournier RA (2014) A model for deriving voxel-level tree leaf area density estimates from ground-based LiDAR. Environ Model Softw 51:184–189. doi: 10.1016/j.envsoft.2013.09.034

Belton D, Moncrieff S, Chapman J (2013) Processing tree point clouds using Gaussian mixture models. Proc ISPRS Ann Photogramm Remote Sens Spat Inf Sci Antalya Turk 11–13.

Binkley D, Campoe OC, Gspaltl M, Forrester DI (2013) Light absorption and use efficiency in forests: Why patterns differ for trees and stands. For Ecol Manag 288:5–13. doi: 10.1016/j.foreco.2011.11.002

Coates KD, Canham CD, Beaudet M, et al (2003) Use of a spatially explicit individual-tree model (SORTIE/BC) to explore the implications of patchiness in structurally complex forests. For Ecol Manag 186:297–310.

Condés S, Del Rio M, Sterba H (2013) Mixing effect on volume growth of Fagus sylvatica and Pinus sylvestris is modulated by stand density. For Ecol Manag

292:86–95.

Coops NC, Hilker T, Wulder MA, et al (2007) Estimating canopy structure of Douglas-fir forest stands from discrete-return LiDAR. Trees 21:295. doi: 10.1007/s00468-006-0119-6

Danson FM, Gaulton R, Armitage RP, et al (2014) Developing a dual-wavelength full-waveform terrestrial laser scanner to characterize forest canopy structure. Agric For Meteorol 198–199:7–14. doi: 10.1016/j.agrformet.2014.07.007

Douglas ES, Martel J, Li Z, et al (2015) Finding leaves in the forest: the dual-wavelength Echidna lidar. IEEE Geosci Remote Sens Lett 12:776–780.

Forrester DI (2014) The spatial and temporal dynamics of species interactions in mixed-species forests: From pattern to process. For Ecol Manag 312:282–292. doi: 10.1016/j.foreco.2013.10.003

Forrester DI, Bauhus J (2016) A Review of Processes Behind Diversity—Productivity Relationships in Forests. Curr For Rep 2:45–61. doi: 10.1007/s40725-016-0031-2

Forrester DI, Benneter A, Bouriaud O, Bauhus J (2016) Diversity and competition influence tree allometric relationships–developing functions for mixed-species forests.

Forrester DI, Collopy JJ, Beadle CL, Baker TG (2012) Interactive effects of simultaneously applied thinning, pruning and fertiliser application treatments on growth, biomass production and crown architecture in a young Eucalyptus nitens plantation. For Ecol Manag 267:104–116. doi: 10.1016/j.foreco.2011.11.039

Forrester DI, Kohnle U, Albrecht AT, Bauhus J (2013) Complementarity in mixed-species stands of Abies alba and Picea abies varies with climate, site quality and stand density. For Ecol Manag 304:233–242. doi: 10.1016/j.foreco.2013.04.038

Forrester DI, Pretzsch H (2015) Tamm Review: On the strength of evidence when comparing ecosystem functions of mixtures with monocultures. For Ecol Manag 356:41–53.

Fournier R, Côté J-F, Bourge F, et al (2015) A method addressing signal occlusion by scene objects to quantify the 3D distribution of forest components from terrestrial lidar. In: 28th-30th September 2015. La Grande Motte. France,

Garber SM, Maguire DA (2005) The response of vertical foliage distribution to spacing and species composition in mixed conifer stands in central Oregon. For Ecol Manag 211:341–355. doi: 10.1016/j.foreco.2005.02.053

Gilmore DW, Seymour RS (1997) Crown architecture of Abies balsamea from four canopy positions. Tree Physiol 17:71–80.

Guisasola R, Tang X, Bauhus J, Forrester DI (2015) Intra- and inter-specific differences in crown architecture in Chinese subtropical mixed-species forests. For Ecol Manag 353:164–172. doi: 10.1016/j.foreco.2015.05.029

Hallé F, Oldeman RAA, Tomlinson PB (1978) Tropical trees and forests: an architectural analysis. Springer-Verlag.

Heiberger RM, Holland B (2015) Statistical analysis and data display: an intermediate course with examples in R. Springer

Hétroy-Wheeler F, Casella E, Boltcheva D (2016) Segmentation of tree seedling point clouds into elementary units. Int J Remote Sens 37:2881–2907.

Horn HS (1971) The adaptive geometry of trees, Princeton University Press. Princeton University Press

Hosoi F, Omasa K (2006) Voxel-based 3-D modeling of individual trees for estimating leaf area density using high-resolution portable scanning lidar. Geosci Remote Sens IEEE Trans On 44:3610–3618.

Jean Jacquelin (2010) 3D linear regression. scribd.com/doc/31477970/Regressions-et-trajectoires-3D

Jucker T, Bouriaud O, Coomes DA (2015) Crown plasticity enables trees to optimize canopy packing in mixed-species forests. Funct Ecol 29:1078–1086. doi: 10.1111/1365-2435.12428

Kükenbrink D, Schneider FD, Leiterer R, et al (2016) Quantification of hidden canopy volume of airborne laser scanning data using a voxel traversal algorithm.

Lafarge T, Pateiro-Lopez B (2014) alphashape3d: Implementation of the 3D alpha-shape for the reconstruction of 3D sets from a point cloud.

Landsberg JJ, Waring RH (1997) A generalised model of forest productivity using simplified concepts of radiation-use efficiency, carbon balance and partitioning. For Ecol Manag 95:209–228. doi: 10.1016/S0378-1127(97)00026-1

Latif ZA, Blackburn GA (2010) The effects of gap size on some microclimate variables during late summer and autumn in a temperate broadleaved deciduous forest. Int J Biometeorol 54:119–129.

Li Y, Guo Q, Tao S, et al (2016) Derivation, Validation, and Sensitivity Analysis of Terrestrial Laser Scanning-based Leaf Area Index. Can J Remote Sens 42:719–729.

Li Z, Douglas E, Strahler A, et al (2013) Separating leaves from trunks and branches with dual-wavelength terrestrial LiDAR scanning. In: Geoscience and Remote Sensing Symposium (IGARSS), 2013 IEEE International. IEEE, pp 3383–3386

Ma L, Zheng G, Eitel JU, et al (2016) Determining woody-to-total area ratio using terrestrial laser scanning (TLS). Agric For Meteorol 228:217–228.

Maguire DA, Bennett WS (1996) Patterns in vertical distribution of foliage in young coastal Douglas-fir. Can J For Res 26:1991–2005. doi: 10.1139/x26-225

Mäkelä A, Vanninen P (2001) Vertical structure of Scots pine crowns in different age and size classes. Trees 15:385–392.

Martin-Ducup O, Schneider R, Fournier RA (2016) Response of sugar maple (Acer saccharum, Marsh.) tree crown structure to competition in pure versus mixed stands. For Ecol Manag 374:20–32. doi: 10.1016/j.foreco.2016.04.047

Martin-Ducup O, Schneider R, Fournier RA (2017) A method to quantify canopy changes using multi-temporal terrestrial lidar data: Tree response to surrounding gaps. Agric For Meteorol 237:184–195.

Medlyn BE (1998) Physiological basis of the light use efficiency model. Tree Physiol 18:167–176.

Messier C, Puettmann KJ, Coates KD (2013) Managing forests as complex adaptive systems: building resilience to the challenge of global change. Routledge

Metz J, Seidel D, Schall P, et al (2013) Crown modeling by terrestrial laser scanning as an approach to assess the effect of aboveground intra- and interspecific competition on tree growth. For Ecol Manag 310:275–288. doi: 10.1016/j.foreco.2013.08.014

MFFP (2007) Normes d'inventaire forestier, placettes- échantillons temporaires. Direction des inventaires forestiers, Forêt Québec. Gouvernement du Québec, Québec, CA.

Millet J (2012) L'architecture des arbres des régions tempérées, MULTIMONDES.

Monteith JL (1972) Solar Radiation and Productivity in Tropical Ecosystems. J Appl Ecol 9:747–766. doi: 10.2307/2401901

Morin X (2015) Species richness promotes canopy packing: a promising step towards a better understanding of the mechanisms driving the diversity effects on forest functioning. Funct Ecol 29:993–994.

Morin X, Fahse L, Scherer-Lorenzen M, Bugmann H (2011) Tree species richness promotes productivity in temperate forests through strong complementarity between species. Ecol Lett 14:1211–1219.

Nelson AS, Weiskittel AR, Wagner RG (2014) Development of branch, crown, and vertical distribution leaf area models for contrasting hardwood species in Maine, USA. Trees 28:17–30. doi: 10.1007/s00468-013-0926-5

Niinemets Ü (2007) Photosynthesis and resource distribution through plant canopies. Plant Cell Environ 30:1052–1071. doi: 10.1111/j.1365-3040.2007.01683.x

Niinemets Ü (2010) A review of light interception in plant stands from leaf to canopy in different plant functional types and in species with varying shade tolerance. Ecol Res 25:693–714. doi: 10.1007/s11284-010-0712-4

Oshio H, Asawa T, Hoyano A, Miyasaka S (2015) Estimation of the leaf area density distribution of individual trees using high-resolution and multi-return airborne LiDAR data. Remote Sens Environ 166:116–125. doi: 10.1016/j.rse.2015.05.001

Pretzsch H (2014) Canopy space filling and tree crown morphology in mixed-species stands compared with monocultures. For Ecol Manag. doi: 10.1016/j.foreco.2014.04.027

Pretzsch H, Rais A (2016) Wood quality in complex forests versus even-aged monocultures: review and perspectives. Wood Sci Technol 50:845–880. doi: 10.1007/s00226-016-0827-z

R Development Core Team (2011) R Development Core Team.

Schneider R, Fortin M, Berninger F, et al (2011) Modeling Jack Pine (Pinus banksiana) foliage density distribution. For Sci 57:180–188.

Seidel D, Beyer F, Hertel D, et al (2011) 3D-laser scanning: A non-destructive method for studying above- ground biomass and growth of juvenile trees. Agric For

Meteorol 151:1305–1311. doi: 10.1016/j.agrformet.2011.05.013

Seidel D, Leuschner C, Scherber C, et al (2013) The relationship between tree species richness, canopy space exploration and productivity in a temperate broad-leaf mixed forest. For Ecol Manag 310:366–374.

Shaw DC (2004) Vertical organization of canopy biota. Elsevier Academic Press: Amsterdam, The Netherlands

Tao S, Guo Q, Su Y, et al (2015) A geometric method for wood-leaf separation using terrestrial and simulated lidar data. Photogramm Eng Remote Sens 81:767–776.

Tucker GF, Lassoie JP, Fahey TJ (1993) Crown architecture of stand-grown sugar maple (Acer saccharum Marsh.) in the Adirondack Mountains. Tree Physiol 13:297–310.

Van der Zande D, Stuckens J, Verstraeten WW, et al (2011) 3D modeling of light interception in heterogeneous forest canopies using ground-based LiDAR data. Int J Appl Earth Obs Geoinformation 13:792–800. doi: 10.1016/j.jag.2011.05.005

Wahabzada M, Paulus S, Kersting K, Mahlein A-K (2015) Automated interpretation of 3D laserscanned point clouds for plant organ segmentation. BMC Bioinformatics 16:248. doi: 10.1186/s12859-015-0665-2

Wang YP, Jarvis PG (1990) Description and validation of an array model—MAESTRO. Agric For Meteorol 51:257–280.

Weiskittel AR, Kershaw Jr. JA, Hofmeyer PV, Seymour RS (2009) Species differences in total and vertical distribution of branch- and tree-level leaf area for the five primary conifer species in Maine, USA. For Ecol Manag 258:1695–1703. doi: 10.1016/j.foreco.2009.07.035

Wiki Computree. http://rdinnovation.onf.fr/projects/computree/wiki/En_wiki.

3.11 TABLES

Table 3-1 : Tree characteristics by site. Mean (standard deviation).

	Intermediate stage			Mature site		
	Site 1	**Site 2**	**Site 3**	**Site 4**	**Site 5**	**Site 6**
Sugar maple						
DBH (mm)	147.33 (20)	136.83 (24.85)	141 (23.29)	254.89 (71.53)	233.65 (61.03)	212.38 (32.8)
Height (m)	15.84 (1.26)	15.45 (1.58)	15.04 (1.18)	19.48 (2.69)	19.45 (1.99)	17.88 (0.92)
Age	27.33 (2.88)	29.67 (6.41)	34.5 (12.06)	63.33 (14.24)	60.6 (14.14)	48.5 (4.93)
Balsam fir						
DBH (mm)	154 (23.82)	149.33 (28.97)	143.5 (28.61)	219.8 (26.58)	267.8 (35.65)	231.5 (50.2)
Height (m)	15.97 (0.99)	14.71 (1.57)	16.34 (1.09)	20.32 (2.24)	20.63 (0.97)	19.84 (2.2)
Age	32 (3.22)	32.83 (13.33)	46.83 (17.42)	56.2 (13.99)	68.17 (12.38)	47 (6.96)

Table 3-2 : Basal area in pure and mixed stands for the two developmental stages. Mean (standard deviation).

	Bal. fir	Whi. spr.	Whi. ced.	Yel. bir.	Pap. bir.	Sug. map.	Red map.	Tre. asp.	Fir. che.	Total BA
Sugar maple										
Mixed-inter	15.5	2.33	0	2.83	0.17	8	1.5	1.5	0.5	32.33
Mixed-Mature	12.55	6	0.91	3.45	2.73	4.91	0	1.45	0.18	32.18
Pure-inter	0.83	0.17	0	2.17	0	17	3.5	0.5	0.33	24.5
Pure-mature	0.33	0.83	0	2	0.17	25.33	0	0.17	0	28.83
Balsam fir										
Mixed-inter	8.17	0.83	0	6.5	1	3.5	4.67	1.33	0.17	26.5
Mixed-Mature	5.4	3.8	0	3.6	2	11.6	1	0.8	0	28.2
Pure-inter	27.2	6.8	0	2	0.2	0.4	2.2	0.6	0	39.4
Pure-mature	17.45	11.09	0.73	1.64	3.27	0.55	0.18	0.91	0.18	36

Bal. fir: Balsam fir (Abies balsamea (L.) Mill.); Whi. spr.: White spruce (Picea glauca (Moench) Voss); Whi. ced.: White cedar (Thuja occidentalis L.); Yel. bir.: Yellow birch (Betula alleghaniensis Britton); Pap. bir.: Paper birch (Betula papyrifera Marshall); Sug. map.: Sugar maple (Acer saccharum Marshall); Red map.: Red maple (Acer rubrum L.); Tre. asp: Trembling aspen (Populus tremuloides Michx.); Fir. che.: Fire cherry (Prunus pensylvanica L. f.); Total BA: Total basal area

Table 3-3: Analysis of variance for both beta distribution parameters (r and s) and the three profile types (equation 5). Fixed effect of stand type (ST), developmental stage (SD) species (PT), the interaction between stand type and developmental stage (ST:DS), between stand type and species (ST:SP) and between developmental stage and species (DS:SP) are shown.

	RDI						LRDI						WRDI					
	r			s			r			s			r			s		
	Df	F-value	P-value	Df	F-value	P-value	Df	F-value	P-value	Df	F-value	P-value	Df	F-value	P-value	Df	F-value	P-value
ST	1	0.14	0.71	1	4.2	0.043 *	1	0.047	0.83	1	4.9	0.03 *	1	2.1	0.15	1	0.3	0.59
DS	1	2.6	0.18	1	4.1	0.047 *	1	3.8	0.055	1	4.2	0.045 *	1	0.0046	0.95	1	1.9	0.25
SP	1	210	0 ***	1	100	<0.0001 ***	1	230	0 ***	1	110	<0.0001 ***	1	56	<0.0001 ***	1	14	<0.0001 ***
ST:DS	1	3.1	0.084	1	1.2	0.28	1	2.6	0.11	1	0.91	0.34	1	3	0.088	1	0.63	0.43
ST:SP	1	12	0.0012 **	1	12	0.00095 ***	1	12	0.0011 **	1	11	0.0012 **	1	4.8	0.032 *	1	0.42	0.52
DS:SP	1	3.3	0.074	1	4.3	0.041 *	1	4.2	0.044 *	1	5	0.029 *	1	0.24	0.62	1	0.22	0.64

Table 3-4: Estimates and standard error for the best models to predict *r* and *s* beta distributions parameters (equation 6). AIC criteria were used to select each best model among 479.

	RDI		LRDI		WRDI	
	r	*s*	*r*	*s*	*r*	*s*
	Est (Std.Er)	**Est (Std.Er)**	**Est (Std.Er)**	**Est (Std.Er)**	**Est (Std.Er)**	**Est (Std.Er)**
Treatment variables						
ST	0.5 (0.26)	—	0.5 (0.25)	—	0.58 (0.42)	—
DS	0.26 (0.26)	—	0.36 (0.25)	—	-0.41 (0.51)	—
SP	-0.59 (0.36)	2 (0.27)***	-0.66 (0.34)	2.1 (0.29)***	-0.28 (0.58)	1.4 (0.41)**
ST:DS	1.1 (0.32)***	—	1.1 (0.31)***	—	1.2 (0.52)*	—
ST:SP	-1.4 (0.34)***	—	-1.4 (0.32)***	—	-1.2 (0.55)*	—
DS:SP	-0.87 (0.31)**	—	-0.95 (0.29)**	—	-0.4 (0.49)	—
Crown metrics						
CrL	—	—	—	—	—	—
CrV	—	—	—	—	—	—
CrD	9.1 (6.4)	-34 (6.8)***	8.9 (6.1)	-36 (7.2)***	5.5 (10)	-5.7 (10)
CrW:CrL	—	—	—	—	—	—
						3.1 (1.5)
Cr%	5.1 (0.84)***	-2.2 (0.99)*	5.1 (0.8)***	-2.6 (1)*	3.9 (1.4)**	

3.12 FIGURES
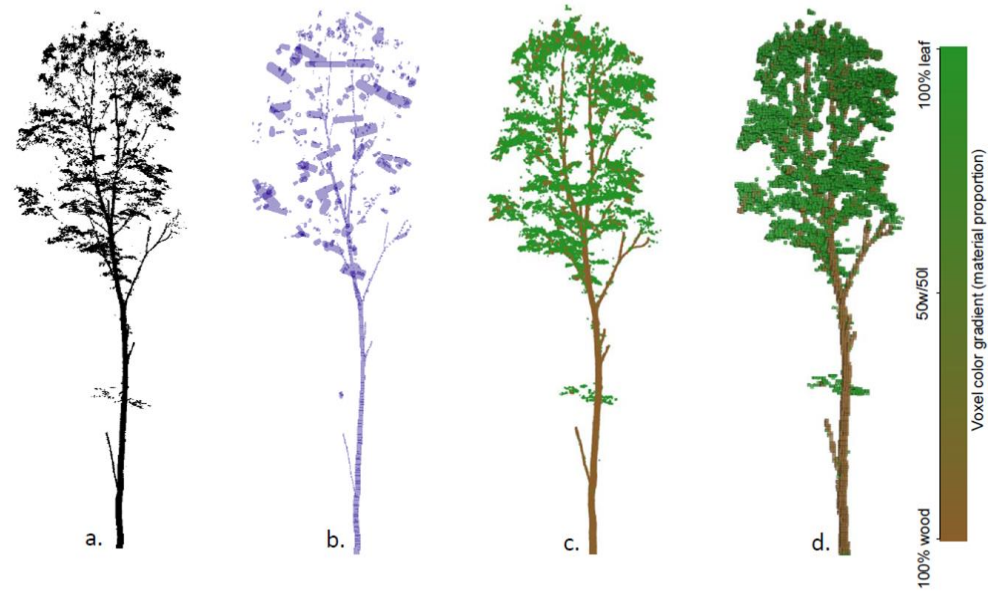
Figure 3-1: Illustration of the steps for wood/leaves discrimination. a. Filtered Sugar maple point cloud. b. Cylinder fitting on point cloud. c. Point cloud discriminated between leaves and wood points. Assignation of wood points to clusters of points retained for cylinders fitting using a threshold fitting error. Leaves points are the rests. d. Voxel grid with wood and leaves points proportion.
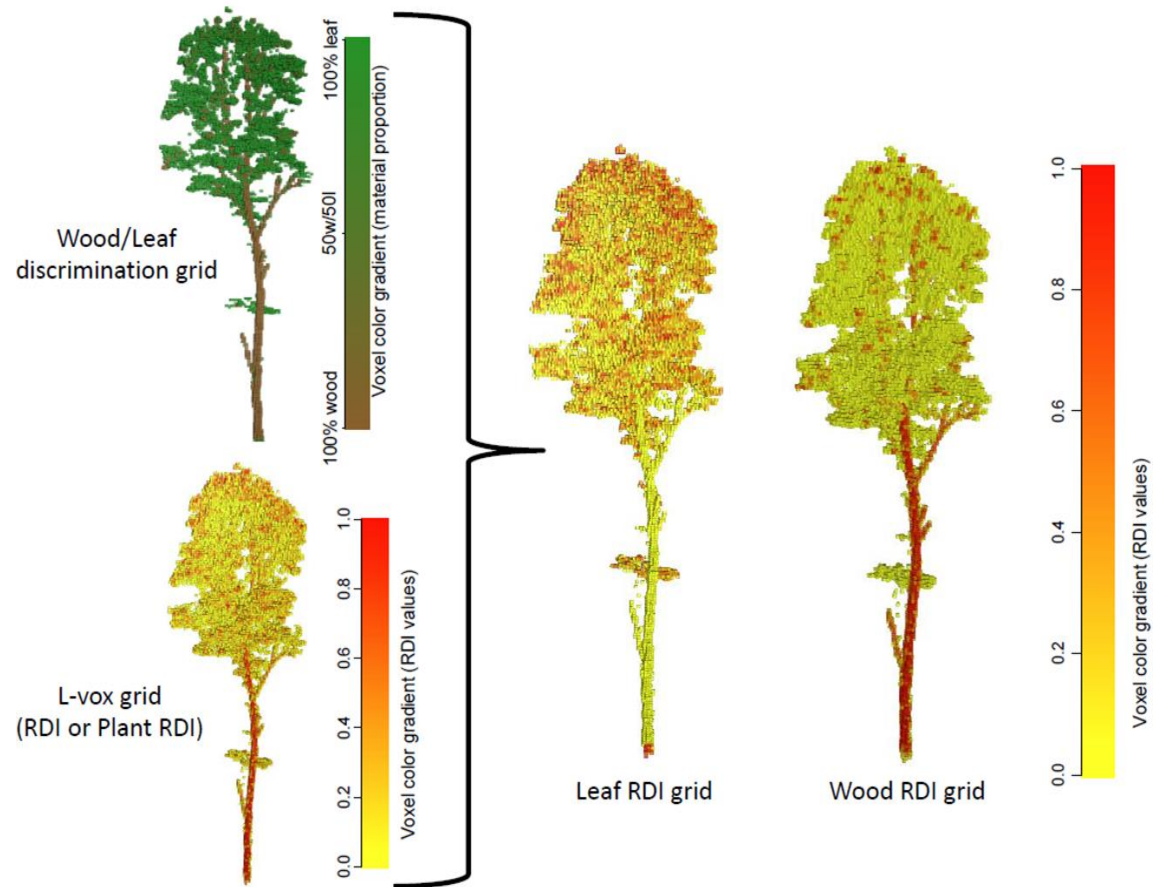
Figure 3-2: Illustration of the L-vox and wood/leaves grid combination. The relative density index (RDI) L-vox output is used to study the Plant relative density index (PRDI) profiles. Combination of RDI voxel grid and wood/leaves voxel grid correspondence allows obtaining leaf density relative index (LRDI) and wood density relative index (WRDI) profiles.

Figure 3-3: Mean beta distribution of Sugar maple. The upper and downer part shows respectively the distributions for intermediate and mature trees. Plain and dashed lines are respectively for trees in pure and mixed stands. Frown left to right plant relative density index (PRDI) profile, leaf relative density index (LRDI) profile and wood relative density index (WRDI) profile. On the Y axis 0 and 1 are respectively the bottom and the top of the crown.

Figure 3-4: Mean beta distribution of Balsam fir. The upper and downer part shows respectively the distributions for intermediate and mature trees. Plain and dashed lines are respectively fo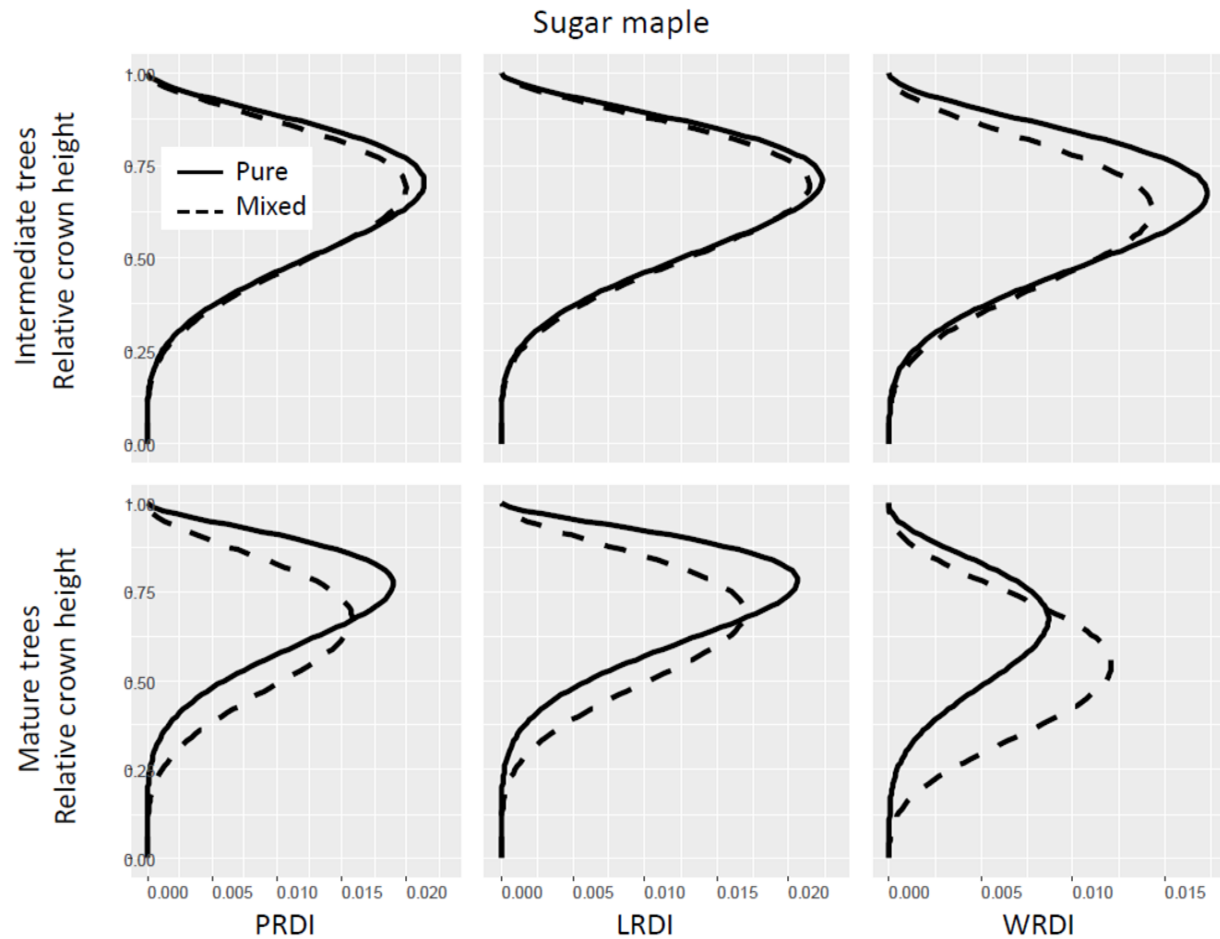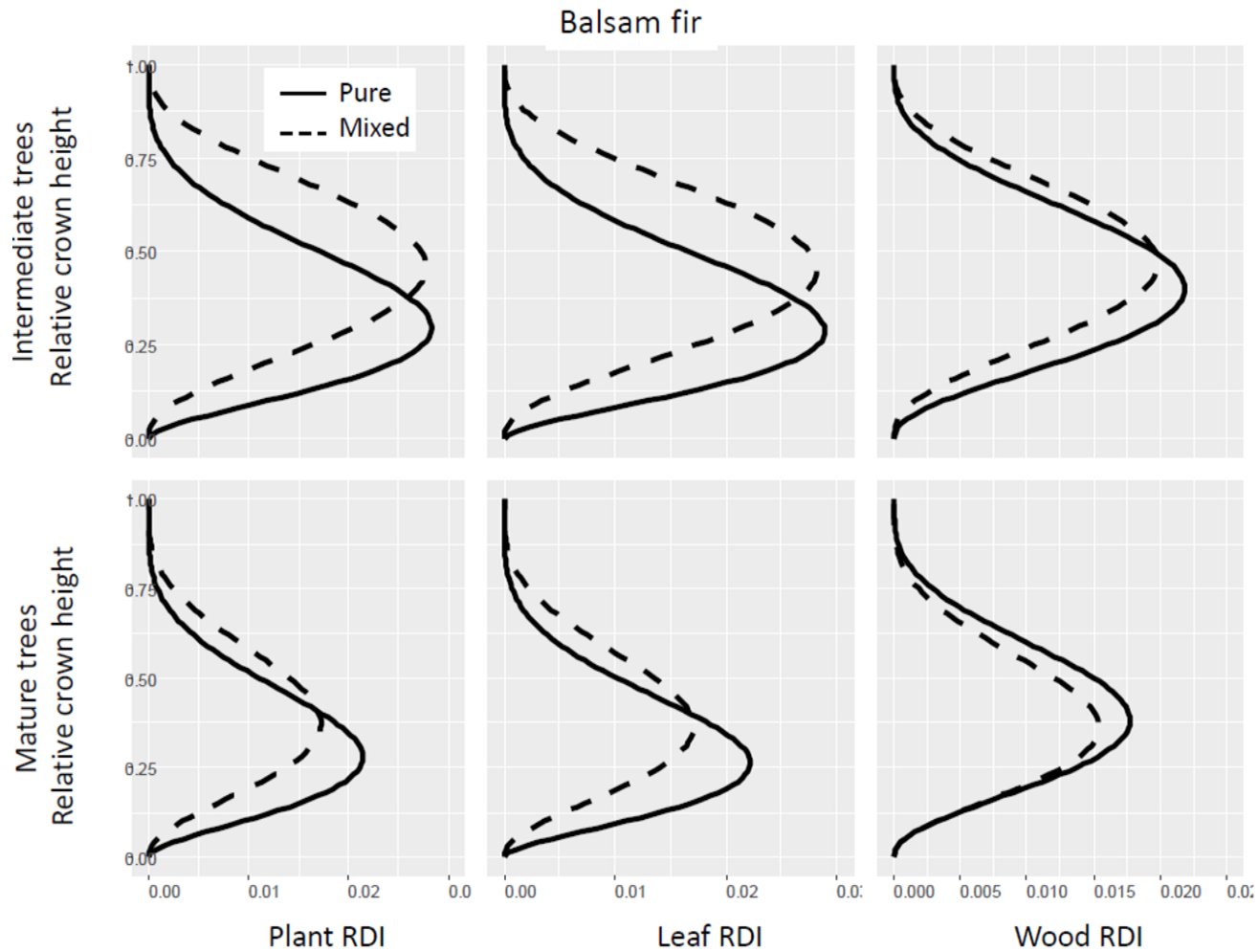r trees in pure and mixed stands. Frown left to right plant relative density index (PRDI) profile, leaf relative density index (LRDI) profile and wood relative density (WRDI).

CHAPITRE IV

UNE METHODE POURQUANTIFIER LES CHANGEMENTS DE LA CANOPEE A PARTIR DE DONNEES MULTI-TEMPORELLES DE LIDAR TERRESTRE : LA REPONSE DES ARBRES AUX TROUEES ENVIRONNANTES

4.1 RESUME

Ce troisième article intitulé « *A method to quantify canopy changes using multi-temporal terrestrial lidar data: tree response to surrounding gaps*», fut rédigé par moi-même ainsi que par les professeurs Robert Schneider et Richard Fournier. Il fut accepté pour publication dans sa version finale en 2017 par les éditeurs de la revue *Agricultural and forest meteorology*. Les contributions des différents coauteurs sont les mêmes que celles évoquées dans le premier chapitre. Une version abrégée de cet article a été présentée en séminaire à l'INIA de Madrid (Espagne) à l'automne 2016.

La croissance des branches et l'expansion du houppier qui en résulte jouent plusieurs rôles à l'échelle de l'arbre et du peuplement. L'expansion du houppier est très difficile à mesurer à cause de son inaccessibilité et de sa complexité. Dans ce troisième chapitre, nous proposons une méthode permettant de quantifier les changements temporels de la végétation dans la canopée. Cette méthode a été appliquée pour faire un suivi de la réponse du houppier à la formation de trouées. Une espèce feuillue (l'érable à sucre) et une espèce résineuse (le sapin baumier) ont été étudiées. La méthode a été développée à partir de données de LiDAR-t. Elle consiste à identifier les limites de la végétation à un temps t_0 et d'isoler le matériel produit ou déplacé entre le temps t_0 et le temps t_x.

102

Les changements de végétation ont été quantifiés à partir de quatre métriques et leurs profils verticaux ont été établis et analysés. Les résultats montrent que l'érable à sucre a une capacité de réponse à la libération de la compétition plus importante que le sapin baumier. Ceci est probablement dû à leurs développements architecturaux contrastés. Les deux espèces montrent une réoccupation de l'espace vers le bas très importante deux ans après la formation de la trouée. Cette réponse inattendue est probablement une conséquence des nouvelles contraintes mécaniques s'exerçant sur l'arbre suite à l'ouverture du couvert. Ce type de résultat révèle l'importance d'analyser les changements de la canopée dans toutes les directions et pas limitée au plan horizontal. La routine méthodologique développée dans cet article peut être adaptée à l'échelle de l'individu aussi bien que sur un groupe d'individus en bordure de trouée. Elle peut ainsi être appliquée dans le but de mieux comprendre comment les arbres réoccupent l'espace suite à la libération de la compétition pour la lumière après la formation d'une trouée.

4.2 A METHOD TO QUANTIFY CANOPY CHANGES USING MULTI-TEMPORAL TERRESTRIAL LIDAR DATA: TREE RESPONSE TO SURROUNDING GAPS.

4.3 ABSTRACT

Branch growth and the resulting crown expansion play many roles in tree and forest processes. Crown expansion is difficult to measure on an adult tree due to the crown's complexity and inaccessibility. The present study proposes a method to quantify vegetation changes over time. It was applied to follow the tree crown response to gap formation for broadleaved (Sugar maple) and coniferous (Balsam fir) species. The method was developed using terrestrial laser scanner (TLS) data. It consists in

identifying the vegetation boundaries at time t_0 and extracting the new material produced or displaced between time t_0 and time t_x. Changes in vegetation form were quantified with four metrics, and vertical profiles of these metrics were analysed. Results show that Sugar maple has a stronger response to gap formation compared to Balsam fir because of the different crown architectures. Both species showed considerable downward space reoccupation within most of the crown two years after the release of competition. These results are probably a consequence of a mechanical rearrangement of the crown and highlight the importance of analysing canopy changes in both the vertical and horizontal directions. The developed methodology can be applied to both individual trees as well as to a group of trees bordering a gap, in order to get insight on how trees recolonize the space that is freed by local and large scale disturbances.

4.4   KEYWORDS

Canopy; Crown expansion; Primary growth; Tree architecture; Gap closure; Mixed stands.

4.5   INTRODUCTION

The crown structure of a tree at a given time determines both the amount of light intercepted for its own growth and the amount of light available for neighbouring trees and the understory vegetation. Crown dimensions are also important inputs for models that simulate forest stand dynamics (Coates et al., 2003; Ligot et al., 2014; Medlyn, 2004). Moreover, canopy structure has major effects on rainfall interception and water availability. Canopies can intercept up to 50% of the annual precipitation in certain

ecosystems (Carlyle-Moses and Gash, 2011). Finally, the vertical organization of the canopy structure is closely related to the fauna diversity by creating specific habitats and microclimates (Shaw, 2004). Tree crown dynamics, defined as the changes over time in crown shape and space occupancy by branches, twigs and leaves, ultimately define crown structure, which is important in understanding stand dynamics for forest ecology and improving forest management. Silvicultural treatments such as fertilization and thinning can have important effects on crown dynamics (Weiskittel et al., 2007). For example, an increase in the growth of the lower part of the crown is observed after trees are released by thinning, due to the changes in the light environment. Furthermore, several studies conducted in managed stands have shown that crown length and width increase after the removal of competitors (Forrester et al., 2013; Gillespie et al., 1994). Crown length increases since self-pruning is reduced whereas crown width increases due to available space for lateral crown expansion. The intensity of the response after a significant structural change in the surroundings of the tree crown depends however on the species considered, the type of thinning and the age of the stand when it is thinned. For example, the growth in the lower part of the crown of Douglas fir increases more when it is thinned earlier (i.e. after precommercial thinning) than later (i.e. after commercial thinning) (Weiskittel et al., 2007). Moreover, crown dynamics will vary between species with shade tolerances, since self-shading is more important for shade tolerant species such as Douglas fir, when compared to certain shade intolerant Pines (Ruha et al., 1997). A good understanding of how tree crowns respond to silvicultural treatments is a key component to predict growth and wood quality, both of which are directly related to crown attributes in managed stands (Achim et al., 2006; Kellomäki et al., 1999; Schneider et al., 2011).

In natural forest dynamics, tree crown response to gap formation has also important implications on canopy closure and thus on tree regeneration (McCarthy, 2001). In this context it has been shown that coniferous species have generally a lower ability to close

a gap when compared to broadleaved species. This is probably due to the less flexible developmental mode of conifers (Getzin and Wiegand, 2007; Muth and Bazzaz, 2002). Vepakomma et al. (2011) observed a different response in boreal forests, where no difference between conifers and broadleaved species was observed. The location of the tree along the gap may also be important, where trees can exhibit higher crown expansions towards the south (Rouvinen and Kuuluvainen, 1997). On saplings or young trees, quantifying crown expansion has allowed a better understanding of how trees modulate their shape according to light availability and a more accurate assessment of species-specific plasticity and growth strategies (Beaudet and Messier, 1998; Canham, 1988; Petriţan et al., 2009). Finally, the importance of crown lateral extension in understanding tree growth, competition for space and persistence in canopy has also been highlighted in recent years (Kellner and Asner, 2014; Seidel et al., 2015a).

In spite of the major roles of crown dynamics on forest functioning and management, very few studies have tried to accurately follow the dynamics of the tree crown on a short time scale. An important reason for this shortcoming is that primary growth (Barthelemy and Caraglio, 2007) of the crown (e.g., shoot growth resulting in the elongation of the different axes) is difficult to quantify. Consequently, for practical reasons, the estimation of the primary growth of the tree crown usually focuses on the tree height increment. This reduces the problem to a unidirectional measurement (i.e. vertical) where orientation is not important. Tree height can be measured routinely in a plot with various devices such as a clinometer, measuring pole or laser altimeter (Clark and Clark, 2011; Larjavaara and Muller-Landau, 2013) or from airborne systems such as lidar and stereo-photogrammetry with large-scale aerial photographs (Wulder et al., 2012). The vertical elongation of the main tree axis is, however, only one of the components of primary growth. It is actually composed of the increment of each branch, with the end result being the expansion of the crown. However, *in situ*

measurements of branch elongation increments or total crown expansion are rarely done on adult trees due to the inaccessibility and the inherent complexity of the branching systems. Mature trees can be destructively sampled (Heuret et al., 2002; Lintunen and Kaitaniemi, 2010; Weiskittel et al., 2007) and primary growth measured retrospectively using markers, but it is generally laborious or impossible and does not allow growth monitoring. Dynamic studies with crown growth monitoring are hard to carry out due to logistical and cost constraints; tree crown studies are thus generally limited to crown attributes at a given time (Barbeito et al., 2014; Getzin and Wiegand, 2007; Longuetaud et al., 2013). Therefore, quantifying primary growth and crown changes over time for adult trees presents a huge methodological challenge.

Aerial (ALS) and terrestrial laser scanners (TLS) provide very accurate three-dimensional (3D) point cloud representations of the spatial distribution of elements composing the forest canopy (Côté et al., 2012). These remote sensing tools enable users to obtain complex and diverse canopy metrics without destructive sampling or climbing trees. In the last decade, many authors have used ALS and TLS systems to quantify canopy structure and its diverse roles in forest dynamics (Kato et al., 2009; Seidel et al., 2012). Metrics can now be easily obtained from point clouds and allow the estimation of canopy density profiles (Ashcroft et al., 2014) or above-ground biomass (Dassot et al., 2012). Indeed, above-ground biomass estimates based on TLS data were reported to be more accurate compared to traditional allometric equations (Calders et al., 2015; Srinivasan et al., 2014). Since laser scanners are non-destructive, changes in forest structure can be obtained (Liang et al., 2012). Furthermore, crown metrics such as crown asymmetry used to estimate crown plasticity can now be much more accurately measured. The envelope of the crown allows a precise quantification of the space occupation and the surface of the crown, both of which can be precisely assessed with TLS data (Bayer et al., 2013; Martin-Ducup et al., 2016). Finally, the potential for some of these new metrics to predict tree growth or tree crown plasticity

have also been highlighted (Seidel et al., 2015b, 2011). Despite these technological advances, to our knowledge, no studies have tried to quantify changes over time of individual tree crowns.

The main objective of this study was to develop a procedure to quantify canopy changes with TLS data. This was achieved by developing computationally easy indicators of growth and displacement that can be quickly extracted from TLS point clouds. More specifically, the proposed method quantifies the amount of displaced vegetation biomass and its global, horizontal and vertical changes using multi-temporal TLS data. The method can be applied to produce vertical profiles of the entire tree crown or by cardinal direction. The proposed method was applied to adult trees in order to characterize their response to canopy openings. Using the proposed method, we were able to test the hypothesis that (i) Sugar maple (*Acer saccharum* Marsh.) trees have a stronger response to canopy openings than Balsam fir (*Abies balsamea* (L.) Mill.), (ii) trees growing in pure stands show no differences compared to trees growing in mixed stands when competition for light was removed, and (iii) both species show a stronger crown response in the most sun exposed direction (south).

4.6 MATERIALS AND METHODS

4.6.1 Study site and species

A total of six Sugar maple and Balsam fir mixed forest sites located in eastern Quebec, Canada, were selected using the provincial eco-forest maps developed by the Quebec Ministry of Forests, Wildlife and Parks (MFFP, 2007). Each site was composed of three stand types: a pure Balsam fir stand, a pure Sugar maple stand, and a mixed stand with both species (see Martin-Ducup *et al.* (2016) for details on the mixed stand composition). Tree characteristics of both species in pure and mixed stands are given

in Table 4.1. Balsam fir and Sugar maple are both very shade tolerant species (Humbert et al., 2007) which present well contrasted architectural developments. On the one hand the Balsam fir is a softwood species with a Massart architectural model (*sensu* (Hallé et al., 1978). The strong apical dominance of the main axis (the trunk) and the horizontal branches yields this species' rigid conic shape with a well-defined trunk. On the other hand the Sugar maple is a hardwood species which presents a combination of several architectural models: Leuwenberg/Koriba/Rauh. Its development changes during the ontogeny and a progressive loss of the apical dominance is observable giving to this species a sparse crown which allows a more flexible crown development (Millet, 2012).

4.6.2   Target-tree measurements

In August 2013, five to six healthy co-dominant trees (i.e. no evidence of damage on the stem or the main branches) per species were selected in both the pure and mixed stands for each site. The direct competitors of each Target-Tree (TT) were felled in order to release the TT from competition on all sides so as to simulate small local gaps surrounding the TT. A neighboring tree was considered as a competitor of the TT when both crowns touched. After release, the TTs were scanned with a Faro Focus 3D set with a resolution angle of 0.036° in both the horizontal and vertical directions and scanner rotation angles from 0 to 360° in the horizontal direction (a full turn) and from -60 to 90° in the vertical direction. The built-in compass was activated in order to have the scan orientation. Each TT was multi-scanned from four opposite viewpoints to minimize occlusion and maximize visible details of the TT crown. Each individual scan was aligned using six spherical targets, with a minimum of three targets seen from each

scan. The TTs were re-scanned during the summer of 2015 using the same scanner settings and the same scan positions, which were marked in the field.

4.6.3 Data preparation

Multi-scan alignments were preprocessed with Faro Scene 5.0.1 (Faro, 2012). Noise points were removed with two filters available in Faro Scene: the dark scan point filter and the stray filter (see Martin-Ducup *et al.* [2016] for more details). This procedure produced one point cloud per tree for 2013 and 2015. The crown base coordinates of each TT were obtained manually from the planar views of the point cloud.

4.6.4 Point cloud processing

Once the point clouds were aligned in Faro Scene and exported as ASCII files, they were processed in CloudCompare (*CloudCompare [GPL software]*, 2015) and R (R Development Core Team, 2011). The R software was used to construct crown meshes, to voxelize point cloud, and to obtain changes in height profiles with and without cardinal directions. CloudCompare was used to orient the normals of the mesh and calculate point-to-point and point-to-mesh distances (Fig. 4.1). The following subsections describe the various steps of the point cloud processing.

Temporal point cloud alignment

The inter-year TT point cloud alignment was a crucial step to reduce possible bias in quantifying crown changes. The annual TT point cloud were manually aligned in CloudCompare, as the automated "iterative closest point" (ICP) algorithm was not precise enough (Fig. 4.2).

Bi-temporal crown comparison

The first step in quantifying crown changes between two different years was to define a boundary in the scene of the first year (S_0 at t_0). This boundary consisted in finding the outer limits of the crown at t_0. They were obtained with an alpha shape 3D being fitted to the TT point cloud belonging to the crown (Lafarge and Pateiro-Lopez, 2014). The parameter α of the alpha shape function was set to 1 for every tree crown, as this value was found to yield accurate crown hulls without creating substantial holes inside the mesh. The result of the algorithm is a hull mesh of the external limits of the crown (Fig. 4.3a). For this case study, differences in tree crowns between 2013 and 2015 (2-year step) are described.

The second step was to identify the points of the t_x scene (S_x) that are outside of the t_0 mesh (defined as CP, or the changed points). The orientation of the normals for each face of the mesh was used. The orientation was, however, not given by the "alpha-shape 3d function" in R. The mesh was thus exported to CloudCompare where the points were sampled on the mesh and normals were associated with these points using a minimum spanning tree algorithm. The mesh was then re-built from the mesh sampled points with normals using the Poisson surface reconstruction plugin (Kazhdan and Hoppe, 2013). Finally, the points from S_x were compared to the S_0 mesh using the cloud-to-mesh distance ("*C2M*") tool available in CloudCompare, yielding the CP that correspond to the points outside the mesh (Fig. 4.3 b and c). The comparison between the mesh and CP can be used to quantify the global changes between t_0 and t_x without, however, providing any information on the direction of the changes.

The CP were then compared to the S_0 cloud point using the cloud-to-cloud distance ("*C2C*") tool in CloudCompare. This algorithm computes the Hausdorff's distance between the point cloud by comparing S_x and the reference cloud (S_0) by searching in S_x for the closest points of each point of S_0 and computing their distance (Girardeau-Montaut et al., 2005) as:

$$d(p_x, S_0) = \min ||p_x - p_0||$$

(1)

where p_x is a point of S_x and p_0 is the nearest point of p_x in S_0. In addition to the distance, the output of the algorithm provides the displacement vector between p_0 and p_x. This vector was then used to obtain the horizontal and vertical changes between t_0 and t_x.

Quantifying changes in the crown after release

Crown changes were quantified by the following:

- The **global expansion (GE),** defined as the distance measured by the cloud-to-mesh algorithm previously described.
- The **horizontal expansion (HE)**, computed as the horizontal distance between p_t and p_{t1} for each CP:

$$Hd_{pt1} = \sqrt{(x_{pt1} - x_0)^2 + (y_{pt1} - y_0)^2} - \sqrt{(x_{pt} - x_0)^2 + (y_{pt} - y_0)^2}$$

(2)

where $(x_{pt1}; y_{pt1})$ are the coordinates of $pt1$, $(x_{pt}; y_{pt})$ are the coordinates of pt and $(x_0; y_0)$ are the coordinates of the center of the scene, that is, the center of the trunk of the TT at its crown base identified using the points in a 1-cm slice of the cloud point from the trunk at the crown base, on which a circle was fit with the Pratt method (Chernov and Lesort, 2014). Moreover, the vertical axis passing through this point is considered as the axis of symmetry of the scene.

- The **vertical expansion (VE)**, quantified using the Z coordinate of the CP output vector of the cloud-to-cloud distance algorithm previously described. Positive values indicate upward vertical changes, and negative values indicate downward vertical changes.

- The **material displaced** (**MD**), defined as the number of non-empty 5-cm edged voxels of the CP and converted into m^3.
- The **relative horizontal expansion (HE:GE)**, which is the ratio between VE and GE.

To obtain between-tree comparable height profiles, the CPs of each tree were divided into 20 vertical slices (5% of crown length). The 95th percentile (or the maximum absolute value between the 5th and the 95th percentile for VE) of the expansion measurements of each slice (GE, HE) in meters (m) was calculated to establish their vertical profiles, whereas the volume per slice in cubic meters (m^3) was used for DB. All the algorithms were developed as functions in the R language.

4.6.5   Data analysis

Species-wise linear mixed models were used to analyse the effect of height within the crown (HL) and stand type (ST, i.e. mixed and pure) on the four crown change variables (GE, HE, VE, DB). For each model, tree and site random effects were used to account for "within site" and "tree within site" correlations, and diameter at breast height (DBH) was considered as a covariable (Eq. 4).

$$Y_{ijkl} = \mu + ST_{ij} + HL_{ijkl} + ST_{ij}HL_{ijkl} + a_1\, DBH + u_k + u_i + \varepsilon_{ijkl} \tag{4}$$

where Y_{ijkl} is one of the structural change variables measured at HL (l) of tree (k) of stand type (j) in the site (i), and where a_1 is a fixed parameter and μ the overall mean. The variable ST_{ij} is a binary variable indicating stand type ($ST_{ij} = 0$ for mixed stand, $ST_{ij} = 1$ for pure stand), and HL_{ijkl} is a factor variable indicating the height level (HL_{ijkl} from 1 to 20 for each 5% height level of the tree). The parameters u_k and u_i are respectively the normally distributed tree within site and site random effects parameters ($u_k \sim N(0, \sigma_k^2)$, $u_i \sim N(0, \sigma_i^2)$), and ε is the residual error ($\varepsilon_{ijkl} \sim N(0, \sigma_i^2)$).

The same model was used to analyse the effects on relative horizontal expansion (HE:GE), except that the effect of species (SP) was analysed and not the stand type:

$$Y_{ijkl} = \mu + SP_{ij} + HL_{ijkl} + ST_{ij}HL_{ijkl} + a_1\,DBH + u_k + u_i + \varepsilon_{ijkl} \tag{5}$$

where Y_{ijkl} is the HE:GE variable, and SP_{ij} is a binary variable to indicate species ($SP_{ij} = 0$ for Sugar maple, $SP_{ij} = 1$ for Balsam fir).

Linear contrasts were used to compare Y_{ijkl} at different HL. Four groups were made to build the contrasts: (i) first quarter crown (HL between 0-25%), (ii) second quarter (HL between 30-50%), (iii) third quarter (HL between 55-75%), and (iv) fourth quarter (HL between 80-100%). In the case of a significant effect of HL, the resulting six contrasts were made to make pairwise comparisons between all groups. In the case of a significant interaction effect between HL and stand type, the same contrasts were used for each stand type (pure and mixed) and another set of contrasts was made to compare differences between pure and mixed stands for a given HL group. A total of 16 contrasts were thus carried out when the interaction effect was significant: six contrasts for pairwise comparisons between groups in pure stands plus six contrasts for pairwise comparisons between groups in mixed stands plus four contrasts for pairwise comparisons for each group between pure and mixed stands.

Finally, the effect of the cardinal direction on GE, HE and DB was analysed with a two degree resolution using circular statistics. A Rayleigh test was performed to evaluate if changes between 2013 and 2015 were uniformly distributed (H_0: random direction) or distributed around the southern direction (H_1: 270°) (Batschelet, 1981) using steps of two degrees. For every test, a difference was considered statistically significant from 0 with an error of 5% (i.e. α=0.05).

4.7   RESULTS

4.7.1   Profile analysis

Changes in crown structure were larger for Sugar maple than for Balsam fir, with the differences particularly evident for GE and DB (Fig. 4.4). Both species showed significant height variations for each profile, while the profile shapes were generally species dependent (Fig. 4.4 and Table 4.2). The relative horizontal expansion (HE:GE ratio) was higher for Balsam fir than for Sugar maple over almost the entire length of the crown (Fig. 4.5). Differences between the two species were, however, significant for the first and second quarters only (*p-value*s < 0.001) (Table 4.4). For Sugar maple, the contrast analysis revealed that the profile was homogeneous with non-significant differences between the different quarters of the crown, but a decreasing tendency in the highest part was observed (Table 4.4 and Fig. 4.5). For Balsam fir, this tendency was statistically significant with the fourth quarter significantly lower than the three others (*p-value*s < 0.001).

Sugar maple trees growing in mixed stands showed larger changes in the bottom half of the crown compared to trees growing in pure stands in all profiles (Fig. 4.4). This interaction was significant for GE, VE and DB (*p-value*s < 0.001 for GE and VE and *p-value*=0.015 for DB) but not for HE (*p-value*=0.066) (Table 4.2). The contrast revealed that the first and second quarters had significantly higher values of GE, VE and DB in mixed stands compared to pure stands (*p-value*s < 0.001 for the first quarter of GE and VE and *p-value*=0.012 for DB; 0.01, < 0.001 and 0.02 for the second quarter of GE, VE and DB respectively) (Table 4.3). For Balsam fir, no significant effect of stand type or its interaction with height level was found for any profile (Table 4.2). For both species and in both stand types, the VE in pure as well as in mixed stands was negative up to 80% to 85% of the crown height (Fig. 4.4). Differences in VE between

the fourth quarter and the first three quarters were always significant for both species; differences between the third and the first two quarters were significant for Sugar maple in mixed stands and for Balsam fir only (Table 4.3).

4.7.2   Cardinal direction effect

Both species expanded their crowns in all cardinal directions. This was true for the three variables GE, HE and DB (Fig. 4.6). Rayleigh's test revealed that Balsam fir expansion was not greater towards the south. Sugar maple, however, had a significantly larger GE, HE and DB towards the south (*p-value*s=0.005 for GE and < 0.001 for HE and DB) (Table 4.5). The mean expansion direction was actually closer to the southwest, with a mean of 229, 230 and 234° for GE, HE and DB respectively (Table 4.5).

4.8   DISCUSSION

We developed an innovative method to quantify 3D vegetation changes in crown structure over time using TLS data. These changes can be presented as vertical profiles and can be decomposed into different azimuthal directions. The method was applied at the individual tree scale in order to quantify tree crown responses to the release of competition. The response was species-dependent and varied with stand type.

4.8.1 Sugar maple and Balsam fir response to release

Sugar maple showed a greater crown response to canopy opening than Balsam fir for all the studied variables, and thus our first hypothesis was confirmed. This is compatible with previous studies showing that broadleaved species usually have greater crown plasticity (often quantified as crown asymmetry) compared to coniferous species (Getzin and Wiegand, 2007; Muth and Bazzaz, 2002). This contradicts Vepakomma *et al*. (2011) who observed that lateral growths of coniferous trees located at gap edges were similar to those of broadleaved trees. In their study, all the broadleaved species were shade intolerant and all the coniferous species were shade tolerant. It is known that the shade tolerant crowns usually have large plastic responses in order to maximize light interception, which could explain their results (Valladares and Niinemets, 2008).

In the present study, both species were highly shade tolerant (Humbert et al., 2007). Moreover, Sugar maple has a high crown plasticity (Brisson, 2001; Martin-Ducup et al., 2016). It was found that the relative horizontal expansion was higher for Balsam fir than for Sugar maple. This was a consequence of the architectural constraints of Balsam fir (and many other conifers) with an indeterminate growth of the apical meristem (Barthelemy and Caraglio, 2007) and strictly horizontal branches (Millet, 2012). But even if the relative horizontal expansion was higher for Balsam fir, the architectural development of Sugar maple, which promotes multidirectional growth through the determinate functioning of primary meristems, seemed to be more efficient for horizontal occupancy following gap formation. It has to be noted that these relative horizontal expansions decrease drastically in the upper part of the crown for both species. This can be explained by the fact that beyond 85% of crown height, a shift between horizontal and vertical growth occurs. This is confirmed by the vertical expansion as we observed an upward vertical expansion increasing above 85% of the crown for both species, which is probably due to the fact that the upper part of the

crown is the most directly exposed to the sun. These observations are based on the comparison of two species only. It would be important to follow the 3D changes in more species in order to generalize our conclusions whereby these trends are due to the developmental mode of these two important taxonomic groups or if the response is species-specific.

It is very surprising to observe such a considerable downward expansion below 80% of the crown, reaching -0.5 m for Sugar maple and -0.23 m for Balsam fir two years after the gap formation. It is difficult to explain this phenomenon physiologically because two years is too short for an adult tree to grow new branches at the base of the crown in order to reshape it. A more probable explanation would be mechanical. The removal of the competing neighbors increases exposure to wind and snow and probably removes support from neighboring trees. The reduced neighboring competition could therefore lead to sagging of the lower branches and global crown opening. This phenomenon was visually observed on most of the trees. An example of this substantial downward expansion due to changes in branch angle is shown for a Sugar maple and a Balsam fir tree in Fig.4.7.

Our results confirmed that trees in mixed stands do not react to release differently from trees found in pure stands (e.g. second hypothesis) for Balsam fir only. We observed a different reaction for Sugar maple. This is probably an indirect mixing effect. Indeed, Martin-Ducup *et al.* (2016) showed that for the same trees, Sugar maple growing in mixed stands has a higher crown volume as well as a deeper and more open crown, which suggests longer branches in the low part of the crown. The fact that Sugar maple trees in mixed stands have larger changes in their crown when gaps are created beside them is likely a consequence of the crown structure of the tree at the time of release, and not directly due to the type of stand. Indeed, these differences were observed in the bottom half of the crown only.

Sugar maple showed the most expansion towards the southwestern direction, but not for Balsam fir which partially confirmed our third hypothesis. This is in accordance with the study by Rouvinen and Kuuluvainen (1997) on Scots pine in Finland (62° N) who also found that crowns grow more in the southwestern direction in the absence of competition. However, most of the studies conducted in lower latitudes (from 40° to 55° N) did not find this trend (Gavrikov et al., 1993; Getzin and Wiegand, 2007; Pedersen and Howard, 2004). Pedersen and Howard (2004) suggested that soil evaporation and the higher transpiration rate in the most sun exposed part could limit the effect of higher light interception. In Quebec, where the present study was conducted (~ 46°N), stress by water deficit and its influence on tree growth is generally not important (Fortin and Langevin, 2010; Franceschini et al., 2016) and could thus explain our results.

4.8.2   Methodological considerations

The new method presented in this study has several advantages in terms of computation. It uses open source algorithms already available in R and in CloudCompare, and it is species independent. Moreover, all algorithms are quick to apply (~90 sec excluding the manual steps). The proposed methodology could thus be adapted to be used on larger areas, therefore including more trees than just a single target tree. The method is not species specific. It was tested on two species with distinct crown morphologies, and it resulted in profiles in accordance with the expected architectural structure of each species. The main limitation encountered was the substantial time required for crown isolation and alignment between years. The procedures are done manually because the automated ICP alignment algorithm in CloudCompare was not precise enough (Fig.4.2). However, depending on the time scale studied (i.e. changes over a decade or more) and the precision required, automatic

alignment could be sufficient. In addition, we did not face the problem of tree isolation or major occlusion as sampled trees were released from all competition. Several automated or semi-automated tools have recently been developed to isolate individual trees in high density forests (Calders et al., 2015; "Computree," 2010; Shendryk et al., 2016) and to correct for occlusions (Fournier et al., 2015), opening the path to apply the proposed methods to follow crown development in closed forests. The proposed method is only interested in the dynamics of the crown beyond its state in 2013, and it only considers crown expansion. The between-year point to point distance within the convex hull could lead to important misinterpretations, as the point-to-point algorithm calculates the distance between the point at time t_x and the closest point at time t_0. It might thus be possible that the point at time t_x might not be from the same branch when compared with the point from time t_0, due to important changes in the branch angles (e.g. branch sagging). The resulting interpretation on directional shrinkage could thus be biased if the branches are not individually identified. The proposed method works with the raw point cloud, where tree topology is not addressed.

This method quantifies with fine spatial detail the vertical profile of crown changes. It be used on the whole crown or applied to specific directions. It is well adapted to study how vegetation re-occupies a gap. It could thus have important applications in forest ecology studies or forest management. For example, studying the effect of silvicultural treatments on changes in tree structure is very important because of the relationship between tree structure and wood quality (Blanchette et al., 2015; Pretzsch and Rais, 2016). The proposed methods could focus on gaps instead of the tree crowns allowing to study gap dynamics without any procedural changes. The only difference between crown or gap analysis would be to use the boundaries of the gap instead of the limit of an individual crown. The same alpha-shape 3D algorithm can create a mesh of the gap, and the points outside of the mesh used to calculate how the gap closes after the disturbance.

Of the four metrics studied (global, vertical and horizontal expansion, and material displaced), total DB is probably the best proxy for primary growth as it quantifies the amount of biomass created (or at least displaced) instead of a distance of potential growth. However, a non-negligible part of the changes observed in our study was due to the mechanical movement of branches and cannot be considered as growth of the primary meristems. It was particularly obvious considering the important negative vertical expansion we observed (Fig. 4.7). Obviously the horizontal expansion is also affected by branch displacement. Thus lateral growth often quantified in gap studies to evaluate lateral gap closure by canopy trees is probably overestimated, as some of the growth is in fact rearrangement of the branches (Runkle and Yetter, 1987; Vepakomma et al., 2011; Young and Hubbell, 1991). For example, Runkle and Yetter (1987) observed for Sugar maple a lateral growth of 20 cm/year seven years after a gap formation and then reported ((Runkle, 1998) a growth of 13 cm/year after 14 years. In our case, we observed for the same species an average maximum horizontal expansion of 32 cm/year only two years after the gap formation (Table 4.1). Basically, the lateral growth measured by projection using manual (visual delimitation) or numerical tools (image or LiDAR data analysis) probably overestimates primary growth because of the crown mechanical rearrangement. However, in a context of quantification of primary growth in an unperturbed environment or a long time after a perturbation, our method should give a good approximation of primary growth.

Our work opens new perspective for studying ecophysiological processes by increasing the number of structural variables available for modelling purposes. For instance, it provides the possibility to use TLS and potentially ALS to measure crown-related characteristics that can then be used to predict tree growth (Seidel et al., 2015b), wood fibre attributes (Blanchette et al. 2015) or timber characteristics (Van Leeuwen et al., 2011). More importantly, gap size and dynamics contribute to many micrometeorological processes like solar radiation, soil temperature and water content or wind pattern which determine fauna habitat and diversity, soil nutrient cycles and

tree regeneration (Latif and Blackburn, 2010; Lowman and Rinker, 2004). Quantifying crown growth rate and speed of canopy closure is thus one part in better understanding of several ecosystem processes. A major advantage of using LiDAR data to assess crown dynamics is that the measurements that are obtained are reproducible, compared to certain measurements obtained from the forest floor. LiDAR based measurements are also better than estimates obtained by allometric relationships, as allometric relationships predict population averages for individuals with the same characteristics. The current work was applied to northern forest ecosystems but can easily be expanded to other ecosystems. The most limiting factor is the availability of specialized algorithms to deal with LiDAR data, the ability to handle some limitations related to the LiDAR datasets such as signal occlusion or handling large datasets of point clouds.

4.9   CONCLUSION

The proposed method quantifies 3D canopy dynamics using TLS data. The method was applied to individual trees and was able to follow short-term changes in crown structure. We were able to analyse vertical profile responses of two species with different architectures to canopy openings. Our approach highlighted an important bias of previous studies quantifying horizontal crown/canopy growth. After being released, tree crowns of the two studied species underwent a mechanical rearrangement. Thus, ground-based estimations of horizontal crown growth could be overestimated if the surrounding environment of the tree was recently disturbed. We therefore suggest decomposing changes in crown structure (e.g. global changes to vertical and horizontal changes) and representing the changes using vertical profiles. Finally, the method could easily be applied at the gap level to conduct gap studies and could be a useful tool for

forest managers to study crown responses to different silvicultural treatments, which is a key element for productivity and wood quality.

4.10 ACKNOWLEDGEMENTS

4.11 REFERENCES

Achim, A., Gardiner, B., Leban, J., Daquitaine, R., 2006. Predicting the branching properties of Sitka spruce grown in Great Britain. N. Z. J. For. Sci. 36, 246.

Ashcroft, M.B., Gollan, J.R., Ramp, D., 2014. Creating vegetation density profiles for a diverse range of ecological habitats using terrestrial laser scanning. Methods Ecol. Evol. 5, 263–272. doi:10.1111/2041-210X.12157

Barbeito, I., Collet, C., Ningre, F., 2014. Crown responses to neighbor density and species identity in a young mixed deciduous stand. Trees 28, 1751–1765. doi:10.1007/s00468-014-1082-2

Barthelemy, D., Caraglio, Y., 2007. Plant architecture: A dynamic, multilevel and comprehensive approach to plant form, structure and ontogeny. Ann. Bot. 99, 375–407.

Batschelet, E., 1981. Circular statistics in biology. Academic press London.

Bayer, D., Seifert, S., Pretzsch, H., 2013. Structural crown properties of Norway spruce (Picea abies [L.] Karst.) and European beech (Fagus sylvatica [L.]) in mixed versus pure stands revealed by terrestrial laser scanning. Trees 27, 1035–1047. doi:10.1007/s00468-013-0854-4

Beaudet, M., Messier, C., 1998. Growth and morphological responses of yellow birch, sugar maple, and beech seedlings growing under a natural light gradient. Can. J. For. Res. 28, 1007–1015. doi:10.1139/x98-077

Blanchette, D., Fournier, R.A., Luther, J.E., Côté, J.-F., 2015. Predicting wood fiber attributes using local-scale metrics from terrestrial LiDAR data: A case study of Newfoundland conifer species. For. Ecol. Manag. 347, 116–129.

doi:10.1016/j.foreco.2015.03.013

Brisson, J., 2001. Neighborhood competition and crown asymmetry in Acer saccharum. Can. J. For. Res. 31, 2151–2159. doi:10.1139/x01-161

Calders, K., Newnham, G., Burt, A., Murphy, S., Raumonen, P., Herold, M., Culvenor, D., Avitabile, V., Disney, M., Armston, J., others, 2015. Nondestructive estimates of above-ground biomass using terrestrial laser scanning. Methods Ecol. Evol. 6, 198–208.

Canham, C.D., 1988. Growth and Canopy Architecture of Shade-Tolerant Trees: Response to Canopy Gaps. Ecology 69, 786–795. doi:10.2307/1941027

Carlyle-Moses, D.E., Gash, J.H., 2011. Rainfall interception loss by forest canopies, in: Forest Hydrology and Biogeochemistry. Springer, pp. 407–423.

Chernov, N., Lesort, C., 2014. Fitting ellipses, circles, and lines by least squares. Br. J. Math. Comput. Sci. 4, 33–60.

Clark, D.A., Clark, D.B., 2011. Assessing Tropical Forests' Climatic Sensitivities with Long-term Data. Biotropica 43, 31–40. doi:10.1111/j.1744-7429.2010.00654.x

CloudCompare [GPL software], 2015.

Coates, K.D., Canham, C.D., Beaudet, M., Sachs, D.L., Messier, C., 2003. Use of a spatially explicit individual-tree model (SORTIE/BC) to explore the implications of patchiness in structurally complex forests. For. Ecol. Manag. 186, 297–310.

Computree [WWW Document], 2010. . RD Innov. ONF. URL http://computree.onf.fr

Côté, J.-F., Fournier, R.A., Frazer, G.W., Niemann, K.O., 2012. A fine-scale architectural model of trees to enhance LiDAR-derived measurements of forest canopy structure. Agric. For. Meteorol. 166, 72–85.

Dassot, M., Colin, A., Santenoise, P., Fournier, M., Constant, T., 2012. Terrestrial laser scanning for measuring the solid wood volume, including branches, of adult standing trees in the forest environment. Comput. Electron. Agric. 89, 86–93. doi:10.1016/j.compag.2012.08.005

Faro, 2012. Faro Scene 5.0 [WWW Document]. Httpwwwfarocomproductsfaro-Softwaresceneoverview.

Forrester, D.I., Collopy, J.J., Beadle, C.L., Baker, T.G., 2013. Effect of thinning, pruning and nitrogen fertiliser application on light interception and light-use efficiency in a young Eucalyptus nitens plantation. For. Ecol. Manag. 288, 21–30. doi:10.1016/j.foreco.2011.11.024

Fortin, M., Langevin, R., 2010. ARTEMIS-2009 : un modèle de croissance basé sur une approche par tiges individuelles pour les forêts du Québec (No. Mémoire de recherche forestière n°156). Ministère des Ressources naturelles et de la Faune, Direction de la recherche forestière, Québec, Canada.

Fournier, R., Côté, J.-F., Bourge, F., Durrieu, S., Piboule, A., Béland, M., Grau, E., 2015. A method addressing signal occlusion by scene objects to quantify the 3D distribution of forest components from terrestrial lidar., in: 28th-30th September 2015. Presented at the Proceedings of SilviLaser 2015. 14th

conference on Lidar Applications for Assessing and Managing Forest Ecosystems, La Grande Motte. France.

Franceschini, T., Martin-Ducup, O., Schneider, R., 2016. Allometric exponents as a tool to study the influence of climate on the trade-off between primary and secondary growth in major north-eastern American tree species. Ann. Bot. mcw003. doi:10.1093/aob/mcw003

Gavrikov, V.L., Grabarnik, P.Y., Stoyan, D., 1993. Trunk-Top Relations in a Siberian Pine Forest. Biom. J. 35, 487–498.

Getzin, S., Wiegand, K., 2007. Asymmetric tree growth at the stand level: Random crown patterns and the response to slope. For. Ecol. Manag. 242, 165–174. doi:10.1016/j.foreco.2007.01.009

Gillespie, A.R., Allen, H.L., Vose, J.M., 1994. Amount and vertical distribution of foliage of young loblolly pine trees as affected by canopy position and silvicultural treatment. Can. J. For. Res. 24, 1337–1344.

Girardeau-Montaut, D., Roux, M., Marc, R., Thibault, G., 2005. Change detection on points cloud data acquired with a ground laser scanner. Int. Arch. Photogramm. Remote Sens. Spat. Inf. Sci. 36, W19.

Hallé, F., Oldeman, R.A.A., Tomlinson, P.B., 1978. Tropical trees and forests: an architectural analysis. Springer-Verlag.

Heuret, P., Barthelemy, D., Guedon, Y., Coulmier, X., Tancre, J., 2002. Synchronization of growth branching and flowering processes in the south american tropical tree Cecropia obtusa (Cecropiaceae). Am. J. Bot. 89, 1180–1187.

Humbert, L., Gagnon, D., Kneeshaw, D., Messier, C., 2007. A shade tolerance index for common understory species of northeastern North America. Ecol. Indic. 7, 195–207.

Kato, A., Moskal, L.M., Schiess, P., Swanson, M.E., Calhoun, D., Stuetzle, W., 2009. Capturing tree crown formation through implicit surface reconstruction using airborne lidar data. Remote Sens. Environ. 113, 1148–1162. doi:10.1016/j.rse.2009.02.010

Kazhdan, M., Hoppe, H., 2013. Screened poisson surface reconstruction. ACM Trans. Graph. TOG 32, 29.

Kellner, J.R., Asner, G.P., 2014. Winners and losers in the competition for space in tropical forest canopies. Ecol. Lett. 17, 556–562.

Kellomäki, S., Ikonen, V.-P., Peltola, H., Kolström, T., 1999. Modelling the structural growth of Scots pine with implications for wood quality. Ecol. Model. 122, 117–134.

Lafarge, T., Pateiro-Lopez, B., 2014. alphashape3d: Implementation of the 3D alpha-shape for the reconstruction of 3D sets from a point cloud.

Larjavaara, M., Muller-Landau, H.C., 2013. Measuring tree height: a quantitative comparison of two common field methods in a moist tropical forest. Methods Ecol. Evol. 4, 793–801. doi:10.1111/2041-210X.12071

Latif, Z.A., Blackburn, G.A., 2010. The effects of gap size on some microclimate

variables during late summer and autumn in a temperate broadleaved deciduous forest. Int. J. Biometeorol. 54, 119–129.

Liang, X., Hyyppä, J., Kaartinen, H., Holopainen, M., Melkas, T., 2012. Detecting Changes in Forest Structure over Time with Bi-Temporal Terrestrial Laser Scanning Data. ISPRS Int. J. Geo-Inf. 1, 242–255. doi:10.3390/ijgi1030242

Ligot, G., Balandier, P., Courbaud, B., Claessens, H., 2014. Forest radiative transfer models: which approach for which application? Can. J. For. Res. 44, 391–403. doi:10.1139/cjfr-2013-0494

Lintunen, A., Kaitaniemi, P., 2010. Responses of crown architecture in Betula pendula to competition are dependent on the species of neighbouring. Trees 24, 411–424. doi:10.1007/s00468-010-0409-x

Longuetaud, F., Piboule, A., Wernsdörfer, H., Collet, C., 2013. Crown plasticity reduces inter-tree competition in a mixed broadleaved forest. Eur. J. For. Res. 132, 621–634. doi:10.1007/s10342-013-0699-9

Lowman, M.D., Rinker, H.B., 2004. Forest canopies. Academic Press.

Martin-Ducup, O., Schneider, R., Fournier, R.A., 2016. Response of sugar maple (Acer saccharum, Marsh.) tree crown structure to competition in pure versus mixed stands. For. Ecol. Manag. 374, 20–32. doi:10.1016/j.foreco.2016.04.047

McCarthy, J., 2001. Gap dynamics of forest trees: a review with particular attention toboreal forests. Environ. Rev. 9, 1.

Medlyn, B.E., 2004. A maestro retrospective. For. Land–Atmosphere Interface CAB Int. 105–121.

MFFP, 2007. Normes d'inventaire forestier, placettes- échantillons temporaires. Direction des inventaires forestiers, Forêt Québec. Gouvernement du Québec, Québec, CA.

Millet, J., 2012. L'architecture des arbres des régions tempérées. Multimondes, Québec, Canada.

Muth, C.C., Bazzaz, F.A., 2002. Tree canopy displacement at forest gap edges. Can. J. For. Res. 32, 247–254. doi:10.1139/x01-196

Pedersen, B.S., Howard, J.L., 2004. The influence of canopy gaps on overstory tree and forest growth rates in a mature mixed-age, mixed-species forest. For. Ecol. Manag. 196, 351–366. doi:10.1016/j.foreco.2004.03.031

Petriţan, A.M., Lüpke, B. von, Petriţan, I.C., 2009. Influence of light availability on growth, leaf morphology and plant architecture of beech (Fagus sylvatica L.), maple (Acer pseudoplatanus L.) and ash (Fraxinus excelsior L.) saplings. Eur. J. For. Res. 128, 61–74. doi:10.1007/s10342-008-0239-1

Pretzsch, H., Rais, A., 2016. Wood quality in complex forests versus even-aged monocultures: review and perspectives. Wood Sci. Technol. 50, 845–880. doi:10.1007/s00226-016-0827-z

R Development Core Team, 2011. R Development Core Team.

Rouvinen, S., Kuuluvainen, T., 1997. Structure and asymmetry of tree crowns in relation to local competition in a natural mature Scots pine forest. Can. J. For.

Res. 27, 890–902.

Ruha, T., Varmola, M., others, 1997. Precommercial thinning in naturally regenerated Scots pine stands in northern Finland.

Runkle, J.R., 1998. Changes in Southern Appalachian Canopy Tree Gaps Sampled Thrice. Ecology 79, 1768–1780. doi:10.2307/176795

Runkle, J.R., Yetter, T.C., 1987. Treefalls Revisited: Gap Dynamics in the Southern Appalachians. Ecology 68, 417–424. doi:10.2307/1939273

Schneider, R., Fortin, M., Berninger, F., Ung, C.-H., Swift, D.E., Zhang, S.Y., 2011. Modeling Jack Pine (Pinus banksiana) foliage density distribution. For. Sci. 57, 180–188.

Seidel, D., Fleck, S., Leuschner, C., 2012. Analyzing forest canopies with ground-based laser scanning: A comparison with hemispherical photography. Agric. For. Meteorol. 154–155, 1–8. doi:10.1016/j.agrformet.2011.10.006

Seidel, D., Hoffmann, N., Ehbrecht, M., Juchheim, J., Ammer, C., 2015a. How neighborhood affects tree diameter increment – New insights from terrestrial laser scanning and some methodical considerations. For. Ecol. Manag. 336, 119–128. doi:10.1016/j.foreco.2014.10.020

Seidel, D., Leuschner, C., Müller, A., Krause, B., 2011. Crown plasticity in mixed forests—Quantifying asymmetry as a measure of competition using terrestrial laser scanning. For. Ecol. Manag. 261, 2123–2132.

Seidel, D., Schall, P., Gille, M., Ammer, C., 2015b. Relationship between tree growth and physical dimensions of Fagus sylvatica crowns assessed from terrestrial laser scanning. IForest-Biogeosciences For. 877.

Shaw, D.C., 2004. Vertical organization of canopy biota. Elsevier Academic Press: Amsterdam, The Netherlands.

Shendryk, I., Broich, M., Tulbure, M.G., Alexandrov, S.V., 2016. Bottom-up delineation of individual trees from full-waveform airborne laser scans in a structurally complex eucalypt forest. Remote Sens. Environ. 173, 69–83. doi:10.1016/j.rse.2015.11.008

Srinivasan, S., Popescu, S.C., Eriksson, M., Sheridan, R.D., Ku, N.-W., 2014. Multi-temporal terrestrial laser scanning for modeling tree biomass change. For. Ecol. Manag. 318, 304–317. doi:10.1016/j.foreco.2014.01.038

Valladares, F., Niinemets, Ü., 2008. Shade tolerance, a key plant feature of complex nature and consequences. Annu. Rev. Ecol. Evol. Syst. 39, 237.

Van Leeuwen, M., Hilker, T., Coops, N.C., Frazer, G., Wulder, M.A., Newnham, G.J., Culvenor, D.S., 2011. Assessment of standing wood and fiber quality using ground and airborne laser scanning: a review. For. Ecol. Manag. 261, 1467–1478.

Vepakomma, U., St-Onge, B., Kneeshaw, D., 2011. Response of a boreal forest to canopy opening: assessing vertical and lateral tree growth with multi-temporal lidar data. Ecol. Appl. 21, 99–121.

Weiskittel, A.R., Maguire, D.A., Monserud, R.A., 2007. Modeling crown structural responses to competing vegetation control, thinning, fertilization, and Swiss

needle cast in coastal Douglas-fir of the Pacific Northwest, USA. For. Ecol. Manag. 245, 96–109.

Wulder, M.A., White, J.C., Nelson, R.F., N\a esset, E., Ørka, H.O., Coops, N.C., Hilker, T., Bater, C.W., Gobakken, T., 2012. Lidar sampling for large-area forest characterization: A review. Remote Sens. Environ. 121, 196–209.

Young, T.P., Hubbell, S.P., 1991. Crown Asymmetry, Treefalls, and Repeat Disturbance of Broad-Leaved Forest Gaps. Ecology 72, 1464–1471. doi:10.2307/1941119

4.12 TABLES

Table 4-1Tree characteristics by species and stand type. Mean (standard deviation).

	Sugar maple		Balsam fir	
	Mixed	**Pure**	**Mixed**	**Pure**
Age	44 (13.9)	48.11 (19.58)	49.25 (15.47)	47.19 (19.56)
DBH (mm)	190.14 (53.18)	188.51 (73)	205.76 (63.35)	171.87 (47.68)
Crown volume (m³)	138.62 (68.07)	81.9 (60.54)	36.21 (33.94)	22.22 (12.43)
Tree height (m)	16.37 (1.6)	18.11 (2.55)	17.44 (2.59)	17.75 (3.08)
Crown Projected Area (CPA,m²)	34.56 (11.75)	21.73 (13.84)	10.3 (7.35)	7.13 (3.5)
Maximum horizontal expansion (m)[1]	0.69 (0.29)	0.59 (0.21)	0.31 (0.07)	0.37 (0.07)
Material displaced (m³)[1]	3.3 (1.52)	2.37 (1.36)	0.63 (0.35)	0.48 (0.22)

[1] Two years after release

Table 4-2: Analysis of variance of the model 4 (equation 4) for each change measure (Global Expansion: GE, Horyzontal expansion: HE, Vertical expansion: VE and Material Displaced: MD). Fixed effect of stand type (SD), height level (HL) and their interaction (HL:ST) and the diameter at breast height (DBH) as a covariable are shown for Sugar maple and Balsam fir. *P-value* < 0.05*; < 0.01**; < 0.001***

	Sugar maple			Balsam fir		
	Df	F-value	*P-value*	Df	F-value	*P-value*
GE						
ST	1	6.3	0.018 *	1	0.035	0.85
HL	19	3	2.3e-05 ***	19	5.9	7.8e-14 ***
DHP	1	0.016	0.9	1	0.016	0.9
HL : ST	19	2.7	1.4 e-04 ***	19	1.2	0.26
HE						
ST	1	2.1	0.16	1	1.1	0.3
HL	19	9.8	0 ***	19	10	0 ***
DHP	1	0.37	0.55	1	0.37	0.55
HL : ST	19	1.5	0.066	19	1.4	0.12
VE						
ST	1	13	1.4e-03 **	1	1.3	0.27
HL	19	19	0 ***	19	17	0 ***
DHP	1	0.34	0.57	1	1.1	0.31
HL : ST	19	3.1	1.2e-05 ***	19	0.8	0.71
MD						
ST	1	5.6	0.025 *	1	0.099	0.76
HL	19	15	0 ***	19	12	0 ***
DHP	1	4.7	0.04 *	1	1.5	0.29
HL : ST	19	1.9	0.015 *	19	1.4	0.13

Table 4-3: *P-value* details of the model 4 (equation 4) for multiple height comparisons for each change variable. When the simple effect of height level was the only significant variable a total of six contrasts are made for pairwise quarter crown height comparisons. When the interaction effect was significant, the same 6 contrasts are made for mixed and pure stands (12 contrasts), moreover four contrasts are made to compare each quarter between pure and mixed stands. *P-value* < 0.05*; < 0.01**; < 0.001***

	Sugar maple				Balsam fir			
	GE	**HE**	**VE**	**MD**	**GE**	**HE**	**VE**	**MD**
HL simple effect								
1/4 vs 2/4	—	6.7e-09 ***	—	—	0.87	1.8e-03 **	0.99	1e-03 **
1/4 vs 3/4	—	3.6e-09 ***	—	—	8.7e-03 **	4.5e-12 ***	2.1e-03 **	1.1e-14 ***
1/4 vs/ 4/4	—	1.8e-04 ***	—	—	9.7e-03 **	0.083	0 ***	0.16
2/4 vs 3/4	—	1	—	—	0.079	2.8e-03 **	6.1e-03 **	3e-04 ***
2/4 vs 4/4	—	0.26	—	—	0.084	0.61	0 ***	0.32
3/4 vs 4/4	—	0.25	—	—	1	1.4e-05 ***	2.9e-12 ***	2.6e-08 ***
HL : ST								
Mixed								
1/4 vs 2/4	0.36	—	0.98	5.6e-07 ***	—	—	—	—
1/4 vs 3/4	1	—	9.5e-04 ***	1.6e-14 ***	—	—	—	—
1/4 vs/ 4/4	0.85	—	0 ***	0.23	—	—	—	—
2/4 vs 3/4	0.11	—	1.9e-05 ***	0.15	—	—	—	—
2/4 vs 4/4	0.0099 **	—	0 ***	0.023 *	—	—	—	—
3/4 vs 4/4	0.99	—	0 ***	2.4e-07 ***	—	—	—	—
Pure								
1/4 vs 2/4	0.0011 **	—	0.084	5e-08 ***	—	—	—	—
1/4 vs 3/4	1.1e-07 ***	—	0.17	0 ***	—	—	—	—
1/4 vs/ 4/4	8.1e-09 ***	—	1.6e-06 ***	1.3e-14 ***	—	—	—	—
2/4 vs 3/4	0.55	—	1	6.7e-06 ***	—	—	—	—
2/4 vs 4/4	0.24	—	6.6e-15 ***	0.3	—	—	—	—
3/4 vs 4/4	1	—	9.6e-14 ***	0.054	—	—	—	—
Pure vs Mixed								

1/4 vs 1/4	8.4e-05 ***	—	2.5e-08 ***	0.012 *	—	—	—	—
2/4 vs 2/4	0.0098 **	—	1.4e-04 ***	0.02 *	—	—	—	—
3/4 vs 3/4	1	—	1	0.71	—	—	—	—
4/4 vs 4/4	1	—	0.95	1	—	—	—	—

Table 4-4: Analysis of variance of the model 5 (equation 5) and contrast details. Fixed effect of species (SP), height level (HL), their interaction (HL:SP) and the diameter at breast height (DBH) as a co-variable are shown. In the bottom part, details on contrast are shown: 6 contrasts are made for Sugar maple (Sug.map) and Balsam fir (Bal.fir) to make pairwise comparisons of crown quarters (total of 12 contrasts). Moreover four contrasts are made to compare each quarter between Sugar maple and Balsam fir. *P-value* $< 0.05^*$; $< 0.01^{**}$; $< 0.001^{***}$

	Df	**F/Z-value**	*P-value*
Model 5			
SP	1	25	5.5e-06 ***
HL	19	4.6	2.2e-10 ***
DHP	1	5.1	0.04 *
SP:HL	19	2.9	2.6e-05 ***
Contrasts			
Sug.map			
1/4 vs 2/4	1	-0.54	0.49
1/4 vs 3/4	1	-0.77	0.1
1/4 vs/ 4/4	1	-0.4	0.83
2/4 vs 3/4	1	-0.23	0.99
2/4 vs 4/4	1	0.15	1
3/4 vs 4/4	1	0.37	0.87
Bal.fir			
1/4 vs 2/4	1	0.22	0.99
1/4 vs 3/4	1	0.64	0.34
1/4 vs/ 4/4	1	1.9	8.6e-09 ***
2/4 vs 3/4	1	0.42	0.82
2/4 vs 4/4	1	1.7	1.2e-07 ***
3/4 vs 4/4	1	1.3	0.00026 ***
Sug.map vs Bal.fir			
1/4 vs 1/4	1	-2.1	4.1e-10 ***
2/4 vs 2/4	1	-1.4	4e-04 ***
3/4 vs 3/4	1	-0.74	0.25
4/4 vs 4/4	1	0.2	1

Table 4-5: Circular statistics on the orientation of the global expansion (GE), horizontal expansion (HE) and material displaced (MD). The null hypothesis is a uniform distribution of the orientation. The alternative hypothesis is a unimodal distribution with a southern direction (270°). The "Statistic" column represents the mean length vector (Rayleigh statistic). *P-value* < 0.05*; < 0.01**; < 0.001***

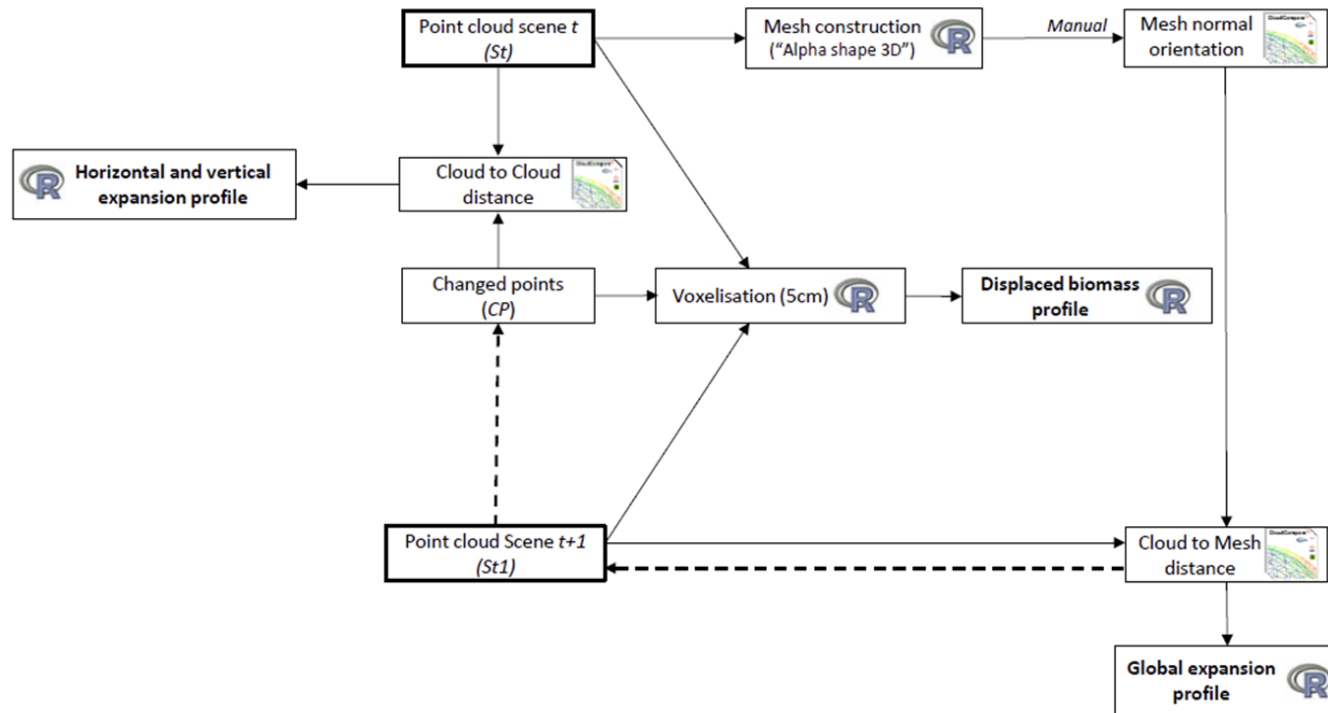|	Mean direction (°)	Statistic	*P-value*
Sugar maple			
GE (m)	229	0.0237	5e-03 ***
HE (m)	230	0.037	2.2e-04 ***
MD (m^{-3})	234	0.0819	3.48e-10 ***
Balsam fir			
GE (m)	32	8.36e-03	0.731
HE (m)	41	0.0141	0.858
MD (m^{-3})	191	6.81e-03	0.241

Figure 4-1: Diagram of the method's main steps. ® indicates the steps performed in R and ▨ those carried out with CloudCompare. The final output (profiles) appear in bold.
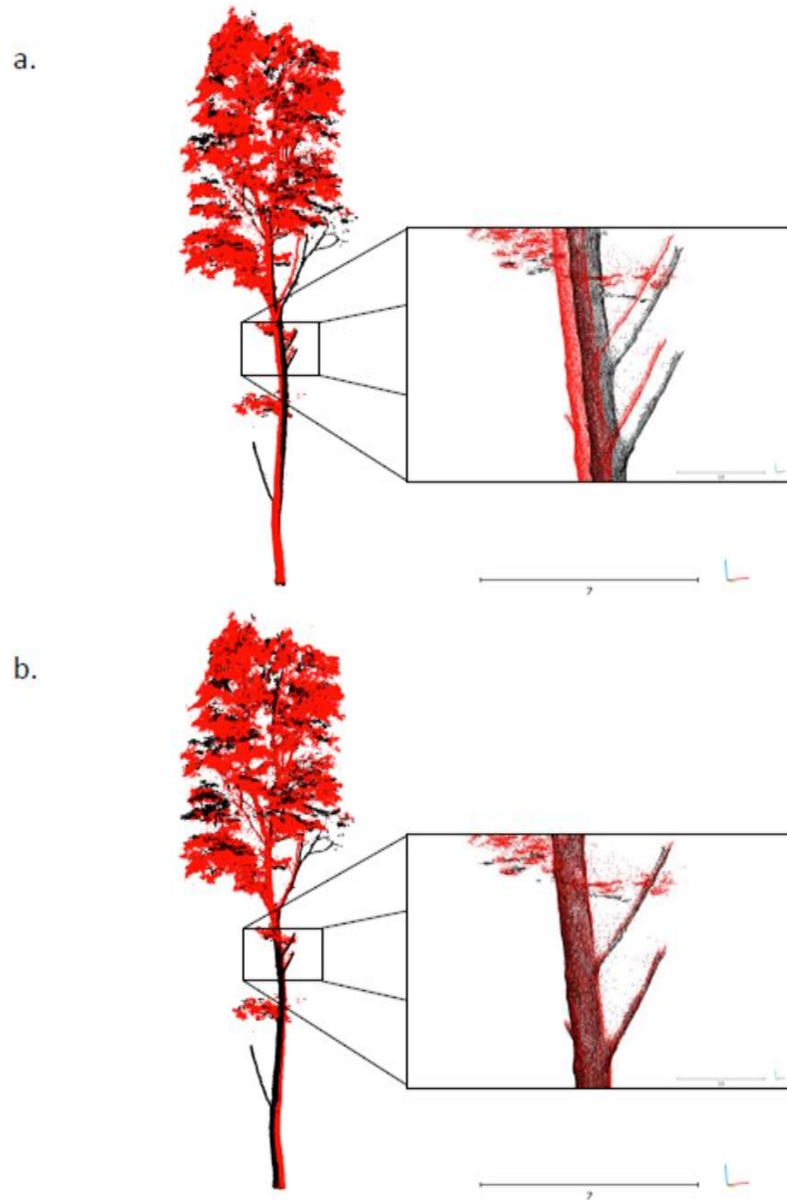
Figure 4-2: Differences between automatic and manual alignment accuracy. a. Automatic alignment performed with ICP CloudCompare algorithm. b. Manual alignment performed with CloudCompare's manual tools. The scale unit is in meters.
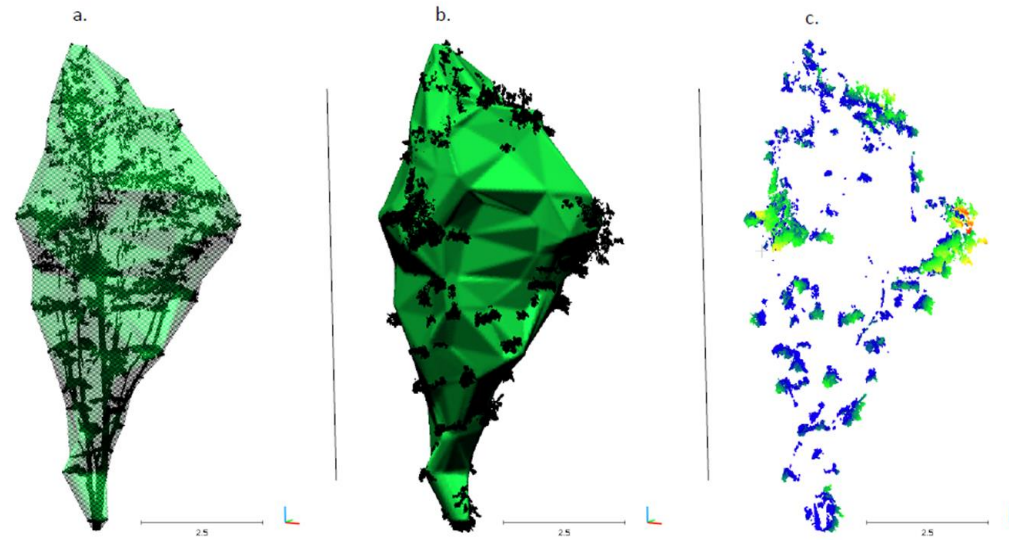
Figure 4-3: Mesh construction and changed points identification. a. In transparent green, the mesh of the crown at t_0t_0 computed using an alpha-shaped algorithm on the crown point cloud, which is in black (S_0). b. The black points are the S_x points outside of the mesh at t_0 (i.e. the changed points: CP). c. Only the CP, with a color gradient (from blue to red) representing the distance between the mesh and the CP (the global expansion: GE). These points are those used to characterise changes between t_0 and t_x. The scale unit is in meters.
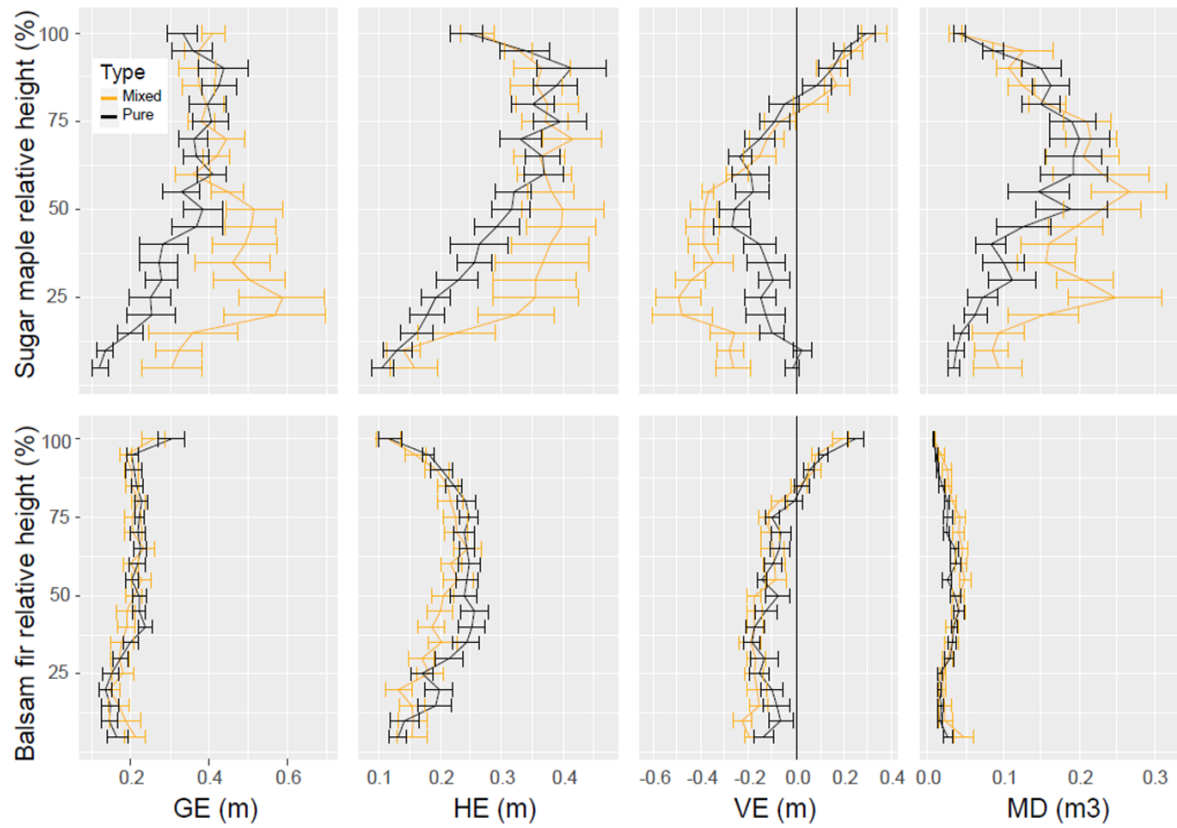
Figure 4-4: Mean tree crown profile by stand type. The upper part of the figure illustrates the 2-year changes in the Sugar maple crowns and the lower part shows changes in the Balsam fir crowns. The mean mixed tree profiles are in orange and the pure tree profiles are in black.
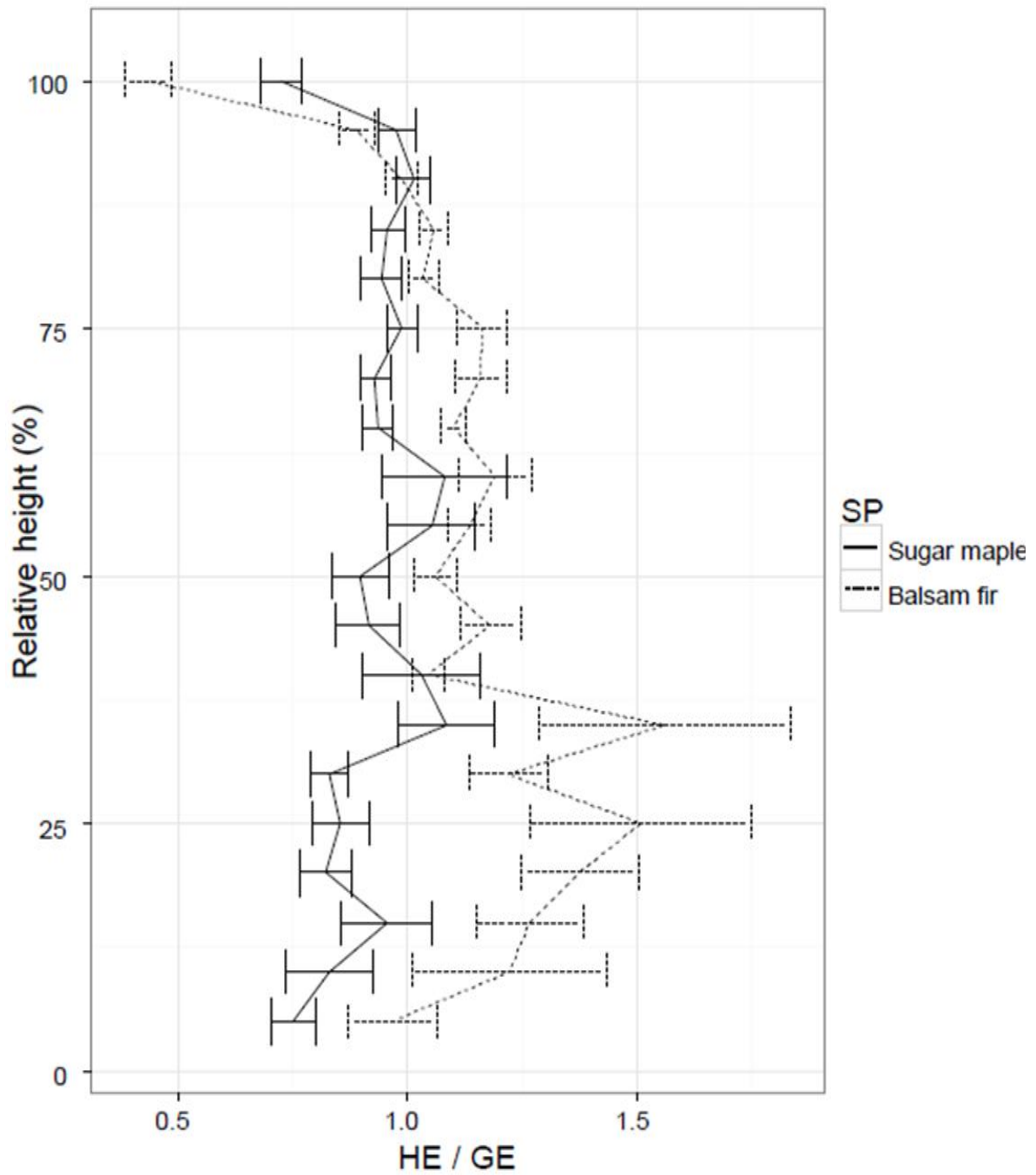
Figure 4-5: Mean tree HE:GE ratio profile by species. Sugar maple profile is shown as a solid line and Balsam fir profile as dashed lines.
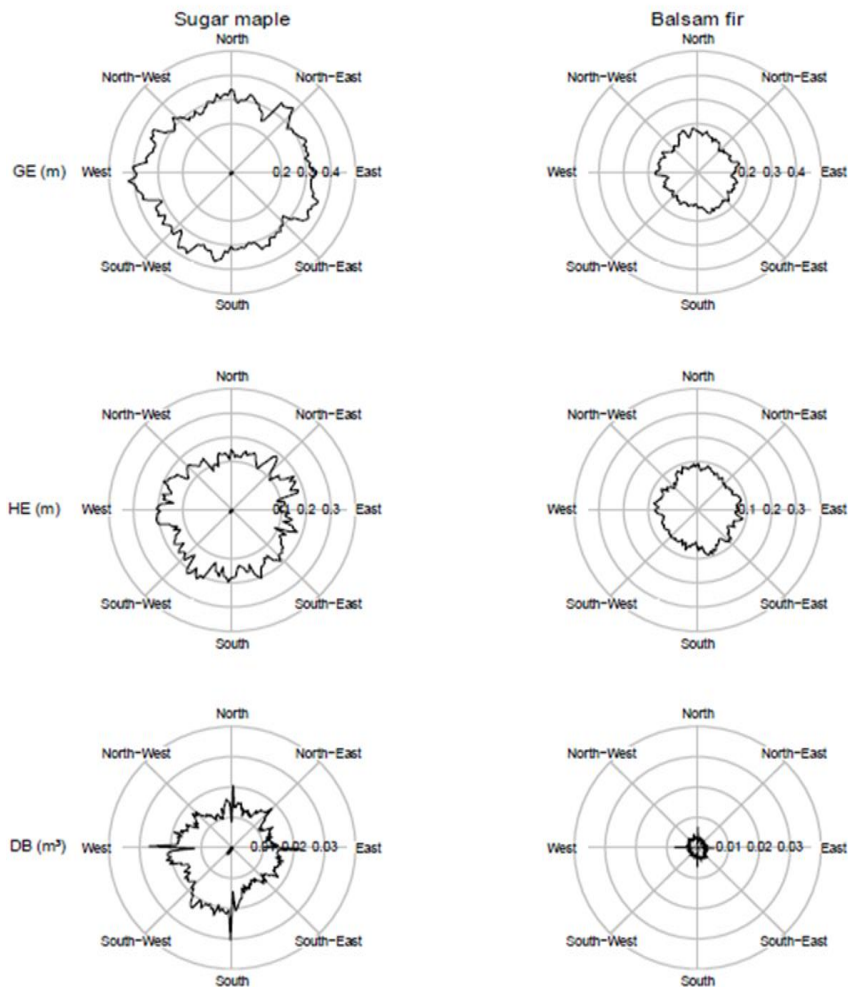
Figure 4-6: Circular plots of change variables by cardinal direction. Sugar maple plots are on the left side and Balsam fir plots on the right side. Circular plots are presented for GE (top), HE (middle) and DB (bottom) measures. The angle step for the circular representations is two degrees (one change variable values every two degrees). The solid line started in the center of each circular plot represents the mean direction and the resultant length (Rayleigh statistic from Batschelet, (1981)) of the change variable. No line is observed for GE and HE for Balsam fir because the Rayleigh statistic is nearly 0. The same circular plots scaled for each change variable are shown for both species for comparison.
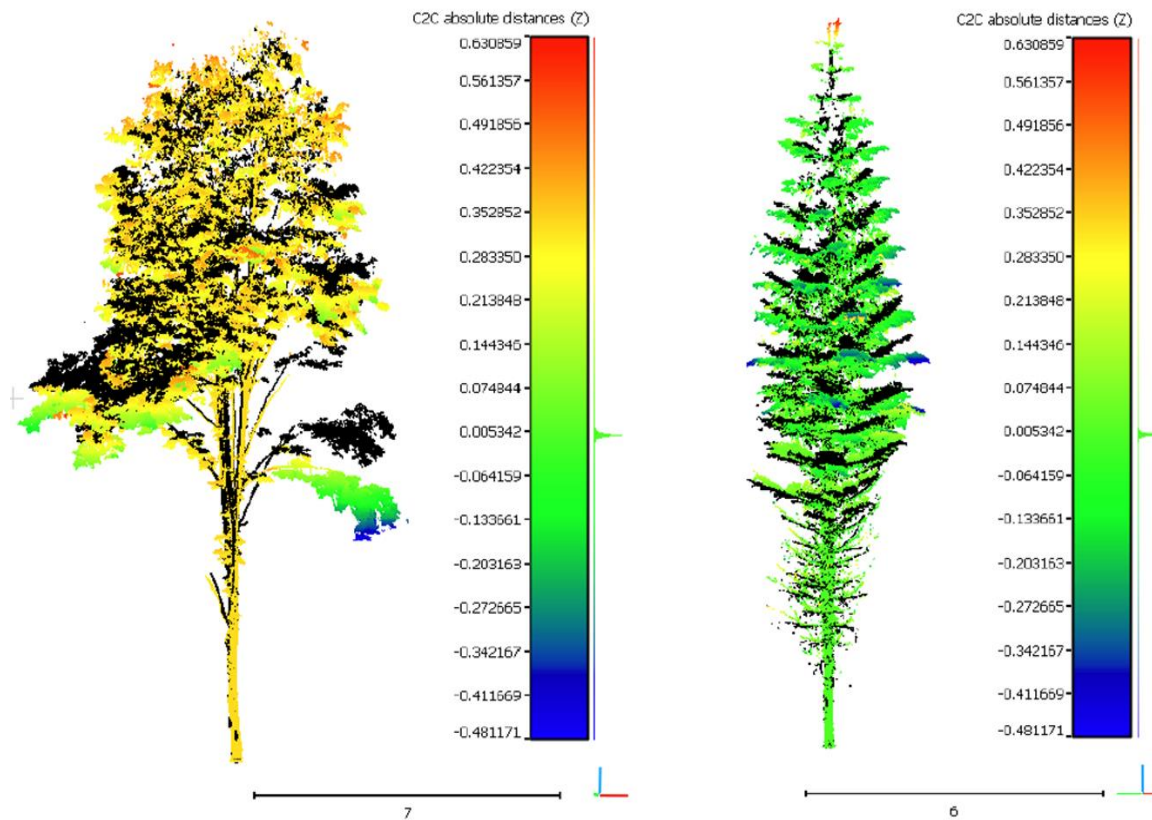
Figure 4-7: Example of point-to-point distance in 2013 vs 2015. A Sugar maple and a Balsam fir example are shown on the left side and on the right side respectively. In black, the point cloud of the trees in 2013. In color, the point cloud of the same trees in 2015. The color gradient corresponds to the vertical distance between the two point clouds (VE) computed with the "*C2C*" algorithm in CloudCompare. We observed substantial negative values for many branches in the bottom part of both trees.

CHAPITRE V
CONCLUSION GÉNÉRALE

La structure des arbres joue de multiples rôles sur le fonctionnement des écosystèmes forestiers. Elle intervient à une échelle très locale en influençant des processus micrométéorologiques (Latif et Blackburn, 2010), à l'échelle du peuplement en créant des habitats pour la faune et en déterminant la compétition et la croissance des arbres (Niinemets, 2010; Shaw, 2004) ainsi qu'à une échelle globale en intervenant dans des processus biogéochimiques (Hardiman et coll., 2013). Il est donc primordial d'étudier avec précision la structure du houppier des arbres et de comprendre comment elle interagit avec l'environnement. Dans ce contexte général, l'objectif de ma thèse de doctorat était d'étudier l'effet de la mixité sur la structure et la dynamique des houppiers chez le sapin baumier et l'érable à sucre à partir de données de LiDAR-t. Des contributions importantes ont alors été apportées en termes de développement technique et de questions d'écologie. Ces travaux pourraient avoir des répercussions sur l'aménagement des forêts. D'un point de vue technique, des méthodes d'études statiques et dynamiques de la structure des arbres ont été développées. D'un point de vue écologique l'étude de la structure et de la dynamique des houppiers dans différentes conditions de compétition ont permis de contribuer à répondre des questionnements liés à la dynamique des forêts mixtes. La conclusion est divisée en trois parties décrivant 1) les contributions techniques, 2) les contributions écologiques et 3) les perspectives d'améliorations et de recherches futures.

5.1   CONTRIBUTIONS TECHNIQUES

La structure du houppier des arbres a longtemps été quantifiée au travers de mesures simples acquises depuis le sol. Ces métriques se limitaient généralement à la profondeur du houppier, son diamètre ou encore sa surface projetée au sol (Pretzsch, 2009). Des mesures plus complexes ou des suivis du développement du houppier ont pu être abordés sur de petits arbres accessibles depuis le sol (Canham, 1988; Laurans et coll., 2012), mais rarement sur des arbres de la canopée. Les études menées sur de grands arbres nécessitaient généralement d'abattre ou de grimper dans ces derniers (Denison, 1973; Gilmore et Seymour, 1997). L'apparition des LiDAR-t permet d'ouvrir un grand nombre de perspectives et de mesurer les composantes de la canopée de façon plus précise. En fait, les LiDAR-t permettent d'obtenir une information 3D avec un détail très fin. Toutefois, le traitement de ces données fait face à de nombreux défis informatiques et conceptuels. Mes trois chapitres de thèse ont tous permis de relever certains de ces défis et de rendre opérationnelles des méthodes de traitements de ces données à l'échelle de l'arbre et de son environnement local. Ces méthodes ont été développées au travers d'approches statiques dans le premier et le deuxième chapitre et dynamique dans le troisième chapitre.

5.1.1   La structure externe des houppiers

L'une des difficultés rencontrées pour caractériser la structure des arbres à partir d'un nuage de point 3D est d'établir ce que sont les limites externes du houppier d'un arbre individuel. Dans le cadre de ma thèse, des algorithmes d'enveloppes alpha et d'enveloppes convexes ont été utilisés à cette fin (Barber et coll., 2014; Lafarge et Pateiro-Lopez, 2014). Cette approche a permis de proposer dans le premier et le deuxième chapitre plusieurs métriques d'occupation 3D de l'espace. C'est le cas par

exemple du volume occupé par le houppier, de sa surface ou de sa sinuosité (ou asymétrie 3D). Dans le premier chapitre, la délimitation externe du houppier a également permis de calculer un houppier théorique (ou lissée). À partir de cette dernière, l'angle d'ouverture du houppier, la rugosité et la proportion de houppier d'ombre ont pu être estimées sur l'érable à sucre. Ces nouvelles métriques ont été utilisées pour caractériser la plasticité des houppiers. Par ailleurs leurs implications écophysiologiques, notamment en termes d'interception de la lumière, ont été discutées.

Le concept de limite 3D du houppier à partir d'enveloppes a été réutilisé dans le troisième chapitre pour étudier la taille des houppiers de façon dynamique. Nous avons alors développé une méthode permettant de quantifier la réoccupation de l'espace dans le temps. Le principe de la méthode est de récupérer tous les points du nuage de points au temps t_x qui se trouvent au-delà de la limite du houppier (c.-à-d., l'enveloppe) au temps t_0. Ces points sont alors considérés comme la matière néoformée ou déplacée entre le temps t_0 et le temps t_x. Ils ont été par la suite utilisés pour quantifier la réoccupation globale, horizontale et verticale de l'espace. Cette méthode présente de grands intérêts pour des questions de dynamique des trouées en milieu naturel ou de réponse à l'éclaircie en forêt aménagée. Dans la littérature, les études sur ces questions se focalisent sur des mesures statiques pour caractériser la capacité de réoccupation de l'espace, notamment au travers de mesure d'asymétrie du houppier (Muth et Bazzaz, 2002; Young et Hubbell, 1991). Le peu d'études dynamiques que l'on retrouve est limité à la réoccupation horizontale de l'espace (Runkle, 1998; Runkle et Yetter, 1987; Vepakomma et coll., 2011). Dans le troisième chapitre de ma thèse, nous avons pu mettre en évidence l'importance de quantifier la réoccupation multidirectionnelle de l'espace.

L'ensemble des métriques et approches décrites ci-dessus sont peu sensibles au phénomène d'occlusion, car elles se focalisent sur des limites externes. En revanche, lorsqu'on s'intéresse à des caractéristiques internes du houppier ou à l'arrangement de

la matière dans la canopée, il est primordial de prendre en compte les biais que l'occlusion peut engendrer.

5.1.2   La structure interne des houppiers et de la canopée

Dans le premier chapitre, trois nouveaux indices de compétition ont été développés. Classiquement, les indices de compétition sont calculés en se basant sur des caractéristiques des compétiteurs en tant qu'individus. Les dimensions de ces individus (caractéristiques de houppier, hauteur ou DHP) ainsi que la distance des compétiteurs déterminent la pression de compétition exercée sur un arbre cible (Pretzsch, 2009). L'originalité de l'approche mise en place dans le premier chapitre de ma thèse a été de calculer des indices basés sur l'arrangement de la matière autour d'un arbre cible. Ces indices sont estimés directement à partir du nuage de point 3D et font abstraction des individus. Cette approche représente théoriquement mieux l'ombrage exercé par l'environnement local d'un arbre que des indices basés sur des individus. Elle offre donc une meilleure estimation de la compétition pour la lumière. L'inconvénient d'une telle approche est qu'elle est sensible à l'occlusion. Ainsi, dans ce premier chapitre l'occlusion a été gérée en utilisant une grille de voxels non vides de 10 cm d'arête comme proposé par Seidel et coll. (2011). Avec cette méthode, un voxel peut donc être plein ou vide. Ceci permet de limiter les bais dus à l'occlusion en simplifiant l'information à l'échelle du voxel. En revanche, cette approche peut avoir tendance à surestimer la quantité de matière puisqu'il en découle qu'un volume de 1000 cm^3 est considéré plein dès que le nombre minimum de points dans le voxel est atteint.

Dans le deuxième chapitre, l'objectif méthodologique était de mettre en place des profils de distribution de matière. Ces métriques sont particulièrement sensibles à l'occlusion puisqu'il s'agit de quantifier la quantité de matière à l'intérieur de l'enveloppe du houppier. Nous avons alors utilisé L-vox (Fournier et coll., 2015), un

algorithme permettant de corriger les biais dus à l'occlusion de façon plus précise que ce qui avait été fait dans le premier chapitre. Cet algorithme estime un indice de densité relative en comparant les scans produits sur le terrain et les mêmes scans simulés à partir d'un modèle de lancer de rayons.

5.1.3 Séparation bois/feuilles

Un défi majeur dans l'utilisation des données de LiDAR-t est la séparation des retours appartenant au feuillage de ceux appartenant au bois. Une méthode basée sur une approche géométrique a été développée pour les besoins du deuxième chapitre. Dans la littérature, une grande partie des méthodes développées se base sur des seuils d'intensité du retour des capteurs, des scans avec et sans feuilles ou encore des approches manuelles (Béland et coll., 2011; Douglas et coll., 2015; Li et coll., 2016; Oshio et coll., 2015). Ces méthodes imposent plusieurs contraintes telles que la nécessité de capteurs particuliers, des dispositifs expérimentaux complexes, un temps de traitement lourd ou encore sont spécifiques aux espèces au feuillage caduc. Les méthodes les plus généralisables semblent être celles qui utilisent des approches géométriques et qui font appel à la donnée LiDAR sous sa forme la plus brute, c'est-à-dire les coordonnées xyz du nuage de point (Tao et coll., 2015). Notre méthode a consisté à la détection de cylindres dans le nuage de points. Les points associés à ces cylindres ont alors été identifiés comme de la matière ligneuse et tous les autres comme de la matière foliaire. Par ailleurs, cette méthode a été développée à partir d'algorithmes déjà existants et opérationnels dans un contexte de détection des arbres pour obtenir des métriques d'inventaires forestiers (http://rdinnovation.onf.fr/, consulté le 14 mars 2017). Certaines limites se sont toutefois révélées, comme l'impossibilité de validation à partir de nos données ainsi que l'occlusion importante dans le cas du sapin baumier.

Des efforts devront être mis en place pour améliorer cette méthode dans de futures recherches.

5.2 CONTRIBUTIONS ÉCOLOGIQUES

L'étude de la relation productivité-diversité suscite depuis quelques années un grand intérêt dans la communauté scientifique. Plusieurs études ont démontré une relation positive entre la diversité et la productivité en milieux forestiers naturels et aménagés (Forrester et Bauhus, 2016). Toutefois, les mécanismes qui expliquent cette relation sont encore mal compris. Une hypothèse souvent mise de l'avant s'appuie sur l'occupation de l'espace aérien des arbres et l'interaction entre leurs houppiers (Morin, 2015; Morin et coll., 2011). La diversité permettrait d'optimiser l'occupation de l'espace grâce à une complémentarité des traits des houppiers. La plasticité des houppiers des arbres serait un des principaux moteurs de cette complémentarité (Jucker et coll., 2015; Niklaus et coll., 2017; Williams et coll., 2017). Les résultats des différents chapitres de ma thèse de doctorat ont permis d'amener des éléments de réponse à l'hypothèse selon laquelle la diversité entraine une meilleure occupation de l'espace ainsi que sur la plasticité des espèces étudiés.

Dans le premier chapitre de la thèse, les résultats illustrent l'importante plasticité du houppier de l'érable à sucre. Sept des huit métriques quantifiées révèlent des différences significatives entre des arbres en peuplements purs et en peuplements mixtes. Les résultats du troisième chapitre appuient cela en révélant la capacité de l'érable à sucre à réoccuper l'espace dans toutes les directions suite à la mise en place d'une trouée. Le sapin baumier se révèle toutefois être moins efficace que l'érable à sucre. Ces résultats s'expliquent par les modes de développement contrastés des deux espèces qui ne permettent pas la même capacité de réoccupation de l'espace.

Les différents résultats de cette thèse mettent largement en évidence l'effet bénéfique de la mixité sur l'occupation de l'espace par l'érable à sucre. Le premier chapitre révèle que les houppiers occupent un volume plus important, sont plus ouverts, plus profonds et ont une proportion de houppier d'ombre moins grande en peuplement mixte qu'en peuplement pur. Ces caractéristiques laissent supposer une structure globale du houppier plus efficace en termes d'interception de la lumière en peuplement mixte qu'en peuplement pur. La pression de compétition exercée sur les arbres (c.-à-d. indice « CPI ») est moins importante en peuplement mixte qu'en peuplement pur et expliquerait ces différences de structure du houppier.

Les résultats du second chapitre appuient ceux du premier chapitre en révélant que les érables à sucre ont globalement une distribution de la matière (totale et foliaire) plus basse sur le houppier en peuplement mixte qu'en peuplement pur. La littérature à ce sujet révèle qu'une distribution de la matière plus basse est entrainée par une compétition pour la lumière moins forte. Ceci entraine par ailleurs une meilleure interception de la lumière (Garber et Maguire, 2005). Finalement, les résultats du troisième chapitre révèlent qu'en peuplement mixte les érables à sucre réoccupent plus d'espace dans la partie inférieure du houppier suite au dégagement des compétiteurs. Ceci est dû aux différences des caractéristiques des houppiers avant le dégagement. La présence de branches plus basses en peuplement mixte permettrait une meilleure réoccupation de l'espace par le bas.

L'ensemble de ces résultats pourraient laisser supposer que la mixité entraine une meilleure occupation de l'espace par les houppiers en termes d'interception de lumière. Toutefois les résultats du second chapitre sur le sapin baumier révèlent une réaction inverse pour cette espèce. En effet, les arbres en peuplement mixte ont une distribution de la matière plus haute sur le houppier. Ceci est généralement une réaction à une pression de compétition plus importante pour optimiser l'accès à la lumière (Forrester et coll., 2012). Par ailleurs, dans le deuxième chapitre, aucune différence de réponse à

148

l'ouverture n'a été détectée entre des sapins en peuplement pur et mixte. La mixité ne serait peut-être donc pas avantageuse pour le sapin baumier.

Il est donc difficile de tirer des conclusions de l'effet bénéfique de la mixité sur l'occupation de l'espace à l'échelle du peuplement à partir de nos résultats. Une hypothèse qui peut être avancée est que nous serions dans le cas où une espèce se développe mieux en condition mixte (l'érable à sucre dans notre cas), mais au détriment d'une autre (le sapin baumier). En revanche, les deux espèces présentent une distribution de la matière plus homogène sur la longueur de l'arbre et pourraient ainsi conduire à une meilleure occupation globale de l'espace et donc un remplissage de la canopée plus important. Finalement, les peuplements mixtes échantillonnés durant ma thèse sont composés de plusieurs autres espèces et toutes devraient être étudiées pour avoir une image complète des interactions entre toutes les espèces des peuplements mixtes étudiés.

Les recherches effectuées durant ma thèse ont donc contribué d'une part au développement de méthodes et d'algorithmes pour rendre opérationnelle l'utilisation de données de LIDAR-t dans le cadre d'études en foresterie et d'autre part d'étudier l'effet de la mixité sur une espèce feuillue et une espèce résineuse. Toutefois, plusieurs améliorations et validations des méthodes proposées doivent être réalisées. Parallèlement, les résultats obtenus quant aux réponses des deux espèces à la diversité ouvrent des perspectives pour étendre ces recherches et les méthodes employées à l'échelle du peuplement**.**

5.3   PERSPECTIVES

Pour l'ensemble des analyses faites durant mon doctorat, les arbres cibles ont été isolés manuellement. Cette approche est précise et était nécessaire pour mener à terme les

analyses de la thèse. Cette méthode reste toutefois laborieuse et n'est pas envisageable à grande échelle. Par ailleurs, elle peut être critiquable par son aspect subjectif. Des méthodes automatisées permettant d'extraire tous les individus d'une scène de LiDAR-t commencent à être développées, mais n'ont pas encore été publiées (Joris Ravaglia USherbrooke, Emmanuel Dûchateau UQAR). L'utilisation de ce type d'approche sur les placettes étudiées durant mon doctorat ouvrirait deux importantes perspectives par rapport à mes recherches :

1. **La validation des indices de compétition développés dans le premier chapitre.** Tous les compétiteurs des arbres ciblent échantillonnés durant mon doctorat pourraient être spatialisés. Des métriques simples telles que le DHP, la hauteur ou la surface du houppier pourraient alors être extraites. Ceci permettrait de calculer des indices de compétition spatialement explicite classique (Biging et Dobbertin, 1992). La capacité de ces indices et des indices développés dans le premier chapitre pour prédire la plasticité des houppiers ainsi que la croissance des arbres cibles pourrait alors être comparée.

2. **L'effet de la mixité à l'échelle de la placette.** Une des limites soulignée par rapport aux résultats de l'ensemble des trois chapitres sur l'effet de la mixité est que les études sont focalisées sur seulement une (premier chapitre) ou deux espèces (deuxième et troisième chapitre). Une segmentation automatique des individus permettrait d'étudier les caractéristiques des houppiers de l'ensemble des espèces présentes. Ceci permettrait d'étudier plus en détail la complémentarité des houppiers dans l'occupation de l'espace et le remplissage de la canopée résultant en peuplement mixte. Nous pourrions alors tirer des conclusions claires à l'échelle du peuplement.

La méthode de séparation du bois et du feuillage proposée dans le deuxième chapitre est un bon point départ. Toutefois, aucune validation de la méthode n'a pu être faite

faute de données terrain sur le feuillage. Ainsi, une prochaine étape serait de valider cette méthode sur différentes espèces feuillues et de conifères. Il serait possible d'employer des données prises sur des arbres avec et sans feuilles ou sinon recourir à des maquettes d'arbres simulées telles que proposées par Côté et coll. (2011).

Finalement, la méthode développée dans le chapitre III consistant à quantifier la réoccupation de l'espace par les arbres peut être appliquée à l'échelle de la trouée. En effet, cette méthode a un grand potentiel pour décrire et étudier la dynamique des trouées. Une enveloppe au temps t_0 serait alors calculée sur l'ensemble de la trouée plutôt que sur un arbre cible. Des questions centrales sur la régénération et les successions végétales liées à la rapidité de la fermeture des trouées en fonction du type de peuplement pourraient alors être abordées.

RÉFÉRENCES BIBLIOGRAPHIQUES

Antin, C., Pélissier, R., Vincent, G., Couteron, P., 2013. Crown allometries are less responsive than stem allometry to tree size and habitat variations in an Indian monsoon forest. Trees 27, 1485–1495. doi:10.1007/s00468-013-0896-7

Ashcroft, M.B., Gollan, J.R., Ramp, D., 2014. Creating vegetation density profiles for a diverse range of ecological habitats using terrestrial laser scanning. Methods Ecol. Evol. 5, 263–272. doi:10.1111/2041-210X.12157

Barber, C.B., Habel, K., Grasman, R., Stahel, A., Stahel, A., Sterratt, D.C., 2014. geometry: Mesh generation and surface tesselation.

Barthelemy, D., Caraglio, Y., 2007. Plant architecture: A dynamic, multilevel and comprehensive approach to plant form, structure and ontogeny. Ann. Bot. 99, 375–407.

Bayer, D., Seifert, S., Pretzsch, H., 2013. Structural crown properties of Norway spruce (Picea abies [L.] Karst.) and European beech (Fagus sylvatica [L.]) in mixed versus pure stands revealed by terrestrial laser scanning. Trees 27, 1035–1047. doi:10.1007/s00468-013-0854-4

Beaudet, M., Messier, C., 1997. Le bouleau jaune en peuplements feuillus et mixtes: autécologie, dynamique forestière et pratiques sylvicoles. Groupe Rech. En Écologie For. GREF Univ. Qué. À Montr. Qué.

Béland, M., Widlowski, J.L., Fournier, R.A., Côté, J.F., Verstraete, M.M., 2011a. Estimating leaf area distribution in savanna trees from terrestrial LiDAR measurements. Agric. For. Meteorol. 151, 1252–1266.

Béland, M., Widlowski, J.L., Fournier, R.A., Côté, J.F., Verstraete, M.M., 2011b. Estimating leaf area distribution in savanna trees from terrestrial LiDAR measurements. Agric. For. Meteorol. 151, 1252–1266.

Biging, G.S., Dobbertin, M., 1992a. A Comparison of Distance-Dependent Competition Measures for Height and Basal Area Growth of Individual Conifer Trees. For. Sci. 38, 695–720.

Biging, G.S., Dobbertin, M., 1992b. A Comparison of Distance-Dependent

152

    Competition Measures for Height and Basal Area Growth of Individual Conifer Trees. For. Sci. 38, 695–720.

Bradshaw, A.D., 1965. Evolutionary significance of phenotypic plasticity in plants. Adv. Genet. 13, 115–155.

Bréda, N.J., 2003. Ground-based measurements of leaf area index: a review of methods, instruments and current controversies. J. Exp. Bot. 54, 2403–2417.

Brisson, J., 2001. Neighborhood competition and crown asymmetry in Acer saccharum. Can. J. For. Res. 31, 2151–2159.

Buda, N.J., Wang, J.R., 2006. Suitability of two methods of evaluating site quality for sugar maple in central Ontario. For. Chron. 82, 733–744.

Burns, R.M., Honkala, B.H., 1990. Silvics of North America. Volume 1. Conifers. Agric. Handb. Wash.

Calders, K., Newnham, G., Burt, A., Murphy, S., Raumonen, P., Herold, M., Culvenor, D., Avitabile, V., Disney, M., Armston, J., others, 2015. Nondestructive estimates of above-ground biomass using terrestrial laser scanning. Methods Ecol. Evol. 6, 198–208.

Canham, C.D., 1988a. Growth and Canopy Architecture of Shade-Tolerant Trees: Response to Canopy Gaps. Ecology 69, 786–795. doi:10.2307/1941027

Canham, C.D., 1988b. Growth and Canopy Architecture of Shade-Tolerant Trees: Response to Canopy Gaps. Ecology 69, 786–795. doi:10.2307/1941027

Canham, C.D., LePage, P.T., Coates, K.D., 2004. A neighborhood analysis of canopy tree competition: effects of shading versus crowding. Can. J. For. Res. 34, 778–787.

Coates, K.D., Canham, C.D., Beaudet, M., Sachs, D.L., Messier, C., 2003. Use of a spatially explicit individual-tree model (SORTIE/BC) to explore the implications of patchiness in structurally complex forests. For. Ecol. Manag. 186, 297–310.

Côté, J.F., Fournier, R.A., Egli, R., 2011a. An architectural model of trees to estimate forest structural attributes using terrestrial LiDAR. Environ. Model. Softw. 26, 761–777.

Côté, J.F., Fournier, R.A., Egli, R., 2011b. An architectural model of trees to estimate forest structural attributes using terrestrial LiDAR. Environ. Model. Softw.

26, 761–777.

Dassot, M., Colin, A., Santenoise, P., Fournier, M., Constant, T., 2012. Terrestrial laser scanning for measuring the solid wood volume, including branches, of adult standing trees in the forest environment. Comput. Electron. Agric. 89, 86–93. doi:10.1016/j.compag.2012.08.005

de Römer, A.H., Kneeshaw, D.D., Bergeron, Y., 2007. Small gap dynamics in the southern boreal forest of eastern Canada: Do canopy gaps influence stand development? J. Veg. Sci. 18, 815–826.

Denison, W.C., 1973. Life in tall trees. Sci. Am. 228, 74–80.

Dieler, J., Pretzsch, H., 2013. Morphological plasticity of European beech (Fagus sylvatica L.) in pure and mixed-species stands. For. Ecol. Manag. 295, 97–108. doi:10.1016/j.foreco.2012.12.049

Douglas, E.S., Martel, J., Li, Z., Howe, G., Hewawasam, K., Marshall, R.A., Schaaf, C.L., Cook, T.A., Newnham, G.J., Strahler, A., others, 2015. Finding leaves in the forest: the dual-wavelength Echidna lidar. IEEE Geosci. Remote Sens. Lett. 12, 776–780.

Forrester, D.I., Bauhus, J., 2016. A Review of Processes Behind Diversity—Productivity Relationships in Forests. Curr. For. Rep. 2, 45–61. doi:10.1007/s40725-016-0031-2

Forrester, D.I., Collopy, J.J., Beadle, C.L., Baker, T.G., 2012. Interactive effects of simultaneously applied thinning, pruning and fertiliser application treatments on growth, biomass production and crown architecture in a young Eucalyptus nitens plantation. For. Ecol. Manag. 267, 104–116. doi:10.1016/j.foreco.2011.11.039

Forrester, D.I., Pretzsch, H., 2015. Tamm Review: On the strength of evidence when comparing ecosystem functions of mixtures with monocultures. For. Ecol. Manag. 356, 41–53.

Fournier, R., Côté, J.-F., Bourge, F., Durrieu, S., Piboule, A., Béland, M., Grau, E., 2015. A method addressing signal occlusion by scene objects to quantify the 3D distribution of forest components from terrestrial lidar., in: 28th-30th September 2015. Presented at the Proceedings of SilviLaser 2015. 14th conference on Lidar Applications for Assessing and Managing Forest Ecosystems, La Grande Motte. France.

Fournier, R.A., Mailly, D., Walter, J.-M.N., Soudani, K., 2003. Indirect measurement

154

of forest canopy structure from in situ optical sensors, in: Remote Sensing of Forest Environments. Springer, pp. 77–113.

Garber, S.M., Maguire, D.A., 2005. The response of vertical foliage distribution to spacing and species composition in mixed conifer stands in central Oregon. For. Ecol. Manag. 211, 341–355. doi:10.1016/j.foreco.2005.02.053

Getzin, S., Wiegand, K., 2007. Asymmetric tree growth at the stand level: Random crown patterns and the response to slope. For. Ecol. Manag. 242, 165–174. doi:10.1016/j.foreco.2007.01.009

Gilmore, D.W., Seymour, R.S., 1997. Crown architecture of Abies balsamea from four canopy positions. Tree Physiol. 17, 71–80.

Godman, R.M., Yawney, H.W., Tubbs, C.H., 1990. Acer saccharum Marsh. sugar maple. Silv. N. Am. 2, 78.

Grau, E., Durrieu, S., Fournier, R., Gastellu-Etchegorry, J.-P., Yin, T., 2017. Estimation of 3D vegetation density with Terrestrial Laser Scanning data using voxels. A sensitivity analysis of influencing parameters. Remote Sens. Environ. 191, 373–388.

Hallé, F., Oldeman, R.A.A., Tomlinson, P.B., 1978. Tropical trees and forests: an architectural analysis. Springer-Verlag.

Hardiman, B.S., Gough, C.M., Halperin, A., Hofmeister, K.L., Nave, L.E., Bohrer, G., Curtis, P.S., 2013. Maintaining high rates of carbon storage in old forests: A mechanism linking canopy structure to forest function. For. Ecol. Manag. 298, 111–119. doi:10.1016/j.foreco.2013.02.031

Hildebrandt, R., Iost, A., 2012. From points to numbers: a database-driven approach to convert terrestrial LiDAR point clouds to tree volumes. Eur. J. For. Res. 1–11.

Horn, H.S., 1971. The adaptive geometry of trees, Princeton University Press. ed. Princeton University Press.

Hosoi, F., Omasa, K., 2009. Estimating vertical plant area density profile and growth parameters of a wheat canopy at different growth stages using three-dimensional portable lidar imaging. ISPRS J. Photogramm. Remote Sens. 64, 151–158. doi:10.1016/j.isprsjprs.2008.09.003

Hosoi, F., Omasa, K., 2006. Voxel-based 3-D modeling of individual trees for estimating leaf area density using high-resolution portable scanning lidar.

Geosci. Remote Sens. IEEE Trans. On 44, 3610–3618.

Jonckheere, I., Fleck, S., Nackaerts, K., Muys, B., Coppin, P., Weiss, M., Baret, F., 2004. Review of methods for in situ leaf area index determination: Part I. Theories, sensors and hemispherical photography. Agric. For. Meteorol. 121, 19–35.

Jucker, T., Bouriaud, O., Coomes, D.A., 2015. Crown plasticity enables trees to optimize canopy packing in mixed-species forests. Funct. Ecol. 29, 1078–1086. doi:10.1111/1365-2435.12428

Lafarge, T., Pateiro-Lopez, B., 2014. alphashape3d: Implementation of the 3D alpha-shape for the reconstruction of 3D sets from a point cloud.

Latif, Z.A., Blackburn, G.A., 2010. The effects of gap size on some microclimate variables during late summer and autumn in a temperate broadleaved deciduous forest. Int. J. Biometeorol. 54, 119–129.

Laurans, M., Martin, O., Nicolini, E., Vincent, G., 2012. Functional traits and their plasticity predict tropical trees regeneration niche even among species with intermediate light requirements. J. Ecol. 100, 1440–1452. doi:10.1111/j.1365-2745.2012.02007.x

Lefsky, M.A., Cohen, W.B., Parker, G.G., Harding, D.J., 2002. Lidar Remote Sensing for Ecosystem Studies: Lidar, an emerging remote sensing technology that directly measures the three-dimensional distribution of plant canopies, can accurately estimate vegetation structural attributes and should be of particular interest to forest, landscape, and global ecologists. BioScience 52, 19–30.

Li, Y., Guo, Q., Tao, S., Zheng, G., Zhao, K., Xue, B., Su, Y., 2016. Derivation, Validation, and Sensitivity Analysis of Terrestrial Laser Scanning-based Leaf Area Index. Can. J. Remote Sens. 42, 719–729.

Liang, J., Crowther, T.W., Picard, N., Wiser, S., Zhou, M., Alberti, G., Schulze, E.-D., McGuire, A.D., Bozzato, F., Pretzsch, H., others, 2016. Positive biodiversity-productivity relationship predominant in global forests. Science 354, aaf8957.

Lin, Y., Herold, M., 2016. Tree species classification based on explicit tree structure feature parameters derived from static terrestrial laser scanning data. Agric. For. Meteorol. 216, 105–114.

Lin, Y., West, G., 2016. Retrieval of effective leaf area index (LAIe) and leaf area

density (LAD) profile at individual tree level using high density multi-return airborne LiDAR. Int. J. Appl. Earth Obs. Geoinformation 50, 150–158. doi:10.1016/j.jag.2016.03.014

Longuetaud, F., Piboule, A., Wernsdörfer, H., Collet, C., 2013. Crown plasticity reduces inter-tree competition in a mixed broadleaved forest. Eur. J. For. Res. 132, 621–634. doi:10.1007/s10342-013-0699-9

McCarthy, J., 2001. Gap dynamics of forest trees: a review with particular attention to boreal forests. Environ. Rev. 9, 1–59.

Medlyn, B.E., 2004. A maestro retrospective. For. Land–Atmosphere Interface CAB Int. 105–121.

Millet, J., 2012. L'architecture des arbres des régions tempérées, MULTIMONDES. ed.

Morin, X., 2015. Species richness promotes canopy packing: a promising step towards a better understanding of the mechanisms driving the diversity effects on forest functioning. Funct. Ecol. 29, 993–994.

Morin, X., Fahse, L., Scherer-Lorenzen, M., Bugmann, H., 2011. Tree species richness promotes productivity in temperate forests through strong complementarity between species. Ecol. Lett. 14, 1211–1219.

Muller-Landau, H.C., Condit, R.S., Chave, J., Thomas, S.C., Bohlman, S.A., Bunyavejchewin, S., Davies, S., Foster, R., Gunatilleke, S., Gunatilleke, N., 2006. Testing metabolic ecology theory for allometric scaling of tree size, growth and mortality in tropical forests. Ecol. Lett. 9, 575–588.

Muth, C.C., Bazzaz, F.A., 2003. Tree canopy displacement and neighborhood interactions. Can. J. For. Res. 33, 1323–1330.

Muth, C.C., Bazzaz, F.A., 2002a. Tree canopy displacement at forest gap edges. Can. J. For. Res. 32, 247–254. doi:10.1139/x01-196

Muth, C.C., Bazzaz, F.A., 2002b. Tree canopy displacement at forest gap edges. Can. J. For. Res. 32, 247–254. doi:10.1139/x01-196

Naesset, E., Gobakken, T., Solberg, S., Gregoire, T.G., Nelson, R., St\a ahl, G., Weydahl, D., 2011. Model-assisted regional forest biomass estimation using LiDAR and InSAR as auxiliary data: A case study from a boreal forest area. Remote Sens. Environ. 115, 3599–3614.

Niinemets, Ü., 2010. A review of light interception in plant stands from leaf to canopy in different plant functional types and in species with varying shade tolerance. Ecol. Res. 25, 693–714. doi:10.1007/s11284-010-0712-4

Niklaus, P.A., Baruffol, M., He, J.-S., Ma, K., Schmid, B., 2017. Can niche plasticity promote biodiversity–productivity relationships through increased complementarity? Ecology n/a-n/a. doi:10.1002/ecy.1748

Oliver, C.D., Larson, B.C., 1990. Forest stand dynamics. McGraw-Hill, Inc.

Oshio, H., Asawa, T., Hoyano, A., Miyasaka, S., 2015. Estimation of the leaf area density distribution of individual trees using high-resolution and multi-return airborne LiDAR data. Remote Sens. Environ. 166, 116–125. doi:10.1016/j.rse.2015.05.001

Othmani, A., Piboule, A., Krebs, M., Stolz, C., Voon, L.F.C.L.Y., 2011. Towards automated and operational forest inventories with T-Lidar.

Othmani, A., Voon, L.F.L.Y., Stolz, C., Piboule, A., 2013. Single tree species classification from terrestrial laser scanning data for forest inventory. Pattern Recognit. Lett. 34, 2144–2150.

Pedersen, B.S., Howard, J.L., 2004. The influence of canopy gaps on overstory tree and forest growth rates in a mature mixed-age, mixed-species forest. For. Ecol. Manag. 196, 351–366. doi:10.1016/j.foreco.2004.03.031

Pedersen, R.Ø., Bollandsås, O.M., Gobakken, T., Næsset, E., 2012. Deriving individual tree competition indices from airborne laser scanning. For. Ecol. Manag. 280, 150–165. doi:10.1016/j.foreco.2012.05.043

Petriţan, A.M., Lüpke, B. von, Petriţan, I.C., 2009. Influence of light availability on growth, leaf morphology and plant architecture of beech (Fagus sylvatica L.), maple (Acer pseudoplatanus L.) and ash (Fraxinus excelsior L.) saplings. Eur. J. For. Res. 128, 61–74. doi:10.1007/s10342-008-0239-1

Pittermann, J., Sperry, J.S., Wheeler, J.K., Hacke, U.G., Sikkema, E.H., 2006. Mechanical reinforcement of tracheids compromises the hydraulic efficiency of conifer xylem. Plant Cell Environ. 29, 1618–1628.

Pothier, D., Savard, F., 1998. Actualisation des tables de production pour les principales espèces forestières du Québec. [Québec]: Ministère des ressources naturelles, Forêt Québec.

Pretzsch, H., 2014. Canopy space filling and tree crown morphology in mixed-

species stands compared with monocultures. For. Ecol. Manag. doi:10.1016/j.foreco.2014.04.027

Pretzsch, H., 2009a. Forest dynamics, growth and yield: from measurement to model. Springer.

Pretzsch, H., 2009b. Forest dynamics, growth and yield, Springer. ed. Berlin Heidelberg.

Pretzsch, H., Dieler, J., 2012. Evidence of variant intra- and interspecific scaling of tree crown structure and relevance for allometric theory. Oecologia 169, 637–649. doi:10.1007/s00442-011-2240-5

Purves, D.W., Lichstein, J.W., Pacala, S.W., 2007. Crown Plasticity and Competition for Canopy Space: A New Spatially Implicit Model Parameterized for 250 North American Tree Species. PLoS ONE 2, e870. doi:10.1371/journal.pone.0000870

Reulke, R., Haala, N., 2005. Tree Species Recognition with Fuzzy Texture Parameters, in: Klette, R., Žunić, J. (Eds.), Combinatorial Image Analysis, Lecture Notes in Computer Science. Springer Berlin Heidelberg, pp. 607–620.

Richards, P.W., Champion, H.G., 1954. The tropical rain forest. Emp. For. Rev. 33, 134–135.

Rigling, A., Braker, O., Schneiter, G., Schweingruber, F., 2002. Intra-annual tree-ring parameters indicating differences in drought stress of Pinus sylvestris forests within the Erico-Pinion in the Valais (Switzerland). Plant Ecol. 163, 105–121.

Robitaille, A., Saucier, J.-P., 1998. Paysages régionaux du Québec méridional. [Québec]: Gouvernement du Québec, Ministère des ressources naturelles.

Runkle, J.R., 1998. Changes in Southern Appalachian Canopy Tree Gaps Sampled Thrice. Ecology 79, 1768–1780. doi:10.2307/176795

Runkle, J.R., Yetter, T.C., 1987. Treefalls Revisited: Gap Dynamics in the Southern Appalachians. Ecology 68, 417–424. doi:10.2307/1939273

Schneuwly, D.M., Stoffel, M., Dorren, L.K.A., Berger, F., 2009. Three-dimensional analysis of the anatomical growth response of European conifers to mechanical disturbance. Tree Physiol. 29, 1247–1257.

Schröter, M., Härdtle, W., Oheimb, G. von, 2012. Crown plasticity and neighborhood interactions of European beech (Fagus sylvatica L.) in an old-growth forest.

Eur. J. For. Res. 131, 787–798. doi:10.1007/s10342-011-0552-y

Schütt, C., Aschoff, T., Winterhalder, D., Thies, M., Kretschmer, U., Spiecker, H., 2004. Approaches for recognition of wood quality of standing trees based on terrestrial laserscanner data. Thies M Koch B Spiecker H.

Seidel, Dominik, Beyer, F., Hertel, D., Fleck, S., Leuschner, C., 2011. 3D-laser scanning: A non-destructive method for studying above- ground biomass and growth of juvenile trees. Agric. For. Meteorol. 151, 1305–1311. doi:10.1016/j.agrformet.2011.05.013

Seidel, D., Hoffmann, N., Ehbrecht, M., Juchheim, J., Ammer, C., 2015. How neighborhood affects tree diameter increment – New insights from terrestrial laser scanning and some methodical considerations. For. Ecol. Manag. 336, 119–128. doi:10.1016/j.foreco.2014.10.020

Seidel, D., Leuschner, C., Müller, A., Krause, B., 2011. Crown plasticity in mixed forests—Quantifying asymmetry as a measure of competition using terrestrial laser scanning. For. Ecol. Manag. 261, 2123–2132.

Shaw, D.C., 2004. Vertical organization of canopy biota. Elsevier Academic Press: Amsterdam, The Netherlands.

Simonse, M., Aschoff, T., Spiecker, H., Thies, M., 2003. Automatic determination of forest inventory parameters using terrestrial laserscanning, in: Proceedings of the ScandLaser Scientific Workshop on Airborne Laser Scanning of Forests. pp. 252–258.

Sultan, S.E., 2000. Phenotypic plasticity for plant development, function and life history. Trends Plant Sci. 5, 537–542.

Tao, S., Guo, Q., Su, Y., Xu, S., Li, Y., Wu, F., 2015. A geometric method for wood-leaf separation using terrestrial and simulated lidar data. Photogramm. Eng. Remote Sens. 81, 767–776.

Thies, M., Spiecker, H., 2004. Evaluation and future prospects of terrestrial laser scanning for standardized forest inventories. Forest 2, 1.

Tilman, D., Wedin, D., Knops, J., 1996. Productivity and sustainability influenced by biodiversity in grassland ecosystems. Nature 379, 718.

Valladares, F., Gianoli, E., Gómez, J.M., 2007. Ecological limits to plant phenotypic plasticity. New Phytol. 176, 749–763.

Vepakomma, U., St-Onge, B., Kneeshaw, D., 2011. Response of a boreal forest to canopy opening: assessing vertical and lateral tree growth with multi-temporal lidar data. Ecol. Appl. 21, 99–121.

Weiss, M., Baret, F., Smith, G.J., Jonckheere, I., Coppin, P., 2004. Review of methods for in situ leaf area index (LAI) determination: Part II. Estimation of LAI, errors and sampling. Agric. For. Meteorol. 121, 37–53.

Williams, L.J., Paquette, A., Cavender-Bares, J., Messier, C., Reich, P.B., 2017. Spatial complementarity in tree crowns explains overyielding in species mixtures. Nat. Ecol. Evol. 1, 0063. doi:10.1038/s41559-016-0063

Wulder, M.A., Bater, C.W., Coops, N.C., Hilker, T., White, J.C., 2008. The role of LiDAR in sustainable forest management. For. Chron. 84, 807–826.

Wulder, M.A., White, J.C., Nelson, R.F., Næsset, E., Ørka, H.O., Coops, N.C., Hilker, T., Bater, C.W., Gobakken, T., 2012. Lidar sampling for large-area forest characterization: A review. Remote Sens. Environ. 121, 196–209. doi:10.1016/j.rse.2012.02.001

Young, T.P., Hubbell, S.P., 1991a. Crown Asymmetry, Treefalls, and Repeat Disturbance of Broad-Leaved Forest Gaps. Ecology 72, 1464–1471. doi:10.2307/1941119

Young, T.P., Hubbell, S.P., 1991b. Crown Asymmetry, Treefalls, and Repeat Disturbance of Broad-Leaved Forest Gaps. Ecology 72, 1464–1471. doi:10.2307/1941119

Zhang, Y., Chen, H.Y.H., Reich, P.B., 2012. Forest productivity increases with evenness, species richness and trait variation: a global meta-analysis. J. Ecol. 100, 742–749. doi:10.1111/j.1365-2745.2011.01944.x